2018

# Reprogramming The Retina: Next Generation Strategies Of Retinal Neuroprotection And Gene Therapy Vector Potency Assessment

Devin Scott Mcdougald
*University of Pennsylvania*, devinmcdougald@gmail.com

# Reprogramming The Retina: Next Generation Strategies Of Retinal Neuroprotection And Gene Therapy Vector Potency Assessment

**Abstract**
Mutations within over 250 known genes are associated with inherited retinal degeneration. Clinical success following gene replacement therapy for Leber's congenital amaurosis type 2 establishes a platform for the development of downstream treatments targeting other forms of inherited and acquired ocular disease. Unfortunately, several challenges relevant to complex disease pathology and limitations of current gene transfer technologies impede the development of gene replacement for each specific form of retinal degeneration. Here we describe gene augmentation strategies mediated by recombinant AAV vectors that impede retinal degeneration in pre-clinical models of acquired and inherited vision loss. We demonstrate distinct neuroprotective effects upon retinal ganglion cell survival and function in experimental optic neuritis following AAV-mediated gene augmentation. Gene transfer of the antioxidant transcription factor, NRF2, improves RGC survival while overexpression of the pro-survival and anti-inflammatory protein, SIRT1, promotes preservation of visual function. In the context of inherited retinal disease, we show stimulation of anabolic metabolism following AKT3 gene transfer preserves photoreceptor viability and delays functional loss in a mouse model of retinitis pigmentosa. In addition to these neuroprotective strategies, we also describe an approach to improve the in vitro potency of AAV vectors that are restricted by tissue-specific regulatory elements. This strategy utilizes genome engineering based on CRISPR/Cas9 gene activation to reprogram cell lines to specifically and potently express tissue-specific promoters of interest from AAV vectors.

**Degree Type**
Dissertation

**Degree Name**
Doctor of Philosophy (PhD)

**Graduate Group**
Cell & Molecular Biology

**First Advisor**
Jean Bennett

**Keywords**
aav, gene therapy, neuroprotection, photoreceptor, retinal degeneration, retinal ganglion cell

**Subject Categories**
Genetics | Molecular Biology | Virology

# REPROGRAMMING THE RETINA: NEXT GENERATION STRAEGIES OF RETINAL NEUROPROTECTION AND GENE THERAPY VECTOR POTENCY ASSESSMENT

Devin S. McDougald

A DISSERTATION

in

Cell & Molecular Biology

Presented to the Faculties of the University of Pennsylvania

in

Partial Fulfillment of the Requirements for the

Degree of Doctor of Philosophy

2018

Supervisor of Dissertation

_____

Jean Bennett M.D., Ph.D., Professor of Ophthalmology and Cell & Developmental Biology

Graduate Group Chairperson

_____

Dan Kessler Ph.D., Chair, Cell & Molecular Biology Graduate Group

Dissertation Committee

Valder Arruda M.D., Ph.D.
Associate Professor of Pediatrics

Kenneth S. Shindler M.D., Ph.D.
Associate Professor of Ophthalmology

Claire H. Mitchell
Professor of Anatomy & Cell Biology

Hansell H. Stedman
Associate Professor of Surgery

## ACKNOWLEDGMENT

I would have not reached this point academically, professionally, or personally without the influence of past scientific mentors. Dr. Anthony Bell Jr. at the University of Southern Mississippi presented my first opportunity to perform laboratory research. His guidance as well as patience provided an excellent foundation in molecular biology techniques, experimental design, and how to conduct oneself within a research lab. Drs. Wade Chien, Lisa Cunningham, and Thomas Friedman at the NIDCD/NIH allowed me to train in an exceptionally fast-paced and cutting edge research environment prior to entering graduate school. Observing their passion, dedication, and relentless work ethic towards improving both the fundamental understanding of human diseases and creation of novel therapeutics reinvigorated my passion for pursuit of a research-based career.

I have been incredibly fortunate to carry out this work alongside a crew of exceptionally talented scientists from very diverse training backgrounds. I want to particularly acknowledge Drs. Adam Wojno, Scott Dooley, Kris Fisher, Jason Mills, and Pavitra Ramachandran for always lending their time for insightful discussions or venting sessions relevant to project design, troubleshooting, career advice, and life. Much of the work shown here could not have been performed without the technical expertise of many individuals including Zhangyong Wei, Alexandra Zezulin, Kimberly Dine, Tyler Papp, and Dr. Ken Shindler. In addition, I must thank members of the CAROT research vector core, especially Drs. Shangzhen Zhou and Jieyan Pan, for producing the AAV vectors used in these studies. I thank my thesis committee for their helpful insight and technical direction in guiding some of the studies presented in this document.

The ideas and concepts behind much of this work would likely have been shot down immediately if I were under the direction of any other scientist besides Jean Bennett. I believe this is one of the many reasons Jean has sustained a highly productive scientific career: she places an incredible amount of trust in her trainees to independently develop and explore creative ideas and solutions to challenging problems in vision research. Beyond all the scientific achievements and medical milestones scattered along her career path, Jean maintains an unwavering humble,

supportive, and congenial nature of a magnitude that I have yet to encounter elsewhere in the research community. Altogether, she is an exceptional scientist and an even better person, and I am forever grateful to her for allowing me to train and grow as a scientist in her laboratory.

I must thank my family and friends for their enduring love and support throughout this very long and tiresome process. I want to specifically acknowledge Terra Kuhn, Bobby French, Steven Zhao, Stephen Bart, Chris Cali, David Walter, and Lucas Van Gorder for their friendship and overwhelming support during the best and worst of times. Finally, I must thank my parents, Glenn and Elizabeth, for their continued support through all avenues of life.

# ABSTRACT

REPROGRAMMING THE RETINA: NEXT GENERATION STRATEGIES OF RETINAL NEUROPROTECTION AND GENE THERAPY VECTOR POTENCY ASSESSMENT

Devin S. McDougald

Jean Bennett M.D., Ph.D.

Mutations within over 250 known genes are associated with inherited retinal degeneration. Clinical success following gene replacement therapy for Leber's congenital amaurosis type 2 establishes a platform for the development of downstream treatments targeting other forms of inherited and acquired ocular disease. Unfortunately, several challenges relevant to complex disease pathology and limitations of current gene transfer technologies impede the development of gene replacement for each specific form of retinal degeneration. Here we describe gene augmentation strategies mediated by recombinant AAV vectors that impede retinal degeneration in pre-clinical models of acquired and inherited vision loss. We demonstrate distinct neuroprotective effects upon retinal ganglion cell survival and function in experimental optic neuritis following AAV-mediated gene augmentation. Gene transfer of the antioxidant transcription factor, NRF2, improves RGC survival while overexpression of the pro-survival and anti-inflammatory protein, SIRT1, promotes preservation of visual function. In the context of inherited retinal disease, we show stimulation of anabolic metabolism following AKT3 gene transfer preserves photoreceptor viability and delays functional loss in a mouse model of retinitis pigmentosa. In addition to these neuroprotective strategies, we also describe an approach to improve the *in vitro* potency of AAV vectors that are restricted by tissue-specific regulatory elements. This strategy utilizes genome engineering based on CRISPR/Cas9 gene activation to reprogram cell lines to specifically and potently express tissue-specific promoters of interest from AAV vectors.

TABLE OF CONTENTS

LIST OF FIGURES

# CHAPTER 1 Introduction

*Organization and composition of the mammalian visual system*

The retina is a thin layer of neural tissue situated at the back the eye that is composed of specialized cellular layers that function in a concerted fashion to convert photo-chemical stimuli into neural impulses that travel to the brain and mediate the sensory perception known as vision. The mammalian retina contains three layers of neurons separated by two additional layers of synaptic connections **(Figure 1.1)**. The outer retina is composed of the retinal pigment epithelium (RPE) and photoreceptor layer. The RPE is the outer most population of retinal cell types and provides structural integrity and support to cells of the neural retina. The RPE mediates the transport of various nutrients, ions, and growth factors from systemic circulation via the choroidal vasculature. In addition, RPE cells supply critical components in the visual cycle maintenance and are essential for the phagocytosis, breakdown, and recycling of photoreceptor outer segments (Sparrow et al., 2010). Photoreceptors are a specialized collection of sensory neurons that capture photons of light as the initial step in the photo-transduction cascade. In mice and humans, photoreceptors account for approximately 70% of retinal cell types and are divided into two major subtypes: rods and cones. Rods are responsible for visual processing in low light (scotopic) conditions mediated by the photo-sensitive pigment, rhodopsin. Cone photoreceptors are responsible for mediating complex features of vision associated with photopic conditions (bright light), color, and high

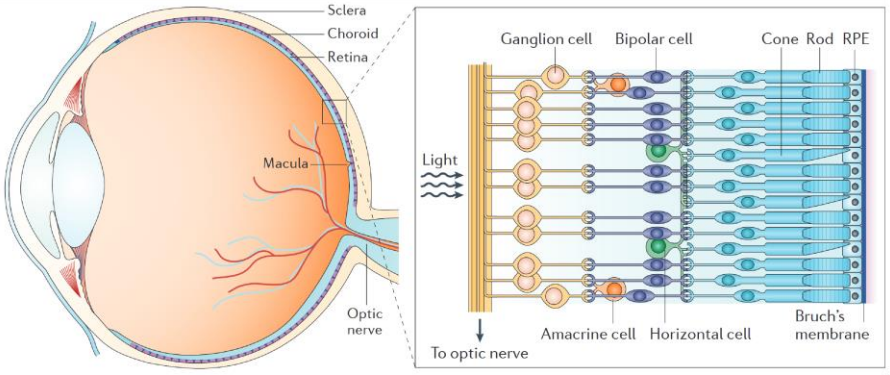


**Figure 1.1. Organization of the mammalian retina.** The retina is composed of three specialized cellular layers that function in a coordinated fashion to process light stimulation into nerve impulses that are transferred to visual centers of the brain. Figure adapted from Kembrel et al., 2015.

resolution/acuity. In vertebrates, cone cells are further divided into two or three subtypes based upon their specific photo-transduction pigment and corresponding responses to various wavelengths of light. For example, humans contain three cone subtypes that are responsive to long (red; L-opsin), medium (green; M-opsin), or short (blue; S-opsin) wavelengths of light (Kolb, 2007). In both mice and humans, rods vastly outnumber the cone cells approximately 30:1 (mice) and 20:1 (humans). Moreover, the anatomical and spatial distribution of rods and cones vary between vertebrate species. Humans and other higher order primates contain a fovea which is composed of cones located in the central retina responsible for high acuity visual processing, whereas rods dominate the retinal periphery (Kolb, 2007). From a structural perspective, photoreceptors are composed of four distinct components: outer segment, inner segment, cell body, and synaptic terminal. The outer segment is a specialized primary cilium composed of several membranous discs saturated with visual pigments and other essential components involved in light capture and signal transduction. The inner segment contains the golgi, mitochondria, and endoplasmic reticulum to support the incredible energetic and metabolic demands of the photoreceptor (Baker et al., 2013). Synaptic terminals provide the critical link in transmission of visual signals from the photoreceptor to second order neurons occupying the inner retina (Kolb, 2007).

Cell types of the inner retinal layer (INL) include bipolar cells, horizontal cells, and amacrine cells. Bipolar cells function as second order neurons and are critical for transmitting signals from the photoreceptors to the ganglion cells via synaptic connections of the inner plexiform layer (IPL). Bipolar cells are typically separated into two major subclasses designated as “ON” or “OFF” cells. Glutamate release from photoreceptors functions as a neurotransmitter and modulates the activity of ON and OFF bipolar cells. In the dark, glutamate release hyperpolarizes (inhibits) the activity of ON bipolar cells and depolarizes (activates) OFF cells (Kolb, 2003). Conversely, hyperpolarization of the photoreceptor following light capture reduces glutamate release leading to depolarization (excitation) of ON bipolar cells and hyperpolarization of OFF cells (Kolb, 2003). ON and OFF bipolar cells can be further subdivided based upon their

connectivity with photoreceptors via synapses that constitute the outer plexiform layer (IPL). Certain subclasses of bipolar cells will synapse with rods while others form connections with multiple or single cone subtypes (Euler et al., 2014). Horizontal cells and amacrine cells function as inhibitory neurons that integrate and regulate inputs between the photoreceptors and retinal ganglion cells (Kolb, 2007). Retinal ganglion cells (RGCs) are the terminal neuron of the retina and mediate the transfer of visual information to the brain. Axonal projections emanating from the RGCs innervate and form the optic nerve, which provides a physical connection between the retina and visual centers of the brain.

*Inherited retinal degenerations (IRDs)*

Given the incredibly complex and coordinated fashion through which retinal neurons process, interpret, and transmit visual input, it is unsurprising that defects within very discrete components can mediate profound consequences upon visual function. Mutations within over 250 genes are associated with retinal degeneration (Bennett, 2017; RetNet). Mendelian forms affect approximately 1 in 2000-3000 individuals with the majority of these manifestations resulting from dysfunction and subsequent death of photoreceptors (Wright et al., 2010). Numerous mechanisms are implicated in photoreceptor cell death ranging from retinal-specific functions to ubiquitous cellular mechanisms such as defects in photo-transduction, the visual cycle, or outer segment maintenance/stability. Perturbations in ubiquitous cellular processes including pre-mRNA splicing, signaling pathways, mitochondrial function, lipid metabolism, and many others **(Figure 1.2)** also contribute to photoreceptor degeneration (Wright

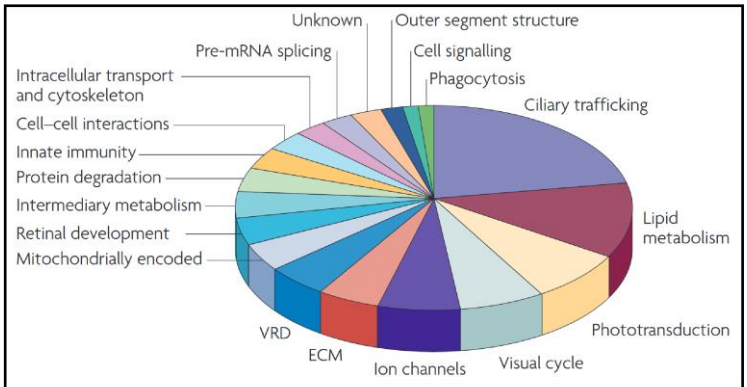


**Figure 1.2. Cellular processes affected in inherited retinal degenerations.** Pie chart demonstrates the functional categorization of retinal disease genes. Figure adapted from Wright et al., 2010.

et al., 2010). Retinitis pigmentosa accounts for the largest and most genetically diverse group of inherited photoreceptor degenerations and is characterized by the onset of rod degeneration and culminating with the progressive demise of cones in later stage disease (Punzo et al., 2012). The genetics, mechanisms of disease, and potential therapeutic strategies for retinitis pigmentosa will be discussed extensively in Chapter 3. Other IRDs, such as Leber's congenital amaurosis (LCA), display early onset vision loss typically within the first year of life resulting from pathogenic mutations within seventeen known genes with functions associated with the visual cycle (ex. *RPE65, RDH12*), connecting cilium structure and transport (ex. *CEP290, LCA5*), and photoreceptor development (ex. *CRX, CRB1*). Other IRDs are characterized by phenotypes that primarily affect one photoreceptor subtype including congenital stationary night blindness (primarily rod involvement) or cone dystrophies (cone degeneration) (Veleri et al., 2015). In the case of many IRDs, the kinetics of vision loss and retinal degeneration can be highly variable between patients depending upon the affected gene and the severity of the pathogenic mutation. Moreover, different mutations with the same gene can be differentially diagnosed based on the clinical presentation. Advancements in genetic testing and DNA sequencing technologies allow us to increase our knowledge of these complex genotype-phenotype correlations associated with IRDs. Understanding these relationships will provide critical information for improving the accuracy and timing of a clinical diagnosis, patient-specific prognosis, and perhaps the opportunity for therapeutic intervention (Bryant et al., 2017).

*Acquired retinal degeneration*

In addition to mendelian forms of vision loss that typically manifest early in life, other retinal diseases may arise later due to complex environmental, genetic, and age-related determinants. Glaucoma is an optic neuropathy characterized by the loss of retinal ganglion cells and is the leading form of irreversible blindness throughout the world (Weinreb et al., 2014). Numerous mechanisms are implicated in the development of glaucoma including elevation in intraocular pressure (IOP) thereby compressing optic nerve fibers/disrupting axonal transport,

dysregulation of autophagic flux within RGCs, vascular alterations, and mitochondrial dysfunction (Davis et al., 2016).

Age-related macular degeneration (AMD) is the primary cause of blindness within the elderly and is an acquired disease that affects the RPE but leads to secondary degeneration of photoreceptors (Ambati et al., 2012). Early signs of AMD involve the accumulation of extracellular aggregates known as drusen. This typically precedes RPE degeneration. AMD is subdivided into two forms termed “dry” or “wet.” Wet AMD is characterized by an additional phenotype beyond primary RPE degeneration: outgrowth and invasion of immature choroidal blood vessels into the outer retina, known as choroidal neovascularization (CNV). These vessels disrupt features of retinal homeostasis by leaking various components into the neural retina (Ambati et al., 2012). Other acquired ocular conditions may arise as secondary features of a broader disease process. In Chapter 2, I will provide a detailed description of one such condition, called optic neuritis, which is characterized by inflammation and demyelination of the optic nerve. Optic neuritis is commonly encountered at the onset of multiple sclerosis. Current treatment strategies for these conditions are aimed at attenuating pathological processes. Medications for glaucoma are aimed at reducing intraocular pressure via hypotensive eyedrops, oral drugs, or laser trabeculoplasty (Weinreb et al., 2014). Wet AMD is treated by intravitreal administration of antibodies directed against VEGF-A, which diminishes vascular outgrowth and stabilizes vision in most patients. Unfortunately, there are currently no effective treatment strategies for the more prevalent dry AMD (Ambati et al., 2012). In most of these disease scenarios where treatments are available, patients must adhere to strict treatment regimens to prevent further retinal degeneration and associated vision loss. Furthermore, these strategies do not address the underlying features driving neurodegeneration of the cell type exhibiting pathology.

*Gene therapy for retinal degenerative diseases*

The practice of gene therapy is an ongoing subject of intense scientific and medical investigation that has spanned well over forty years. Friedmann & Roblin (1972) introduced the

concept and transformative potential of gene therapy to ameliorate substantial forms of human suffering in their landmark article published in the journal, *Science*. However, the authors also cautioned against its immediate application in human clinical studies given the incomplete understanding of basic processes governing gene regulation, delivery of recombinant DNA to human cells, and fundamental molecular mechanisms of many inherited diseases. Decades that followed observed rapid advancements in each of these specific areas. The first retinal disease gene involved in a form of X-linked retinitis pigmentosa was successfully mapped in 1984 (Bhattacharya et al., 1984). Continued advancements in DNA cloning, sequencing, and results of the human genome project propelled unprecedented discovery and functional interrogation of thousands of human disease genes (International Human Genome Sequencing Consortium, 2001). Because of such efforts, we have successfully identified over 250 genes associated with inherited retinal degeneration (Bennett, 2017; RetNet) **(Figure 1.3)**. Possibly the most critical advancements in priming gene therapy for clinical translation involved the discovery and engineering of safe and effective gene delivery vehicles, referred to as "vectors," for targeting diverse cellular and tissue populations (Thomas et al., 2003). The most efficient vector platforms for *in vivo* directed gene therapy are derived from human and primate viruses. Viral vectors are composed of two major functional components: the capsid and expression cassette. The viral capsid dictates tropism for specific cell types (Srivastava, 2016). Engineering of the vector expression cassette includes removal of viral elements encoding structural or functional features

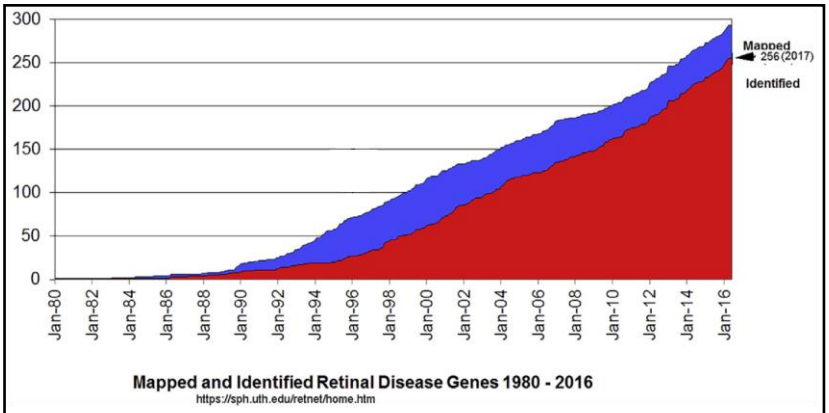


**Figure 1.3. Timeline depicting the mapping and identification of retinal disease genes.** Over 250 disease genes have been identified since 1980. Figure adapted from Bennett, 2017.

that aid in their replication cycle. Such elements are replaced with transgenes that encode cDNA sequences of therapeutic interest and various regulatory elements **(Figure 1.4)**.

The eye provides a favorable environment to interrogate the efficacy of gene-based treatments. The small anatomical size of the organ allows the use of small vector volumes and doses to achieve substantial targeting of retinal cell types. In addition, the presence of the second eye enables the use of a within-subject control to determine the effects of an experimental treatment. Moreover, ocular health and therapeutic outcomes can be easily assessed with various noninvasive imaging techniques including fundoscopy and optical coherence tomography (OCT). Finally, the eye is considered an "immunoprivileged" compartment, meaning it can tolerate the introduction of foreign antigens, such as viral vectors, without eliciting a robust inflammatory response (Willett & Bennett, 2013). This feature is largely due to the presence of the blood-retinal barrier, which is composed of retinal pigment epithelia (RPE) and the retinal vascular endothelium. Tight junctions between the RPE prevent contact between the neural retina and systemic circulation of the choroid (Forrester et al., 2012). RPE cells also secrete various soluble factors such as CD95L (fas ligand), that induce effector T cell apoptosis, thus contributing another layer of immune modulation (Jorgensen et al., 1998). Moreover, the presence of distinct proteins such as B7-1 and B7-2 on the surface of different retinal cell types are involved in the conversion of naïve T cells to regulatory T cells (Tregs), which contribute additional immunosuppressive properties (Stein-Streilein & Taylor, 2007; DiCarlo et al., 2018).

*AAV-mediated gene therapy for Leber's congenital amaurosis type 2 (LCA2)*

Decades of scientific inquiry to identify retinal disease genes, animal models that accurately reflect human disease conditions, and the continued development of safe and durable vector platforms culminated in proof-of-concept studies and subsequently the first human clinical trials for an inherited form of vision loss (Bainbridge et al., 2008; Hauswirth et al., 2008; Maguire et al., 2008). Initial studies interrogated the pre-clinical efficacy of a gene replacement therapy for an inherited retinal disease in animal models of Leber's congenital amaurosis type 2 (LCA2)

using an adeno-associated virus serotype 2 (AAV2) vector as the gene delivery vehicle. Similar to the human disease, these animals contain loss-of-function mutations in the *RPE65* gene, which encodes an enzyme critical for the conversion of all-trans retinal to 11-cis retinol in the visual cycle. Acland et al. (2001) was the first to demonstrate visual recovery in a naturally occurring dog model of LCA2 using AAV2-mediated gene replacement of *RPE65.* Downstream investigations achieved similar findings within the same dog model as well as the *Rpe65*$^{-/-}$ mouse (Dejneka et al., 2004; Acland et al., 2005; Jacobson et al., 2006; Bennicelli et al., 2008), which provided the pre-clinical framework for translation to human clinical testing. Initial clinical studies examined safety and efficacy of AAV2 vector delivery to the subretinal space in a small cohort of patients diagnosed with LCA2. Patients exhibited no adverse events to the AAV2 vector at a dose of $1.5x10^{10}$ vector genomes. Moreover, patients showed improvement in pupillary light reflex and visual acuity (Maguire et al., 2008). A phase 1 dose-escalation trial in 12 patients between ages 8 to 44 years revealed age-dependent effects upon visual recovery following treatment with younger individuals demonstrating the greatest improvement in vision (Maguire et al., 2009). Moreover, this trial reinforced the robust safety and efficacy data observed in the initial cohort of patients (Maguire et al., 2008; Maguire et al., 2009). Furthermore, the effects upon visual function remained durable over time (Simonelli et al., 2010; Bennett et al., 2016). In addition to recovery of retinal function, incredibly, the effects of gene replacement also led to reactivation and reorganization of synaptic connectivity within the visual cortex, suggesting the durable effects of gene replacement may also impact neural plasticity (Ashtari et al., 2011; Ashtari et al., 2015). Based on the robust safety and efficacy profile demonstrated in the phase 1 studies, a phase 3 trial enrolling 31 total patients was initiated (Russell et al., 2017). The AAV2 vector used in these studies was ultimately approved by the US Food & Drug Administration in December 2017 under the commercial name, Voretigene neparvovec-ryzl, or more simply, Luxturna. This landmark scientific and medical achievement sets the stage for the development of additional gene therapy products targeting other forms of inherited and acquired vision loss.

*Gene transfer with adeno-associated virus (AAV) vectors*

Vectors based upon recombinant adeno-associated virus (AAV) have become the current standard for targeting retinal cell populations safely and effectively (Bennett, 2017). AAV was first identified as a contaminant of adenovirus preparations (Atchison et al., 1965). The AAV genome consists of a small, single-stranded DNA molecule of approximately 4.7 kilobases in length encoding two genes flanked by two 145 base pair inverted terminal repeats (ITRs) **(Figure 1.4)**. The *Rep* gene encodes various proteins (Rep40, Rep52, Rep68, Rep78) associated with viral DNA replication and packaging, whereas the *Cap* gene encodes three structural proteins involved in assembly of the viral capsid (VP1, VP2, VP3) (Salganik et al., 2015). Recombinant AAV (rAAV) genomes can be generated through excision of the *Rep* and *Cap* genes and inclusion of a transgene cassette between the ITR sequences **(Figure 1.4)**. These recombinant genomes are readily packaged into infectious AAV particles by supplying the *Rep* and *Cap* genes in *trans* and in the presence of adenovirus (Tratschin et al., 1984). Downstream investigations elucidated the specific adenovirus factors that contribute to the AAV replicative cycle (Ferrari et al., 1997; Xiao et al., 1998). Identification of these factors led to development of the "triple transfection" method in which three plasmids encoding the AAV expression cassette, *Rep*/*Cap* genes, and the adenoviral "helper" genes (respectively) are transiently transfected into human embryonic kidney 293 cells (HEK293). This has become the standard procedure for generation of research and clinical grade rAAV vectors (Mingozzi & High, 2011).

AAV exhibits several favorable properties as a gene transfer vector for *in vivo* directed applications. Foremost, the wild-type virus has not been associated with any human disease. This is a unique feature compared to other conventional viral vector platforms including lentivirus (HIV/AIDS), HSV-1 (herpes), and adenovirus (respiratory infections). While the wild-type virus has been shown to preferentially integrate into a specific genomic region located on the long arm of chromosome 19 (19q13-qter), later termed the AAV safe harbor locus (AAVS1), this process occurs at an exceptionally low frequency (approximately 0.1%) (Deyle et al, 2009; McCarty et al., 2004). In most cases, the incoming single-stranded AAV genome is converted to a non-

integrating, double-stranded circular episome that provides durable transgene expression in quiescent cell types. This feature reduces the possibility of insertional mutagenesis commonly associated with other vector platforms including lentiviral and retroviral vectors (Bokhoven et al., 2009; Uren et al., 2005). Compared to other viral vectors, rAAV exhibits a low immunogenic profile perhaps due to its relatively poor transduction efficiency of antigen presenting cells (APCs) (Mays et al., 2014) or its complete lack of viral-associated genes (Basner-Tschakarjan et al., 2014). Despite its weak immunogenicity, the immune system can still detect other vector components including the capsid proteins, vector genome, and transgene products. Thus components of humoral immunity, including T cells and pre-existing neutralizing antibodies, may limit the efficacy of gene transfer and lead to the elimination of successfully transduced cells (Louis Jeune et al., 2013). Moreover, this presents a substantial challenge for the prospect of vector re-administration (Mingozzi & High, 2013).

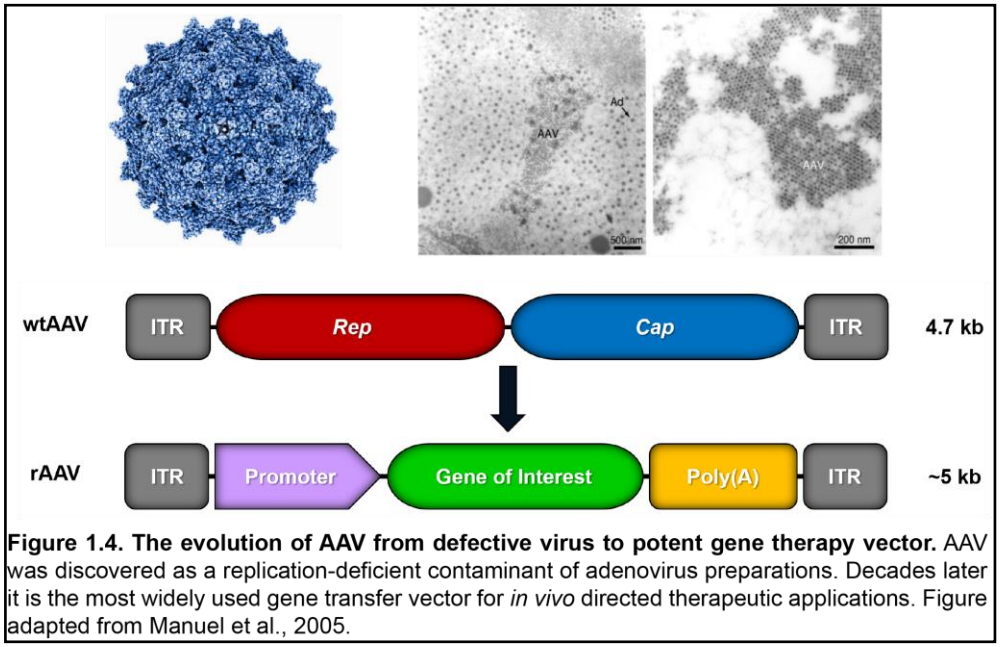


**Figure 1.4. The evolution of AAV from defective virus to potent gene therapy vector.** AAV was discovered as a replication-deficient contaminant of adenovirus preparations. Decades later it is the most widely used gene transfer vector for *in vivo* directed therapeutic applications. Figure adapted from Manuel et al., 2005.

*Ocular gene delivery: vectors, routes of administration, and cell targeting considerations*

Gene transfer vectors are introduced in clinical trials to retinal cell types via two routes of administration. The intravitreal injection is a common outpatient procedure by which a small needle is inserted through the pars plana followed by release of the reagent into the vitreous

cavity **(Figure 1.5)**. This approach is used to administer medication for a variety of retinal conditions including age-related macular degeneration (AMD) and diabetic retinopathy. Delivery of AAV vectors with this injection approach has revealed tropism for retinal ganglion cells (RGCs) and their axons projecting through the optic nerve. Moreover, various studies have utilized this combination of vector and delivery approach to demonstrate RGC protection in various animal models of optic neuropathy (Qi & Lewin et al., 2007; Qi & Sun et al., 2007; Talla et al., 2013; Talla et al., 2014; Talla et al., 2015; McDougald et al., 2018). The insufficient transduction of outer retinal cell types, including photoreceptors and RPE, through intravitreal administration is partly due to presence of the inner limiting membrane (ILM), which serves as a basement membrane in the eye and provides physical separation of the retina and vitreous humor. Thus, the ILM likely acts as a barrier for the penetration of viral particles (Dalkara et al., 2009). Moreover, the structure is coated with various extracellular matrix proteins that may bind and sequester vector particles from reaching the retina (Candiello et al., 2007). Various studies suggest outer retinal targeting with gene transfer vectors can be enhanced through pharmacological digestion or physical removal of the ILM (Dalkara et al., 2009; Takahashi et al., 2017). However, sufficient targeting of photoreceptors and other cell types localized to the outer retina with conventional AAV vectors relies upon delivery of these particles to the subretinal space. This approach involves a somewhat invasive procedure in which the physician delicately places the injection needle between the neural retina and retinal pigment epithelium **(Figure 1.5)**. Vector preparation is dispensed in a controlled fashion and generates a localized retinal detachment commonly referred to as a “subretinal bleb.” This region typically re-attaches to the underlying RPE within a few days.

Beyond the route of administration, other features that must be taken into consideration to achieve targeting of a specific retinal cell population include selection of an appropriate capsid and regulatory elements. The amino acid sequence of the *Cap* gene dictates the tropism of the rAAV particle. Pioneering studies examined the retinal tropism of AAV2 encoding reporter genes under the regulation of ubiquitous promoters via intravitreal or subretinal delivery. This vector was

shown to readily transduce retinal ganglion cells and optic nerve following intravitreal administration (Dudus et al., 1999). If the vector is injected within the subretinal space, it displays exceptional tropism for retinal pigment epithelia (RPE) (Bennett et al., 1997). Downstream studies examined the retinal tropism of various naturally isolated and rationally designed AAV capsids. Vectors such as AAV5, AAV8, and AAV9 demonstrate efficient targeting of photoreceptors following subretinal delivery (Lotery et al., 2003; Lebherz et al., 2008; Vandenberghe et al., 2011; Vandenberghe et al., 2013). Since photoreceptors are the primary cell type affected in the majority of IRDs, the emergence of these vectors expanded the utility of AAV-mediated gene replacement to target these diseases. Additional investigations performed site directed mutagenesis of surface exposed tyrosine residues within the AAV2 capsid sequence to broaden its retinal tropism and utility. It is suggested that changing these tyrosine residues protects vector particles from ubiquitination and proteasome-mediated degradation thus enhancing successful transduction events (Petrs-Silva et al., 2009; Petrs-Silva et al., 2011; Mowat et al., 2014). More recent efforts aimed to identify synthetic AAV capsids via *in vivo* evolution/selection to achieve outer retinal targeting with the less invasive intravitreal delivery approach (Boyd RF et al., 2016; Dalkara et al., 2013; Kay et al., 2013). However, anatomical differences between species continue to pose formidable barriers for translation of these vectors with respect to penetration of retinal cell layers after intravitreal injection and cellular specificity (Ramachandran et al., 2017).

In addition to capsid selection, features of the AAV expression cassette can be modified to drive tissue-selective transgene expression. Numerous promoter elements are available to drive cell-specific expression within distinct retinal cell types including photoreceptors, bipolar cells, and retinal ganglion cells (Flannery et al., 1997; Lu et al., 2016; Chaffiol et al., 2017). These regulatory elements provide an additional layer of safety by reducing the possibility of off target transgene expression within otherwise healthy cell types. Many of these promoter elements will be described in subsequent chapters. Collectively, selection of the appropriate capsid, regulatory elements, and delivery route allows precise targeting of a specific retinal cell population with gene transfer.

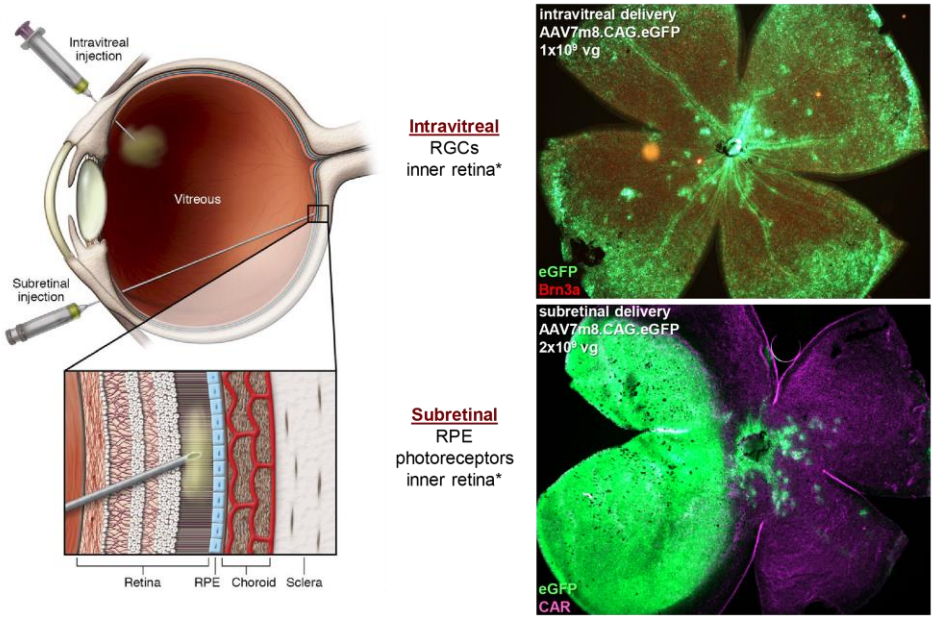


Targeting a specific cell population: capsid + regulatory elements + route of administration

**Figure 1.5. Routes of administration for targeting retinal cells with gene therapy vectors.** Panels to the right depict representative gene expression patterns following intravitreal or subretinal delivery of AAV vectors. Figure adapted from DiCarlo et al., 2018.

*Limitations of AAV-mediated gene replacement therapies for ocular disease*

Despite the overwhelming pre-clinical and clinical evidence to support the continued development of AAV-based gene replacement for various ocular diseases, features associated with complex disease pathology and biophysical limitations of rAAV vectors impede the application of such strategies for many inherited and acquired conditions. The “Achilles heel” of the AAV gene transfer platform concerns its limited DNA packaging capacity of approximately five kilobases. Numerous genes implicated in IRDs unfortunately exceed this size restriction, and thus are not candidates for gene replacement using conventional AAV vectors. Several efforts are underway to deliver genes using alternative vector platforms that can accommodate these large cDNA and promoter sequences. However, these systems present additional challenges including unstable gene expression patterns, immunogenic concerns, and insufficient targeting of the

desired cell population (Thomas et al., 2003). Another strategy to deliver large transgene cassettes utilizes the delivery of two AAV vectors that each encode one half of the transgene sequence. In this scenario, the two vector sets may undergo homologous recombination and reconstitute the fully intact cDNA sequence (Hirsch et al., 2016; Carvalho et al., 2017). Moreover, other strategies harness the advantages of a single AAV to deliver partial coding sequences capable of editing endogenous pre-mRNA transcripts through a process known as spliceosome-mediated pre-mRNA trans-splicing (Berger et al., 2015; Dooley et al., 2018). Unfortunately, the current iterations of these technologies display particularly low efficiency in their respective processes to mediate a therapeutic effect (Carvalho et al., 2017; Dooley et al., 2018).

*Neuroprotective gene transfer strategies for retinal degeneration*

While gene replacement is an attractive strategy to ameliorate ocular pathology associated with mendelian forms of vision loss, other forms of retinal degeneration as described previously are characterized by disease etiologies due to complex genetic and environmental factors rather than single gene defects. Furthermore, limitations of the conventional vector systems as described in the previous section also present substantial challenges to address certain monogenic conditions. It may be possible to alleviate or slow retinal degeneration in many inherited or acquired forms of ocular disease by targeting “conserved” features of the pathological process. This concept, often referred to as “neuroprotection,” utilizes pharmacological or gene transfer strategies to counteract common mechanisms that lead to progressive neurodegeneration. In the context of retinal degeneration, trophic factors such as ciliary neurotrophic factor (CNTF) and rod-derived cone viability factor (RdCVF) have been the subject of rigorous basic and translational research investigation within several inherited and acquired disease models (Liang et al., 2001; Maier et al., 2004; Ait-ali et al., 2015; Byrne et al., 2015). Other strategies involve direct manipulation or reprogramming of cellular pathways by targeting critical mechanisms involved in the degenerative process. Several candidate interventions mitigate oxidative damage by direct scavenging of reactive oxygen species or

manipulation of gene expression programs associated with antioxidant defense (Qi & Lewin et al., 2007; Qi & Sun et al., 2007; Xiong et al., 2015; Liang et al., 2017; McDougald et al., 2018). Other reagents non-specifically impede cell death by interrupting key components in the apoptotic signaling cascade (Petrin et al., 2003; Leonard et al., 2007). Finally, other strategies induce large scale reprogramming of key metabolic pathways that become dysregulated during disease progression (Venkatesh et al., 2015; Zhang & Justus et al., 2016; Zhang & Du et al., 2016; Rajala et al., 2018).

*Thesis aims*

My thesis research examined novel neuroprotective strategies in pre-clinical models of retinal degeneration utilizing AAV-mediated gene transfer. Specifically, Chapters 2 and 3 will examine strategies to impede retinal degeneration in complex forms of acquired and inherited vision loss through reprogramming the metabolism of retinal neurons with gene augmentation. Chapter 2 will focus on the design and testing of potential therapeutic interventions to attenuate inflammatory and oxidative stress-induced retinal degeneration in a mouse model of optic neuritis. Chapter 3 describes a neuroprotective strategy to delay photoreceptor degeneration in a mouse model of retinitis pigmentosa. This approach involves stimulating pathways associated with anabolic metabolism and cell survival to nonspecifically impede photoreceptor death during disease progression.

Later in my studies, I became interested in the development of translational research tools to more accurately characterize the effects of gene transfer vectors driven by tissue or cell-specific regulatory elements. Specifically, I engineered cell-based platforms to interrogate the function and potency of AAV vectors regulated by promoters that are only active within mammalian photoreceptors. Potency assays are an essential component in all phases of a drug development timeline and ensure purity, stability, and function of the product. One of the underappreciated yet key impediments in developing cell-based potency assays for gene therapy products concerns the use of tissue or cell-specific promoters driving transgene expression. In

many cases, these elements display robust expression and specificity *in vivo* but exceptionally poor activity across several well characterized cell lines, thus hindering our ability to assess vector expression and potency in a cell-based setting. Chapter 4 will discuss a genome engineering approach that effectively and robustly activates photoreceptor-specific promoters from AAV vectors.

# CHAPTER 2 Stimulating anti-inflammatory/antioxidant pathways in experimental optic neuritis with AAV-mediated gene transfer

*Multiple sclerosis: clinical phenotype and genetics*

Multiple sclerosis is a chronic neuroinflammatory disease characterized by infiltration of the central nervous system by autoimmune effector cells targeting conserved components of neural tissue such as myelin and oligodendrocytes. Extensive demyelination, axonal degeneration, and neuronal death implements a phenotype of progressive neurological impairment and physical disability (Dendrou et al., 2015; Mahad et al., 2015). While disease presentation is highly heterogeneous, common clinical symptoms include sensory deficits, fatigue, pain, cognitive decline, and loss of mobility. Most patients are diagnosed with relapsing-remitting MS (RRMS), which is characterized by the onset of recurrent neurological defects followed by a phase of recovery. The disease varies between patients with respect to episode frequency and duration. Patients with RRMS enter a second phase of disease termed secondary progressive MS (SPMS) which is characterized by a steady and permanent neurological decline in the absence of clinical relapses (Mahad et al., 2015). Approximately ten percent of patients

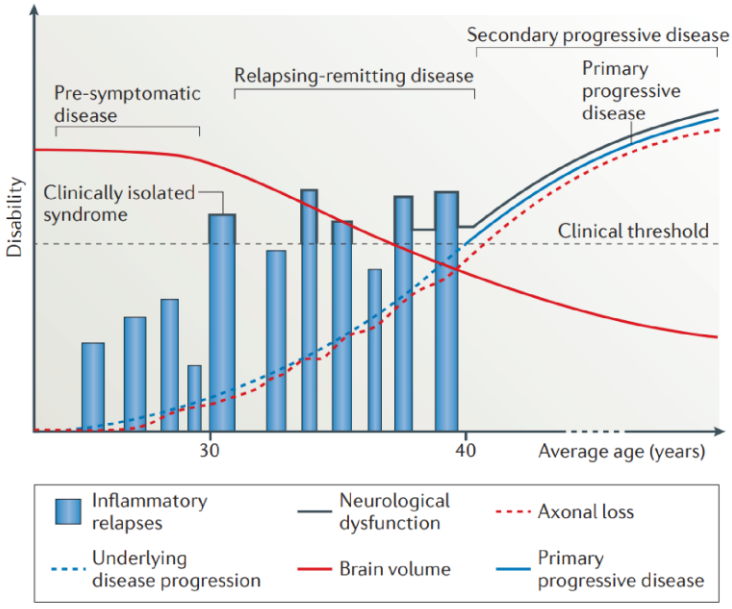


**Figure 2.1. Clinical progression and heterogeneity of multiple sclerosis.** RRMS is diagnosed following an intial episode of neurological dysfunction (clinically isolated syndrome). Brain volume and axonal loss increases over time and as the patient enters progressive phases of disease. Ten percent of patients experience PPMS which is characterized by progressive neurological decline in the absence of relapse/recovery periods. Figure adapted from Dendrou et al., 2015.

experience primary progressive MS (PPMS). Age of onset typically begins in the second or third decades for RRMS patients while PPMS manifests later in life.

MS is largely considered an autoimmune disease with arms of both innate and adaptive immunity contributing to the neurodegenerative process. The disease is largely thought to be driven by the $CD4^+$ T cell response based upon data from animal models of MS. Immunization of animals with components to generate an auto-inflammatory response against conserved neuronal antigens stimulates a $CD4^+$ T cell response. Moreover, these cells can be adoptively transferred to naïve animals and prompt disease progression (Pettinelli et al., 1981), whereas antibody transfer does not generate a similar phenotype. $CD8^+$ T cells mediate direct cytotoxicity following antigen recognition upon oligodendrocytes (Huseby et al., 2001; Sun et al., 2001; Na et al., 2008; Saxena et al., 2008; Mahad et al., 2015). Components of humoral immunity, including B cells and plasma cells, are also found within active MS lesions and secrete pathogenic antibodies that amplify the pro-inflammatory environment (Weber et al., 2011). Interestingly, the target antigens of antibodies in MS remain largely unknown. However, treatment of MS models with monoclonal antibodies directed against myelin oligodendrocyte glycoprotein (MOG) was shown to exacerbate the severity of disease progression (Linington et al., 1998). Innate immune responses in MS are mediated primarily by microglia within the lesion. These cells secrete various pro-inflammatory factors and exhibit a process known as oxidative burst that amplifies critical mechanisms of neurodegeneration including oxidative injury, mitochondrial stress, and ultimately neuronal energy failure, which will be discussed in further detail later in this chapter.

Despite decades of research, a central “trigger” of MS onset is largely undefined but likely influenced by a combination of complex genetic risk factors and environmental cues. Variations within numerous immune loci such as *HLA*, *IL-2Rα*, and *IL-7Rα* are implicated in genetic predisposition to MS (Sospedra et al., 2016). A recent study combined whole exome sequencing with homozygosity mapping to identify a recessive missense mutation in the *NLRP1* gene as a causative variant for familial MS. This gene encodes a critical sensory component involved in inflammasome-associated innate immune function. Interestingly, pathogenic mutations in a

related gene (*NLRP3*) are associated with other rare autoimmune syndromes (Maver et al., 2017) further supporting involvement/dysregulation of the inflammasome and other inflammatory pathways in autoimmune disease pathogenesis. Non-genetic risk factors for MS acquisition are mostly undefined from a mechanistic standpoint. However, several external factors including lifestyle choices, behavior, and exposure to certain infections are proposed to influence disease onset (Coo et al., 2004).

*Optic neuritis*

Optic neuritis is a condition commonly associated with multiple sclerosis and involves acute episodes of visual impairment mediated via inflammation and demyelination of the optic nerve (Kale, 2016). Extensive demyelination and axonal degeneration may culminate in permanent vision loss corresponding with the loss of retinal ganglion cells (RGCs) whose axons innervate and form the optic nerve (Costello et al., 2006; Fisher et al., 2006; Trip et al., 2005). Patients typically experience unilateral vision loss associated with orbital pain eye movement. These features correspond with decreased visual acuity in which two-thirds of patients register a visual acuity below 0.5 (0 = no light perception, ≥1 = normal). Fundoscopic examination is normal in most patients, but the optic disc may appear slightly edematous in the affected eye(s) (Wilhelm et al., 2015). Typically, visual function improves a few weeks following an episode of optic neuritis with visual acuity improving to normal in most patients. However, approximately 6% of patients still experience reduced visual acuity several months after disease presentation (Beck et al., 1992; Wilhelm et al., 2015).

*Treatment strategies for multiple sclerosis & optic neuritis*

Conventional treatments for MS and optic neuritis are directed at managing the inflammatory response. A large multicenter, randomized clinical trial examined the efficacy of corticosteroids for the treatment of relapsing optic neuritis via intravenous or oral routes of administration (Beck et al., 2002). The high dose intravenous cohort demonstrated faster visual

recovery but no change in long-term visual outcomes compared to placebo treated controls. Patients administered oral doses showed no improvement in visual outcomes and, surprisingly, increased the risk of new episodes (Beck et al., 2002). Furthermore, another investigation concluded that the use of corticosteroids did not prevent optic nerve degeneration in acute optic neuritis (Hickman et al., 2003). Subsequent reports suggest there is no definitive evidence to support the use of corticosteroids to achieve normal visual recovery (Gal et al., 2015).

In addition to corticosteroids, treatment with interferon-β has been extensively studied and demonstrated partial therapeutic efficacy particularly in RRMS (Paty et al., 1993; Jacobs et al., 1996; Ebers et al., 1998; Rog et al., 2006). Interferon-β is a cytokine that binds to the heterodimeric surface receptor, IFNAR1/2, and mediates a signal transduction cascade via the JAK/STAT pathway (Rudick et al., 2011). Signaling components form an activated transcriptional complex that translocates to the nucleus and modulates expression of genes containing interferon sensitive response elements (ISRE). While the exact function and influence of these gene expression programs in MS pathogenesis are largely uncharacterized, many of these products are associated with putative therapeutic responses including the activation of antiviral mechanisms, modulation of T cell activity, and stimulation of anti-inflammatory pathways (Rudick et al., 2011). Three formulations of interferon-β have been approved for the treatment of RRMS (Avonex, Betaferon, and Rebif). These treatments demonstrated an approximately 30% reduction in relapse rates, reduced development of new lesions as measured via MRI, and delayed the progression towards MS in the case of patients with clinically isolated syndromes (Paty et al., 1993; Jacobs et al., 1996; Ebers et al., 1998; Rog et al., 2006). While interferon-β-based therapies do provide partial therapeutic efficacy in RRMS, these treatments do not impede the clinical progression of patients that have advanced to SPMS (La Mantia et al., 2012). Moreover, clinical efficacy is reduced in patients who develop neutralizing antibody (NAb) responses against the treatment (Rog et al., 2006).

Recent therapeutic strategies have shifted toward monoclonal antibody-based therapies (mAbs) that target specific surface proteins to modulate the peripheral immune response

(Fontoura, 2010). For example, the United States Food & Drug Administration (FDA) approved ocrelizumab (also known as Ocrevus), which is a humanized monoclonal antibody that targets the CD20 domain on the surface of B cells for the treatment of RRMS and PPMS (Greenfield et al., 2018). Two clinical trials, termed OPERA I and OPERA II, demonstrated reduced annual relapse rates in individuals suffering from RRMS following treatment with ocrelizumab compared to treatment with interferon β-1a (Hauser et al., 2017; Greenfield et al., 2018; Syed, 2018). An additional trial, termed ORATORIO, followed patients with PPMS for ≥120 weeks following intravenous injection of ocrelizumab or placebo every 24 weeks. The primary clinical endpoint for this trial was a diagnosis of disability progression. Ocrelizumab led to reduced disability progression compared to the placebo treatment (Montalban et al., 2017). In addition, interferon-based therapy requires multiple courses of treatment per month whereas ocrelizumab is administered one time over a six month period thus reducing the burden upon patients to maintain a consistent treatment regimen (Syed et al., 2018). Clinical trials for ocrelizumab were specifically designed to include individuals diagnosed with RRMS and PPMS and did not examine the effect upon patients with SPMS. Therefore, it is unclear how ocrelizumab affects mechanisms associated with later stage neurodegeneration associated with SPMS.

*Role of oxidative injury in multiple sclerosis pathogenesis*

Reactive oxygen and nitrogen species (ROS, RNS) are compounds generated as byproducts of normal cellular metabolism and include superoxide, hydroxyl radical, peroxide, and dioxygen. Under conditions of cellular homeostasis, reactive oxidants are generated in a controlled fashion and serve as key signaling molecules for a diverse array of physiological processes including cell growth, immunity, inflammation, and autophagy (Finkel et al., 2011). Oxidative stress occurs when environmental insults or disease states allow uncontrolled production of these molecules which promotes damage to proteins and lipids thereby impairing function and accelerating their degradation.

Accumulating evidence points to oxidative stress as an important contributor in both the early stages of MS progression and later stage chronic neurodegeneration (Qi et al., 2006) **(Figure 2.2)**. Oxidative injury in RRMS is primarily associated with inflammatory processes driven by activated microglia and macrophages as these cells are considered critical reservoirs of reactive oxygen and nitrogen species. Specifically, the cells exhibit a process known as oxidative burst which involves the release of pro-inflammatory cytokines and ROS/RNS in response to a foreign antigens typically associated with infectious agents (Dendrou et al., 2015). High concentrations of ROS/RNS promote damage and destruction of neighboring axons, neurons, and oligodendrocytes. (Lassmann et al., 2016). Neurons are particularly susceptible to oxidative insults because they are quiescent cell types and cannot dilute these cytotoxic components with successive cell divisions (Campbell et al., 2018). Reactive species can diffuse through the plasma membrane and mediate covalent modifications to mitochondrial respiratory chain members and impair ATP production via oxidative phosphorylation (Haider, 2015). Moreover, oxidative injury can also induce irreversible mutations within mitochondrial DNA thereby disrupting normal gene expression programs and further impairing mitochondrial activity. These collective deficits in mitochondrial function, oxidative phosphorylation, and subsequent production of ATP mediates a cellular phenotype of energy failure leading to neuronal death (Lassmann et al., 2012). In addition to inflammatory mechanisms, generation of reactive oxygen species is amplified by the presence of iron liberated into the extracellular space through the loss of myelin and oligodendrocytes (Lassmann et al.,

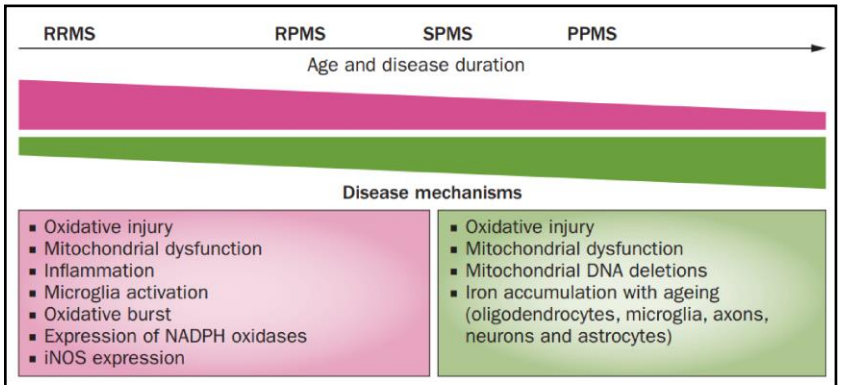


**Figure 2.2. Mechanisms of MS disease progression.** Cytotoxic insults in the relapsing phases of disease coincide with pro-inflammatory and oxidative features of activated immune cells. Oxidative burst of activated microglia drives axonal loss, oligodendrocyte death, and neuronal dysfunction within the MS lesion. Progressive disease mechanisms are highlighted by continued oxidative damage that drives mitchondrial impairment and energy failure that underlies neuronal loss. Figure adapted from Lassmann et al., 2012.

2012; Haider, 2015). Furthermore, iron is taken up by other cell types within the lesion such as microglia and can mediate apoptosis via numerous mechanisms (Dixon et al., 2014). Release of iron via cell death mediates a second wave of oxidative damage within the lesion (Lassmann et al., 2012; Haider, 2015). Interestingly, ablation of microglia was shown to inhibit the development and generation of CNS lesions in the experimental autoimmune encephalomyelitis (EAE) animal model of MS further supporting the role of these cells in mediating MS lesion formation and pathogenesis (Heppner et al., 2005).

Clinical studies observed increased byproducts of oxidative damage including peroxidized lipids and oxidized glutathione in cerebrospinal fluid (CSF) and plasma of MS patients (Hunter et al., 1985; Naidoo et al., 1992). Patient-derived erythrocytes showed reduced activity in the antioxidant enzymes, superoxide dismutase and glutathione peroxidase, suggesting deficits in cellular ROS defense mechanisms (Zagorski et al., 1991; Karg et al., 1999). In addition, isolated mononuclear cells from patients produce higher levels of ROS and nitric oxide compared to those from healthy patients supporting their role in promoting disease progression (Sarchielli et al., 1997). Importantly, molecular examination of MS lesions in postmortem brain samples displayed increased markers of ROS damage corresponding with decreased levels of key antioxidants such as glutathione (Langemann et al., 1992). Moreover, these plaques also show increased oxidized DNA content compared to control specimens (Vladimirova et al., 1998). Collectively, these findings support the contribution of oxidative injury as a conserved mechanism throughout disease progression and a potential therapeutic target in MS etiology.

*Experimental autoimmune encephalomyelitis*

Current understanding of MS pathogenesis is largely attributed to studies of experimental autoimmune encephalomyelitis (EAE). EAE can be elicited in a variety of species by immunization with myelin derived peptides including myelin oligodendrocyte glycoprotein (MOG), myelin basic protein (MBP), or myelin proteolipid protein (PLP) emulsified with an adjuvant (Lublin et al., 1984). This combination stimulates an autoimmune response similar to that found in MS

patients. Furthermore, breakdown of the blood-brain barrier with reagents such as pertussis toxin allows infiltration of autoinflammatory cells into the CNS. The phenotype is characterized by development of inflammatory and demyelinating lesions within the brain and spinal cord and limb paralysis. In addition, the model exhibits an ocular phenotype paralleling optic neuritis with features such as optic nerve thinning, RGC loss, and reduced visual function (Quinn et al., 2011). Collectively, this model provides a robust *in vivo* system to understand neurodegenerative processes and testing of novel therapeutic interventions for MS and optic neuritis.

Amplification of antioxidant or anti-inflammatory mechanisms has shown therapeutic promise in attenuating pathological features of EAE. Several gene therapy strategies have successfully ameliorated ocular disease manifestations in EAE animals. AAV2 overexpression of ROS scavengers such as superoxide dismutase (SOD2) or catalase reduced features of optic nerve pathology including demyelination, optic nerve head swelling, immune infiltration, and RGC loss (Guy et al., 1998; Qi et al., 2006; Qi & Lewin et al., 2007; Qi & Sun et al., 2007). Similarly, amplifying components involved in mitochondrial function commonly dysregulated in MS pathogenesis conferred neuroprotective features. AAV-mediated augmentation of NADH-dehydrogenase type 2 complex 1 (NDl1) attenuated vision loss, axonal loss, oxidative stress, and RGC death in EAE mice (Talla et al., 2013). Gene augmentation of another NADH dehydrogenase subunit (NDUFA6) promoted similar neuroprotective effects (Talla et al., 2015). In addition, overexpression of mitochondrial heat shock protein 70 (mtHSP70), a chaperone involved in mitochondrial protein import and folding, rescued similar disease features as well as activities associated with the mitochondrial respiratory chain (Talla et al., 2014). Collectively, these investigations support further development of gene-based treatment strategies to prevent or reverse MS pathogenesis by amplifying antioxidant pathways or promoting mitochondrial function.

*Modulation of oxidative metabolism by targeting the NRF2/ARE pathway*

Nuclear factor (erythroid-derived 2)-like 2 (NRF2) is a basic leucine zipper transcription factor that stimulates expression of genes associated with antioxidant defense and cellular detoxification. It was originally identified as a DNA binding protein with considerable homology to NF-E2 and bound hypersensitive site 2 of the β-globin control locus (Moi et al., 1994). Structurally, NRF2 contains six NRF2-ECH homology domains (Neh1-6) which participate in DNA binding, nuclear localization, and regulation **(Figure 2.3A)**. Neh2 contains critical functional motifs that are critical for negative regulation of protein activity (Katoh et al., 2005). Neh3 contains a conserved sequence among bZIP transcription factors that is essential for stimulation of genes containing antioxidant response elements (AREs) (Nioi et al., 2005). Neh4 and Neh5 function as additional transactivation domains by binding the cAMP responsive element binding protein (CBP), a conserved co-factor for many transcription factors (Katoh et al., 2001; Abed et al., 2015).

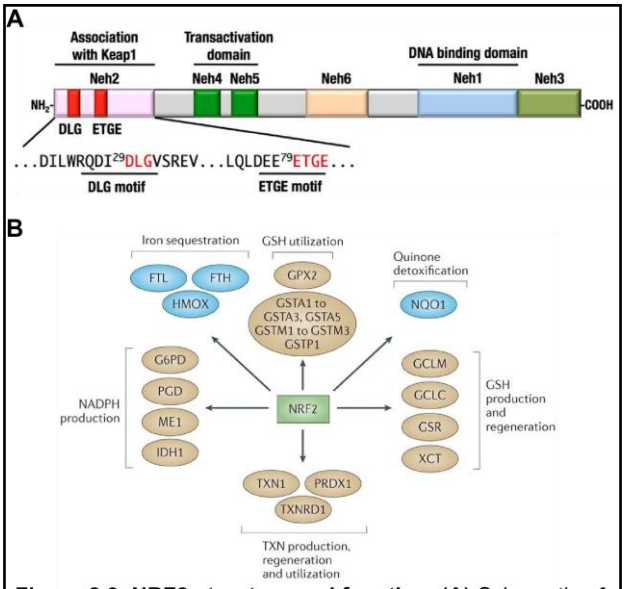


**Figure 2.3. NRF2 structure and function. (A)** Schematic of NRF2 protein structure. NRF2 is composed of six Neh domains which mediate various interactions associated with DNA binding, transcriptional co-factors, and the Keap1 cytoplasmic scaffold. **(B)** NRF2 transcriptional targets. NRF2 stimulates expression various genes associated with antioxidant metabolism, detoxification, iron sequestration, and NADPH production. Figures adapted from Mitsuishi et al., 2012; Gorrini et al., 2013.

In the absence of an oxidative insult, NRF2 is translated and associates with its cytoplasmic scaffold Kelch-like ECH-associated protein 1 (KEAP1). This interaction sequesters NRF2 within the cytoplasm and prevents it from entering the nucleus (Itoh et al., 1999; Ito et al., 2003). In this scenario, NRF2 is eventually targeted for proteasomal-mediated degradation (McMahon et al., 2003). Upon oxidative challenge, critical cysteine residues within KEAP1 become modified by rising oxidant and electrophile concentrations thereby altering its conformation and facilitating dissociation from NRF2. Under such circumstances, newly

synthesized NRF2 freely translocates into the nucleus where it recognizes and binds antioxidant response elements (ARE) in upstream regulatory sequences of genes with antioxidant or detoxification value including heme oxygenase 1 (HMOX1), NADPH quinone oxidoreductase 1 (NQO1), and glutathione S transferases (GSTs) (Dinkova-Kostova et al., 2002; Dinkova-Kostova et al., 2015) **(Figure 2.3B)**. Moreover, NRF2 contributes a critical role in mitochondrial biogenesis and function, and *Nrf2* knockout cells exhibit mitochondrial deficits (Dinkova-Kostova et al., 2015; Kovac et al., 2015). Transgenic ablation of *NRF2* during EAE development generates a phenotype of accelerated demyelination, immune cell infiltration, and pro-inflammatory cytokine signaling compared to the phenotype in wild-type animals also subjected to EAE (Johnson et al., 2010). In addition, *Nrf2* knockout mice demonstrate enhanced decline in visual function, loss of RGCs, and exacerbated optic nerve atrophy (Larabee et al., 2016).

Accumulating evidence supports therapeutic modulation of NRF2 activity via pharmacological approaches or transgenic overexpression in neurodegenerative disease states driven by oxidation (Johnson et al., 2015). EAE mice treated with the NRF2 inducer, TFM-735, demonstrated reduced disease severity and inflammatory cytokine production (Higashi et al., 2017). Similarly, administration of melatonin ameliorated EAE pathophysiology that was associated with activation of the NRF2/ARE pathway (Long et al., 2018). Several investigations have also interrogated the possibility of NRF2-mediated neuroprotection with gene therapy approaches. Xiong et al. (2015) developed a gene augmentation strategy that promoted survival and function of cone photoreceptors in pre-clinical

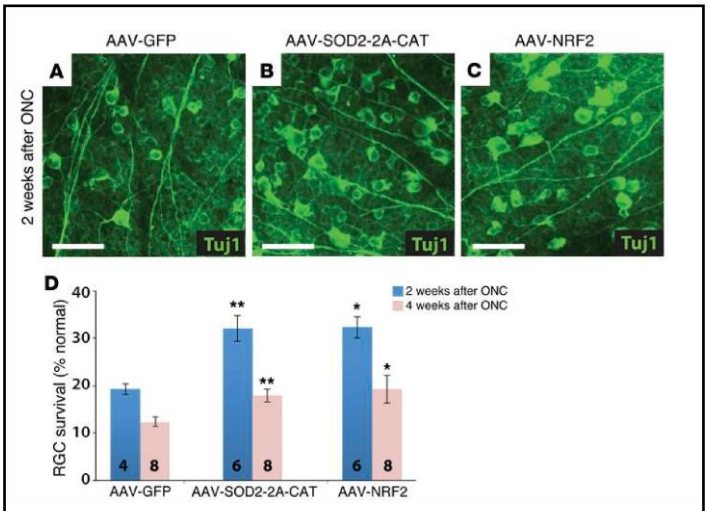


**Figure 2.4. NRF2 gene transfer improves RGC survival following optic nerve crush. (A-C)** Representative images of retinal flatmounts stained with Tuj1 antibodies to label RGCs following treatment with AAV2 vectors. **(D)** Quantification of RGC survival two and four weeks following optic nerve crush. Eyes treated with AAV2.NRF2 display increased survival at both time points compared to eyes that received the AAV2.eGFP control vector. Figure adapted from Xiong et al., 2015.

models of retinitis pigmentosa. In addition, this study demonstrated a transient increase in survival of RGCs targeted with NRF2 expression vectors following optic nerve crush **(Figure 2.4)**. Liang et al. (2017) explored a similar approach within mouse models of retinal degeneration induced by light damage. Based on the collective data, we hypothesized that stimulation of NRF2 activity may provide an effective means to protect RGCs in experimental optic neuritis.

*Role of SIRT1 in multiple sclerosis and optic neuritis*

Sirtuins are a class of enzymes that regulate numerous cellular processes associated with aging, metabolism, stress response, and DNA repair. Seven members comprise the mammalian sirtuin family, and each share a conserved catalytic core domain responsible for carrying out various protein modifications such as deacetylation **(Figure 2.5)**. Sirtuins are largely classified based upon their protein domains flanking this enzymatic core, which dictate features such as substrate specificity and compartmental localization (Michan et al., 2007). The mammalian homologue of Sir2, Sirtuin 1 (SIRT1), is the most well characterized family member and an evolutionarily conserved $NAD^+$-dependent deacetylase that regulates various components of cellular metabolism with respect to aging, DNA repair, mitochondrial biogenesis, and apoptosis (Martin et al., 2015). SIRT1 inhibits apoptosis by direct deacetylation of p53 thereby inactivating its cell death signaling cascade (Luo et al., 2001; Vaziri et al., 2001). SIRT1 has been shown to enhance DNA damage repair by forming a complex and deacetylating Ku70, which is a critical mediator for resolving double-stranded DNA breaks (Jeong et al., 2007). Moreover, SIRT1 improves mitochondrial function by enhancing gene expression and direct

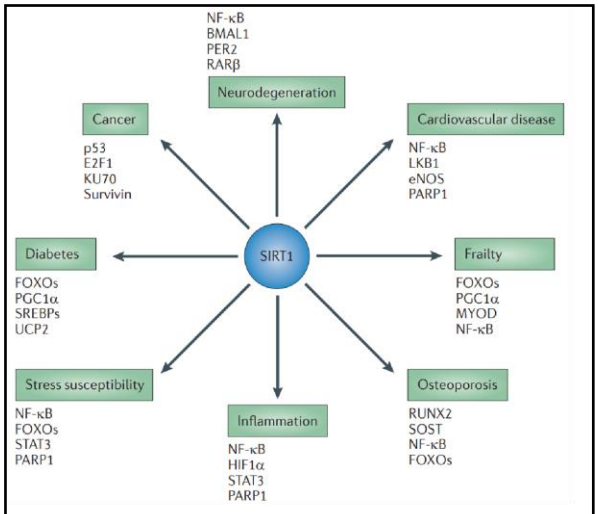


**Figure 2.5. Beneficial effects of SIRT1 activity in age-related disease.** SIRT1 regulates various pathways and processes associated with age-related disease conditions via deacetylation of numerous protein targets. Figure adapted from Baur et al., 2012.

activation of PGC-1α, an essential transcriptional regulator of mitochondrial-associated and antioxidant genes (Amat et al., 2009; Nemoto et al., 2005).

Several lines of evidence suggest modulating SIRT1 activity via pharmacological induction or transgenic overexpression may promote therapeutic outcomes in neurodegenerative disease (Fonseca-Kelly et al., 2012; Jeong et al., 2011; Kahn et al., 2012; Khan et al., 2014; Kim et al., 2007; Martin et al., 2015; Nimmagadda et al., 2013; Shindler et al., 2007; Shindler et al., 2010; Zuo et al., 2013). Neuron-specific deletion of SIRT1 exacerbates the CNS phenotype in a mouse model of Huntington's disease while transgenic overexpression increases survival and rescues neurodegeneration in this model (Jeong et al., 2011). Similarly, pharmacological induction with the known SIRT1 activator, resveratrol, or lentivirus-mediated overexpression of SIRT1 in the hippocampus promoted neuroprotection in a mouse model of Alzheimer's disease/tauopathies (Kim et al., 2007). In experimental optic neuritis, pharmacologic activators of SIRT1, including resveratrol and structurally similar polyphenolic compounds, are effective in sustaining RGC survival in EAE (Shindler et al., 2007; Shindler et al., 2010). Prophylactic or reactive administration of SIRT1 activators including SRT501 and SRT647 attenuated RGC loss in EAE. Moreover, administration of sirtinol, a well characterized SIRT1 inhibitor, effectively blocked the therapeutic effects of SRT501 and SRT647 further emphasizing the neuroprotective role of SIRT1 in EAE pathogenesis (Shindler et al., 2007). In addition to pharmacological inducers, Nimmagadda et al. (2013)

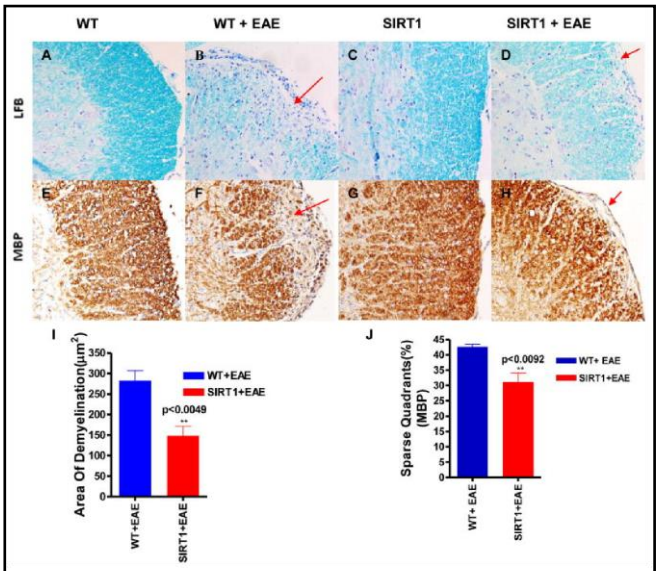


**Figure 2.6. Transgenic SIRT1 overexpression reduces demyelination in EAE. (A-H)** Histology depicts spinal cord sections from respective animal groups stained with two different makers of myelin. **(I-J)** Quantification of myelination. EAE mice harboring a neural-specific SIRT1 overexpression cassette demonstrate improved preservation of myelin compared to control EAE animals. Figure adapted from Nimmagadda et al., 2013.

demonstrated reduced inflammation and demyelination following EAE sensitization in a transgenic mouse harboring a neural-restricted SIRT1 overexpression cassette. This investigation specifically examined MS lesions localized to the spinal cord and did not interrogate the contribution of SIRT1 overexpression in ameliorating ocular disease manifestations **(Figure 2.6)**. Based upon the collective evidence supporting the neuroprotective role of SIRT1 in MS pathogenesis, I sought to explore the therapeutic potential of SIRT1 gene transfer within RGCs during EAE.

## Results

*Design and characterization of first generation RGC neuroprotection vectors*

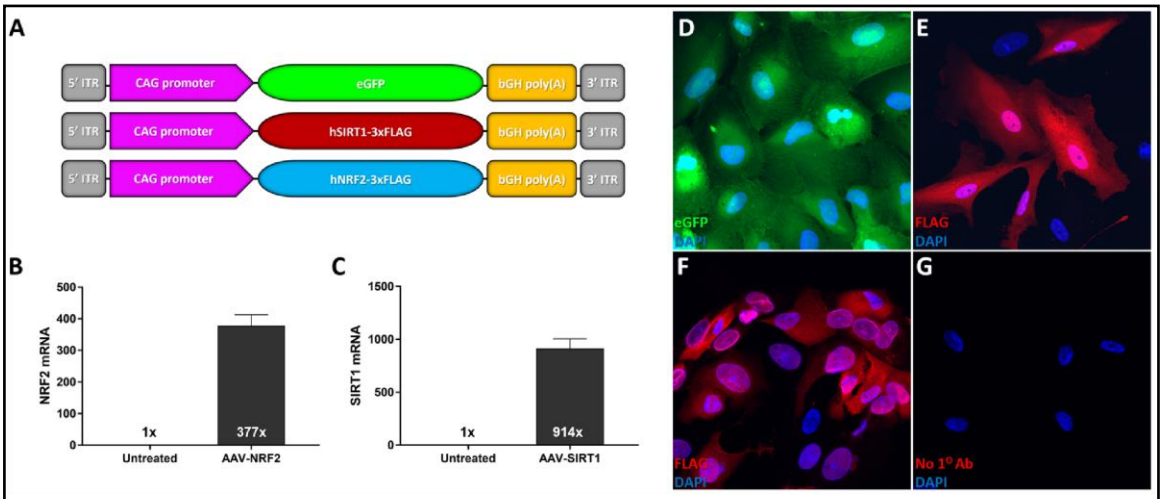


**Figure 2.7. Design and *in vitro* characterization of AAV2 vectors. (A)** Outline of AAV expression cassettes used in the study. RT-qPCR analysis of relative quantities of human NRF2 or human SIRT1 mRNA in 84-31 cells treated with **(B)** AAV2.NRF2 or **(C)** AAV2.SIRT1 compared to untreated cells. Micrographs displaying vector protein expression following ARPE-19 cell transduction with **(D)** AAV2.eGFP, **(E)** AAV2.NRF2, and **(F)** AAV2.SIRT1. **(G)** Control micrograph of ARPE-19 cells transduced with AAV2.NRF2 without anti-FLAG primary antibody incubation. Figure from McDougald et al., 2018.

I designed AAV expression cassettes that allow ubiquitous expression of eGFP, human NRF2, or human SIRT1 **(Figure 2.7A)**. Proviral expression cassettes were packaged into the AAV2 capsid by the CAROT research vector core. These vectors display exceptionally robust *in vitro* activity as shown with RT-qPCR and immunofluorescent analysis. Infection with AAV2.NRF2

and AAV2.SIRT1 yielded a several hundred-fold increase in *Nrf2* and *Sirt1* mRNA compared to levels found in non-transduced cells **(Figure 2.7B-C)**. At the protein level, both vectors display robust nuclear and cytoplasmic distribution following transduction in ARPE-19 cells **(Figure 2.7D-G)**. I examined the retinal transduction profile of AAV2 following intravitreal administration of the AAV2 vector expressing eGFP in a cohort of wild-type mice. Similar to previously described reports, AAV2.eGFP displayed transduction of the ganglion cell layer and optic nerve head **(Figure 2.8A-B).** This vector achieved approximately 21% RGC transduction. RGC transduction was quantified by counting the number of eGFP positive RGCs co-labeled with Brn3a antibody **(Figure 2.8C).** I also assessed the activity of AAV2.NRF2 and AAV2.SIRT1 vectors in the murine retina by immunolabeling retinal cross-sections with antibodies targeting the 3xFLAG epitope tag on each vector. Immunofluorescent analysis revealed FLAG positive labeling of several cells in the ganglion cell layer and sparse labeling of cell types localized to the inner nuclear layer **(Figure 2.8D-F).**

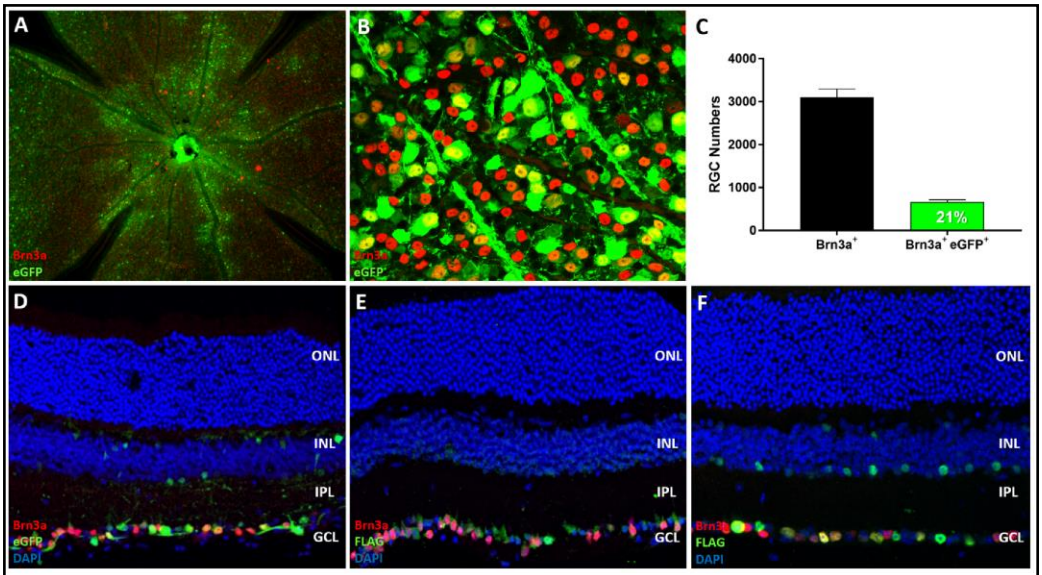


**Figure 2.8. AAV2 transduction profile and RGC transduction efficiency following intravitreal delivery.** **(A)** Representative micrograph of retinal flat mount following intravitreal injection of AAV2.eGFP. RGCs are labeled with Brn3a (red). **(B)** Representative visual field of a retinal flat mount used for calculating RGC transduction efficiency with AAV2. **(C)** Quantification of RGC transduction (N=5 retina). **(D)** Representative cross-section of mouse retina following intravitreal injection of AAV2.eGFP, **(E)** AAV2.NRF2, and **(F)** AAV2.SIRT1. RGCs are labeled with Brn3a (red). Cells positively transduced with NRF2 or SIRT1 vectors are labeled with FLAG (green). Data represented as mean ± SEM. Figure from McDougald et al., 2018.

*AAV2.SIRT1 gene transfer preserves visual acuity during EAE*

Animals received bilateral injections of AAV vectors or empty buffer alone. Animals were induced with EAE at eight weeks of age by immunization with myelin oligodendrocyte glycoprotein (MOG) and complete freunds adjuvant (CFA). This experiment included a cohort of control animals which did not develop the EAE phenotype as they received immunizations with phosphate buffered saline (PBS) and CFA. Clinical features of EAE appeared approximately twelve days post-immunization, while sham-induced control animals exhibited a completely healthy phenotype throughout the experimental timeline **(Figure 2.9)**. Visual acuity was assessed with optokinetic response (OKR) recordings prior to EAE induction and once per week following immunization **(Figure 2.10)**. All treatment groups exhibited robust OKR scores prior to EAE immunization suggesting vector delivery and transgene expression had negligible impact upon visual function. Visual decline was observed approximately 14 days post-immunization. Animals treated with AAV2.SIRT1 display a trending increase in OKR compared to control treatments throughout the experimental timeline. There was statistically significant preservation at day 35 (AAV2.SIRT1=0.292 ± 0.016; AAV2.eGFP=0.19 ± 0.035; *P*=0.032) and day 42 (AAV2.SIRT1=0.274 ± 0.022; AAV2.eGFP=0.161 ± 0.029; *P*=0.049) compared with the AAV2.eGFP control group. This finding supports the neuroprotective potential of *SIRT1* gene transfer in preserving visual function in optic neuritis. NRF2 gene augmentation was unable to prevent visual decline in EAE mice.

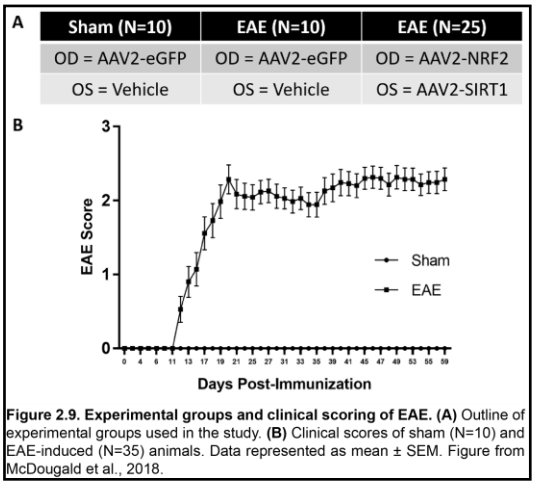


**Figure 2.9. Experimental groups and clinical scoring of EAE. (A)** Outline of experimental groups used in the study. **(B)** Clinical scores of sham (N=10) and EAE-induced (N=35) animals. Data represented as mean ± SEM. Figure from McDougald et al., 2018.

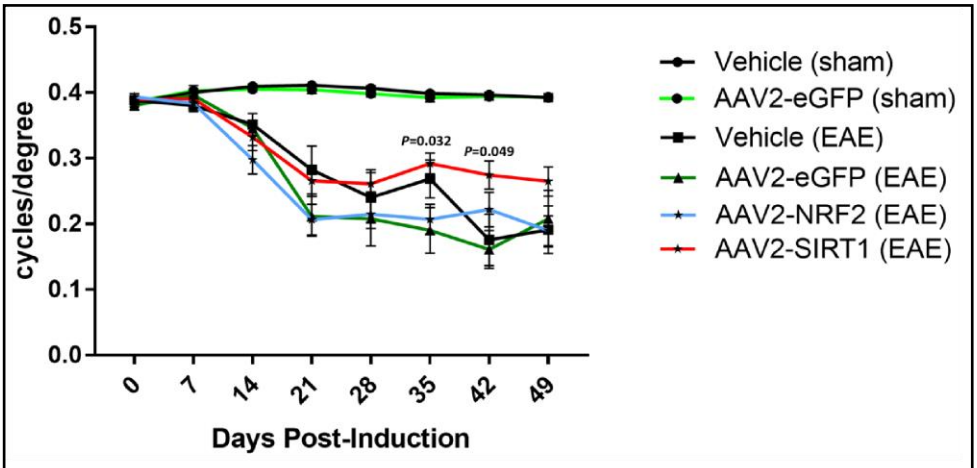


**Figure 2.10. Effect of gene transfer on visual acuity during EAE.** OKR recordings demonstrate signficantly decreased visual acuity in eyes of EAE mice treated with vehicle (N=10) or AAV2.eGFP (N=10). Treatment with AAV2.NRF2 (N=25) did not improve visual function. Mice treated with AAV2.-SIRT1 (N=25) show trending improvement in OKR at days 35 (P=0.032) and 42 (P=0.049) compared to AAV2.eGFP injected eyes also subjected to EAE. Data represented as mean ± SEM. **P*<0.05, ***P*<0.01 by 1-way ANOVA with Turkey's HSD post-test. Figure from McDougald et al., 2018.

*AAV2.NRF2 promotes RGC survival in EAE*

Visual decline in EAE mice corresponds with the loss of RGCs. To investigate the effect of anti-oxidant gene augmentation on RGC survival, I isolated retinas from each treatment group and immunolabeled them with antibodies directed against the canonical RGC marker, Brn3a **(Figure 2.11)**. Reporter vector injected control (non-EAE) eyes displayed RGC numbers comparative to those that received sham intravitreal injections suggesting the AAV2 capsid and associated dose were well tolerated. RGC numbers were significantly reduced in all treatment groups subjected to EAE immunization compared to the non-induced controls (*P*<0.01). Eyes treated with AAV2.SIRT1 demonstrated non-significant but upward trend in RGC survival compared to EAE-induced controls. Surprisingly, AAV2.NRF2, while it did not promote functional retention, was able to significantly improve total RGC survival compared to what was measured in EAE-induced eyes treated with vehicle (*P*=0.027) **(Figure 2.11B)**. In addition to counting total

RGCs per retina, I also examined the effects of gene transfer on regional density of RGCs (central, mid-peripheral, peripheral). NRF2 gene transfer increased the survival of RGCs located within peripheral regions of the retina compared to vehicle (*P*=0.001) and AAV2.eGFP (P=0.002)

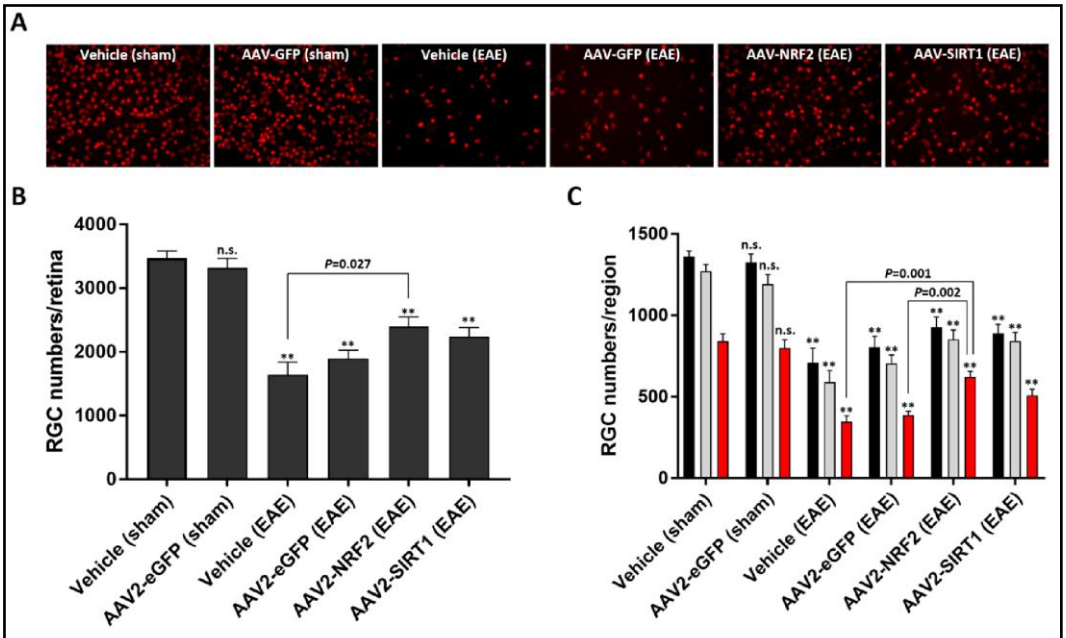


**Figure 2.11. Effect of gene transfer on RGC survival during EAE. (A)** Representative micrographs of RGC survival from each treatment group. RGCs are immunolabeled with Brn3a (red). **(B)** Total RGC numbers quantified per retina. **(C)** RGC numbers quantified per retinal region. Black bars: central, gray bars: mid-peripheral, red bar: peripheral. Data represented as mean ± SEM. *P<0.05, **P<0.01 by 1-way ANOVA and Turkey's HSD post-test. Figure from McDougald et al., 2018.

control groups sensitized to EAE **(Figure 2.11C)**. SIRT1 gene therapy mediated a non-significant but trending increase in regional survival of RGCs.

*Gene therapy with NRF2 and SIRT1 fails to attenuate optic nerve pathology*

EAE animals display progressive thinning, demyelination, axonal loss, and cellular infiltration of the optic nerve. Thus, I examined the effect of NRF2 or SIRT1 gene therapy on features of optic nerve pathology. Optic nerve sections were processed with H&E staining to label immune cell infiltrates. Non-EAE samples displayed minimal evidence of immune infiltration. However, all treatment groups subjected to EAE immunization showed enhanced evidence of cellular infiltrates. Moreover, neither NRF2 nor SIRT1 gene augmentation was able to attenuate this feature **(Figure 2.12A)**. To examine the effect of gene transfer on demyelinaton, optic nerves

were stained with luxol fast blue (LFB). Optic nerve sections derived from healthy control animals showed robust staining of myelin supporting absence of the disease phenotype. All treatment groups subjected to EAE displayed a reduction in myelination. Likewise, treatment with AAV2.NRF2 or AAV2.SIRT1 did not preserve the myelin coating compared to controls **(Figure 2.12B)**.

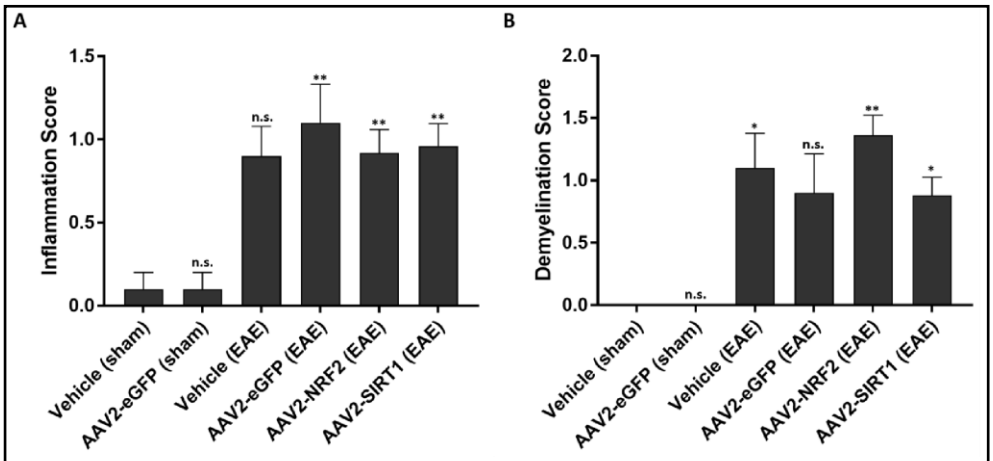


**Figure 2.12. Effect of gene transfer on optic nerve inflammation and demyelination. (A)** Inflammation scores quantified from optic nerve sections following H&E staining. **(B)** Demyelination scores from optic nerve sections following LFB staining. Data represented as mean ± SEM. **P*<0.05, ***P*<0.01 by 1-way ANOVA and Turkey's HSD post-test. Figure from McDougald et al., 2018.

*Optimization of RGC-specific gene transfer*

While we were able to observe some evidence of retinal neuroprotection with NRF2 or SIRT1 gene therapy, these effects were particularly small and did not successfully ameliorate all aspects of ocular EAE pathogenesis. One potential approach to enhancing this therapeutic response in the future is to increase transduction efficiency as this is only 21% using the AAV2 vector. Various methods incorporating rational design or *in vivo* selection have generated novel AAV capsids with improved potency and tropism for retinal cell types compared to naturally isolated serotypes such as AAV2. While AAV7m8 does enhance RGC gene transfer, its activity is not specific to the ganglion cell layer. In fact, this capsid was initially developed to bypass the GCL and inner retina to reach cell types occupying the ONL including photoreceptors and RPE

when coupled with a less surgically invasive intravitreal injection. Recently, Chaffiol et al. (2017) identified a minimal promoter sequence from the human gamma synuclein *(SNCG*) gene that drives robust and specific transgene expression within RGCs **(Figure 2.13)**. I adapted this promoter to an AAV expression cassette encoding a reporter gene, and packaged it into the AAV7m8 capsid. I hypothesized that the AAV7m8 capsid would provide greater transduction of RGCs than AAV2. In addition, coupling this capsid with the *SNCG* promoter would restrict gene expression to the RGC layer. Wild-type animals received intravitreal injection of AAV7m8.SNCG.eGFP.WPRE ($1x10^{10}$ vg) and histology was evaluated four weeks later. The AAV7m8 vector provided potent transduction of the ganglion cell layer (GCL). Transgene expression was observed mostly to the GCL with slight off target expression observed in the inner retina, suggesting this promoter is not truly an "RGC specific" regulatory element. Nonetheless, off target transgene expression was not observed in cell types of the outer nuclear layer **(Figure 2.14B)**. Next, I generated an additional SNCG-driven AAV vector encoding the *SIRT1* transgene. Unlike the previously described construct based on AAV2, this vector contains a codon-optimized human *SIRT1* sequence (copt.SIRT1) and terminates into a woodchuck hepatitis posttranscriptional regulatory element (WPRE) followed by the bovine growth hormone (bGH) polyadenylation signal **(Figure 2.14A).** Vectors were generated and tested in the mouse retina following intraviteal delivery at a $1x10^{10}$ vg dose. Since the copt.SIRT1 sequence did not contain an epitope tag, retinal sections were stained with antibodies directed against SIRT1 protein. Fluorescent microscopy revealed enhanced SIRT1 expression within the GCL, suggesting potent expression of the SNCG-driven

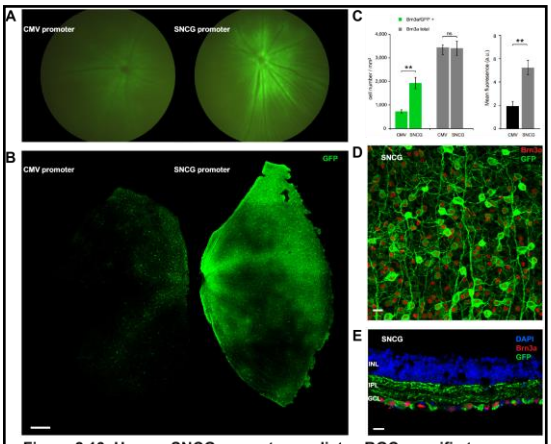


**Figure 2.13. Human SNCG promoter mediates RGC-specific transgene expression with AAV2. (A)** Representative fundus images of *rd1* mouse retinae injected with AAV2.CMV.hCatCh.eGFP or AAV2.hSNCG.hCatCh.eGFP. **(B)** Retinal flat mounts depicting eGFP expression from different vectors. **(C)** Quantification of Brn3a$^{+}$/eGFP$^{+}$ cells per square millimeter between vector treatments. **(D)** Representative confocal stack projection across the RGC layer in an *rd1* mouse retina treated with hSNCG-driven vectors. **(E)** Representative cross of *rd1* mouse retina treated with AAV2.hSNCG.hCatCh.eGFP. Figure adapted from Chaffiol et al., 2017.

vector **(Figure 2.14B)**. The therapeutic utility of this vector is currently being tested within the EAE mouse model.

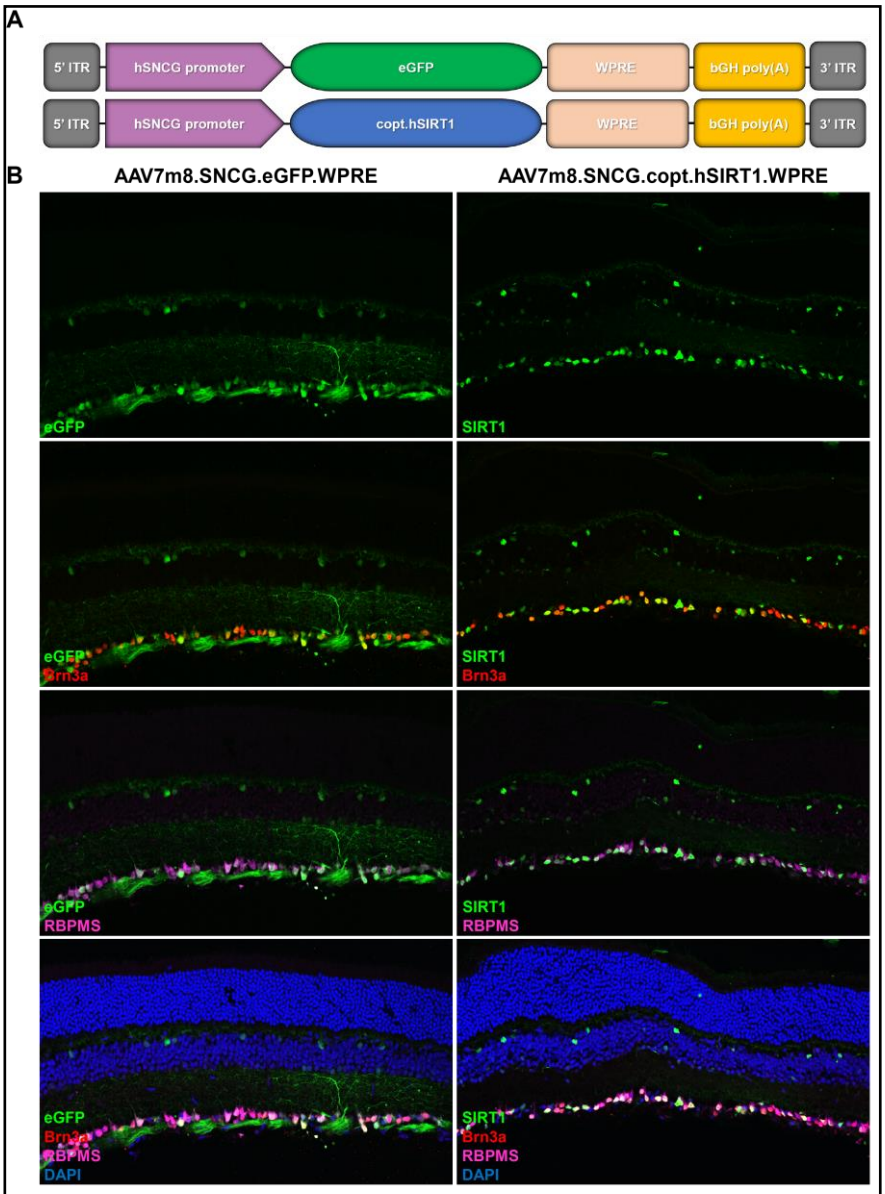


**Figure 2.14. Characterization of AAV7m8 vectors driven by the SNCG promoter. (A)** Outline of vector expression cassettes. **(B)** Vector transduction profile following intravitreal delivery in C56BL/6 mice at $1x10^{10}$ vector genome dose. RGCs are dual labeled with antibodies directed against Brn3a (red) and RBPMS (pink).

## Materials and methods

*Animals*

C57Bl/6J mice were obtained from the Jackson Laboratory and raised in a 12-hour light/dark cycle. Animals were housed at the University of Pennsylvania vivarium in compliance with ARVO guidelines on the care and use of laboratory animals as well as with institutional and federal regulations.

*First generation AAV vector design and production*

Human *SIRT1* (transcript variant 1) and human *NRF2* (transcript variant 1) cDNA clones were obtained from Origene. Sequences were amplified with Q5 DNA polymerase (NEB) and cloned into an AAV expression plasmid using the In-Fusion HD cloning kit (Clonetech). Transgene expression was driven by the CAG promoter cassette derived from pDRIVE-CAG (Invivogen). Both cDNA sequences contained a C-terminal 3xFLAG epitope tag that terminates into a bovine growth hormone (bGH) polyadenylation sequence. AAV expression cassettes were flanked by the AAV2 inverted terminal repeats. A proviral plasmid driving expression of enhanced green fluorescent protein (*eGFP*) was obtained from Dr. Jean Bennett (University of Pennsylvania) and contains identical *cis* regulatory elements. AAV2.NRF2, AAV2.SIRT1, and AAV2.eGFP vectors were generated using previously described methods and purified with CsCl gradient centrifugation by the CAROT research vector core at the University of Pennsylvania[2].

*RGC-specific AAV vector design and production*

The human *SNCG* promoter sequence was obtained from Chaffiol et al. (2017) and synthesized by DNA2.0/ATUM. This sequence was cloned into an AAV proviral plasmid containing the enhanced green fluorescent protein cDNA sequence terminating into a woodchuck hepatitis virus posttranscriptional regulatory element (WPRE) and bovine growth hormone (bGH) polyadenylation signal. The human *SIRT1* cDNA sequence was codon optimized and synthesized

by DNA2.0/ATUM. The sequence was cloned into the SNCG-driven AAV proviral backbone plasmid with the In-Fusion HD cloning system. AAV7m8.SNCG.eGFP.WPRE and AAV7m8.SNCG.copt.SIRT1.WPRE vectors were generated by the CAROT research vector core.

*Cell culture*

ARPE-19 cells were supplied by ATCC (Manassas, VA, USA) and grown at 37$^{o}$C with 5% $CO_2$. Cells were maintained in Dulbecco's modified eagle medium: nutrient mixture F-12 (DMEM/F12; Gibco) and supplemented with 10% fetal bovine serum (FBS) and 1% penicillin-streptomycin. 84-31 cells were provided by Dr. James Wilson (University of Pennsylvania) and were cultured in DMEM-GlutaMax (Gibco) and supplemented with 10% FBS and 1% penicillin-streptomycin. 84-31 cells were seeded at a density of 350,000 cells and transduced with AAV2 vectors at an MOI of 100,000. Cells were harvested for expression analysis at 48 hours post-transduction. For AAV transduction in ARPE-19 cells, 150,000 cells were plated and transduced with AAV2 vectors at an MOI of 100,000. Cells were harvested for expression analysis at 72 hours post-transduction. Cells were rinsed with PBS and fixed in 4% paraformaldehyde for fifteen minutes at room temperature. Afterwards, cells were blocked in 0.1% Triton X-100 and 1% bovine serum albumin (BSA) for 30 minutes at room temperature. Cells were incubated with primary antibody solution containing 1%BSA and rabbit anti-FLAG antibody (CST #14793; 1:200) for 1 hour at room temperature. Cells were washed with PBS and incubated in secondary antibody solution containing 1%BSA and goat anti-rabbit Alexa Fluor-594 antibodies (1:500) for 1 hour at room temperature. Cells were removed from secondary incubation, washed in PBS, and mounted with Fluoromount-G (Southern Biotech) containing DAPI.

*Quantitative real-time PCR (RT-qPCR)*

RNA was isolated from 84-31 cells (provided by Dr. James Wilson) using the Macherey-Nagel Nucleospin RNA kit. First-strand cDNA synthesis was performed using 500 ng of total RNA with the SuperScript III first-strand synthesis system according to manufacturer's protocol. Real-

time PCR was performed with the Applied Biosystems 7500 Fast system using the Power SYBR green PCR master mix (Invitrogen). The following primer sequences were used: 5' CCACTCCTCCACCTTTGAC 3' (human *GAPDH* Forward), 5' ACCCTGTTGCTGTAGCCA 3' (human *GAPDH* Reverse), GAGCTGGGGTGTCTGTTTCA (human *SIRT1* Forward), GGAAGTCTACAGCAAGGCGA (human *SIRT1* Reverse), GTCACATCGAGAGCCCAGTC (human *NRF2* Forward), and AGCTCCTCCCAAACTTGCTC (human *NRF2* Reverse). Relative gene expression was quantified with the $\Delta\Delta C_T$ method and normalized to *GAPDH*.

*Intravitreal injections*

Four week old mice were anesthetized by isoflurane inhalation. A 33 ½ gauge needle was used to create a small incision at the limbus. Afterwards, a ten microliter Hamilton syringe (701 RN, Hamilton Company, Reno, NV, USA) attached to a 33 gauge blunt-end needle was inserted into the vitreous cavity with the needle tip placed directly above the optic nerve head. 1-2 microliters of AAV preparation were dispensed into each eye bilaterally.

*Induction and score of EAE*

Eight week old C57Bl/6 mice were anesthetized by isoflurane inhalation and injected at two sites subcutaneously with 200 micrograms of myelin oligodendrocyte glycoprotein peptide ($MOG_{35-55}$, Genscript, Piscataway, NJ, USA) emulsified in Complete Freund's Adjuvant (CFA; Difco, Detroit, MI, USA) with 2.5 mg/mL mycobacterium tuberculosis (Difco). Control mice that were not induced for EAE were injected with an equal volume of PBS and CFA. All mice were given 200 ng pertussis toxin (List Biological, Campbell, CA, USA) in 0.1 milliliters of PBS by intraperitoneal injection at 0 hours and 48 hours post-immunization with $MOG_{35-55}$. Clinical EAE was assessed using a previously described five-point scale[19]: no disease = 0, partial tail paralysis = 0.5, tail paralysis or waddling gait = 1.0, partial tail paralysis and waddling gait = 1.5, tail paralysis and waddling gait = 2.0, partial limb paralysis = 2.5, paralysis of one limb = 3.0,

paralysis of one limb and partial paralysis of another = 3.5, paralysis of two limbs = 4.0, moribund state = 4.5, death = 5.0.

*Optokinetic response recordings*

Visual function was assessed by measuring the optokinetic response (OKR) using the OptoMotry software and apparatus (Cerebral Mechanics, Inc, Medicine Hat, AB, Canada) as previously described (Prusky et al., 2004; McDougald et al., 2018). OKR was determined as the highest spatial frequency where mice track a 100% contract grating that is projected at different spatial frequencies. Measurements were performed by an investigator masked to the experimental treatments.

*Retinal histology and RGC quantification*

Eyes were harvested and placed in 4% paraformaldehyde (PFA) in phosphate buffered saline (PBS) overnight at 4 degrees celsius. Eyes were washed in PBS followed by dissection of retinal cups. Tissues were permeabilized and blocked in 2% Triton X-100, 10% normal donkey serum, and PBS and then incubated with goat anti-Brn3a antibody (Santa Cruz Biotechnology, Dallas, TX, USA) diluted 1:100 at 4$^{o}$C. Retinal cups were washed and then incubated in secondary antibody solution containing 2% Triton X-100, 10% normal donkey serum, and donkey anti-goat Alexa Fluor 594 antibody (1:500 dilution). After washing, samples were prepared as flatmounts and mounted onto glass slides with Fluoromount-G (Southern Biotech) containing 4',6-diamidino-2-phenylindole (DAPI). RGCs were quantified as previously described[7,19,25,26]. Briefly, retinal micrographs were recorded at 40X magnification in 12 standard fields (1/6, 3/6, and 5/6 of the retinal radius from the center of the retina in each quadrant). Total RGC counts from the 12 fields per retinal sample covering a total area of 0.45mm$^2$/retina were recorded by an investigator masked to the experimental conditions using the ImageJ software. Retinal cross-sections were incubated in blocking buffer containing PBS, 2% Triton X-100, and 10% normal donkey serum for 1 hour at room temperature. Next, sections were incubated in primary antibody solution

containing the previously described components and a rabbit anti-FLAG antibody (CST #14793) at 1:100 dilution overnight in a humidified chamber at room temperature. Sections were washed in PBS three times and incubated in secondary antibody solution containing donkey anti-rabbit Alexa Fluor 488 antibody diluted at 1:200 for two hours at room temperature. Slides were then washed in PBS three times and mounted with Fluoromount-G containing DAPI.

*Optic nerve histology and scoring*

Histologic staining and scoring was performed as in prior studies. Optic nerves were harvested, fixed in 4% PFA, and embedded in paraffin. Nerves were subsequently cut into 5 μm longitudinal sections. To examine immune cell infiltration, sections were stained with hematoxylin and eosin (H&E). Inflammation was scored by an investigator blinded to the experimental treatments, and nerves were graded on a 0-4 point scale: no infiltration = 0, mild cellular infiltration = 1, moderate infiltration = 2, severe infiltration = 3, massive infiltration = 4. Sections were stained with luxol fast blue (LFB) to assess myelination. These sections were graded on a 0-3 point scale: 0 = no demyelination; 1 = scattered foci of demyelination; 2 = prominent foci of demyelination; and 3 = large (confluent) areas of demyelination.

*Statistics*

All data are represented as means ± SEM. Differences between treatment groups with respect to OKR responses, RGC quantification, and optic nerve histopathology were compared using a one-way ANOVA followed by Turkey's honest significant difference test using GraphPad Prism 7.0. Differences were considered statistically significant at $P < 0.05$.

CHAPTER 3 Metabolic reprogramming of photoreceptors in retinitis pigmentosa

*Retinitis pigmentosa: clinical phenotype, genetics, and treatment*

Retinitis pigmentosa (RP) comprises a heterogenous group of photoreceptor degenerative diseases associated with a peripheral-to-central mode of vision loss. The earliest pathological hallmark includes deficits in dim light vision typically beginning in the second decade of life. Loss of night vision is followed by decreased visual fields and advancing tunnel vision. Central vision associated with daylight, color, and high acuity vision deteriorates in later stage disease via the secondary degeneration of cone photoreceptors culminating in a condition of complete blindness by 40-50 years of age (Hartong et al., 2006). Clinical hallmarks can be identified with a fundoscopic evaluation and include abnormal coloration of the optic disc, bony spicule pigmentation, and narrowing of the retinal blood vessels (O'neal et al., 2018) **(Figure 3.1)**. Approximately 1 in 3000-7000 individuals are affected by retinitis pigmentosa on a global scale (Ferrari et al., 2011). Mutations in over 60 known genes are responsible for onset of clinical disease **(Figure 3.2)**. Defects in these genes may be associated with structural deficits and/or a variety of unique cellular functions and pathways including photo-transduction, ciliary transport, or protein trafficking. Pathogenic mutations can be transmitted via autosomal recessive (50-60%), dominant (30-40%), or X-linked

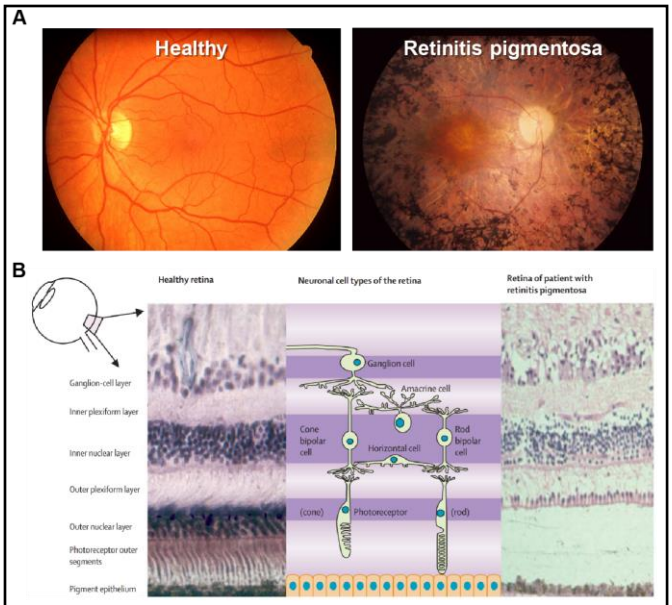


**Figure 3.1. Pathological features of retinitis pigmentosa. (A)** Comparison of fundus images from a healthy patient (left) and an RP patient (right). **(B)** Cross section of a healthy retina (left) compared to a retina with advanced stage RP (right). Figure adapted from Hartong et al., 2006; NEI.NIH.GOV.

(5-15%) inheritance patterns (Hartong et al., 2006). Mutations in the rod phototransduction pigment rhodopsin (*RHO*) account for 20-30 percent of all autosomal dominant forms of RP (Hartong et al., 2006; Ferrari et al., 2011). The vast genetic heterogeneity of this disease is also met with extensive clinical variation. Mutations within the same gene may confer vastly different clinical outcomes. Many of these genes listed in Figure 3.2 are also associated with other forms of inherited retinal degeneration including juvenile macular degeneration (*ABCA4*), cone-rod dystrophy (*CRX)*, and Leber's congenital amaurosis (*CRB1, RPE65*). In addition, defects in many of these genes may also present with extra-ocular clinical symptoms. For example, approximately 20-40% of recessive diseases are associated with Usher's syndrome, which is characterized by retinitis pigmentosa and severe hearing loss due to dysfunction and death of mechanosensory hair cells of the inner ear (Boughman et al., 1984). Bardet-Biedl syndrome (BBS) is a multisystemic, neurodevelopmental disease that may present with retinitis pigmentosa, renal complications, polydactyly, obesity, and cognitive impairment (Weihbrecht et al., 2017). Finally, some RP subtypes manifest via incomplete penetrance further complicating genotype-phenotype correlations (Ferrar et al., 2011).

There are currently no approved treatments to effectively halt or reverse vision loss in RP. Several studies interrogated the effects of dietary supplements in delaying visual decline (Berson et al., 1993; Massof et al., 1993). A randomized trial investigated the protective value of oral vitamin A and/or E in 601 patients aged 18 to 49 suffering from various RP subtypes. Patients that received high dose vitamin A treatment displayed a significantly slower yet modest decline in cone

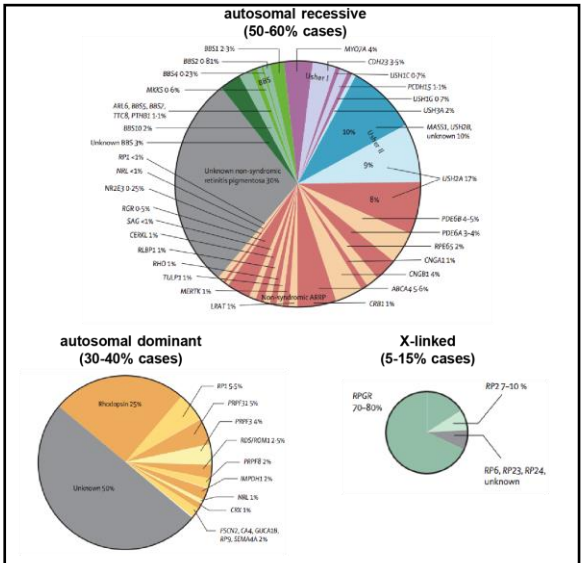


**Figure 3.2. Genetic heterogeneity of retinitis pigmentosa.** Diagrams illustrating the genes and modes of inheritence associated with retinitis pigmentosa. Figure adapted from Hartong et al., 2006.

ERG amplitudes compared to other groups (Berson et al., 1993). However, other outcome measures of visual function including visual field area and visual acuity did not differ between groups in this initial study. Moreover, a recent review of this evidence concluded there is no significant benefit of vitamin A supplementation in impeding disease progression (Rayapudi et al., 2013). Therapeutic strategies currently in development are centered around gene and cell-based treatment platforms. The clinical success and recent FDA and anticipated European Medicines Agency approval of Luxturna provides a framework for the downstream development of gene replacement therapies for other forms of IRD. However, developing a gene therapeutic tailored to each specific RP subtype is met with extensive challenges, as described below.

*Challenges of gene replacement therapy for retinitis pigmentosa*

Although many RP subtypes may be amenable to gene replacement, several challenges impede development of a treatment for all disease manifestations. Foremost, RP is an incredibly genetically heterogeneous collection of diseases. Pathological mutations may be inherited via an autosomal recessive, dominant, or X-linked fashion (Hartong et al., 2006) **(Figure 3.2)**. Therefore, gene augmentation may not be a suitable therapeutic approach for dominant mutations, which in most cases, will require alternative strategies to silence the mutant allele. Moreover, many RP-associated disease genes contain coding sequences that exceed the approximately five kilobase DNA packaging capacity of conventional AAV vectors. However, other vector platforms that can accommodate larger DNA sequences contain significant drawbacks including unstable gene expression patterns, insufficient tropism for photoreceptors and other retinal cell types, heightened immunogenicity, and potential for insertional mutagenesis in the case of integrating vectors (Thomas et al., 2003). Finally, many clinical cases remain undiagnosed with respect to the underlying genetic aberration, further complicating the course of action for therapeutic intervention.

*Conserved mechanisms of photoreceptor degeneration in RP*

The early onset and loss of rod-mediated visual function is characterized by deficits in genes associated with rod photo-transduction and homeostasis, providing a direct explanation for the loss of this photoreceptor subtype. Interestingly, cone photoreceptors which degenerate in later stage disease are typically unaffected by many of these pathogenic mutations. This secondary degenerative event has led to extensive exploration of potential conserved neurodegenerative mechanisms discussed in detail below. Various treatment strategies in

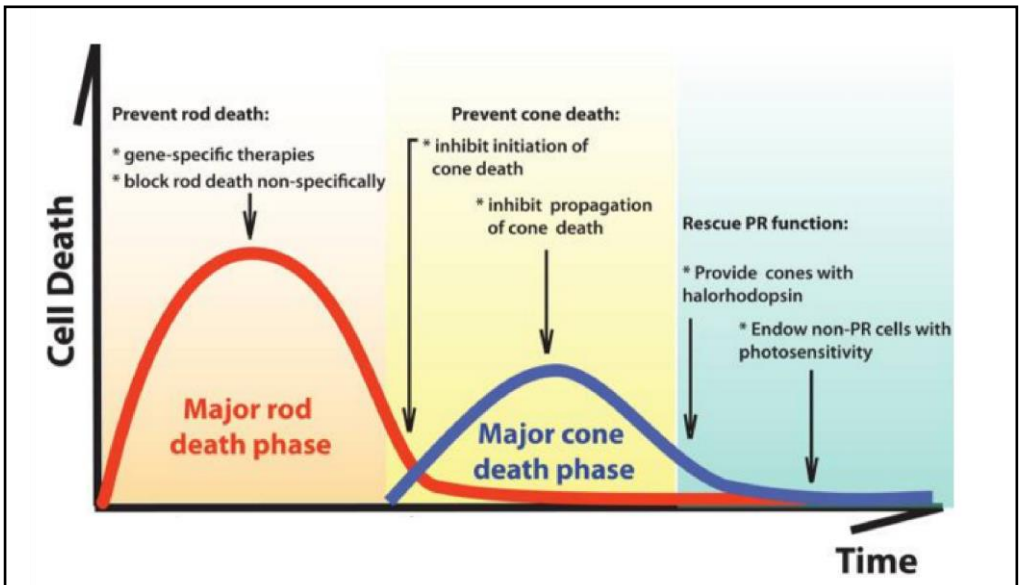


**Figure 3.3. Kinetics of photoreceptor degeneration in RP and therapeutic windows of rescue.** Figure adapted from Punzo et al., 2012.

development aim to preserve retinal function at various therapeutic "windows of rescue" based on the patient's stage of degeneration **(Figure 3.3)**

*Oxidative injury*

Oxidative stress is implicated to play a significant role in RP pathophysiology (Punzo et al., 2012; Shen et al., 2005). The major hypothesis to support this mechanism involves dysregulated oxygen consumption and redox imbalance in the retina following rod death. Rods comprise >90% of the photoreceptor population and consume the vast majority of oxygen delivered to the outer retina via the choroid. Following rod clearance, the remaining cone cells are exposed to an aberrant increase in oxygen levels as the choroid cannot autoregulate the output of oxygen transport to the retina. This hyperoxic environment leads to the generation of ROS within the retina thereby promoting oxidative damage to proteins, lipids, and DNA. Cones may be particularly vulnerable to changes in oxygen content as they contain 2-10 times more mitochondria, which provide an endogenous source of ROS production via mitochondrial respiration, as rod photoreceptors (Hoang et al., 2002; Perkins et al., 2003). Various lines of evidence from animal models and patients support the role of oxygen toxicity in RP pathogenesis. Canonical markers of oxidative stress such as acrolein, 4-hydroxynonenal (HNE), nitrotyrosine, and 8-hydroxy-2'-deoxyguanosine (8-OHdG) are elevated in various animal models of RP (Shen et al., 2005; Trachsel-Moncho et al., 2018; Xiong et al., 2015). Peripheral blood from RP patients revealed heightened levels of lipid

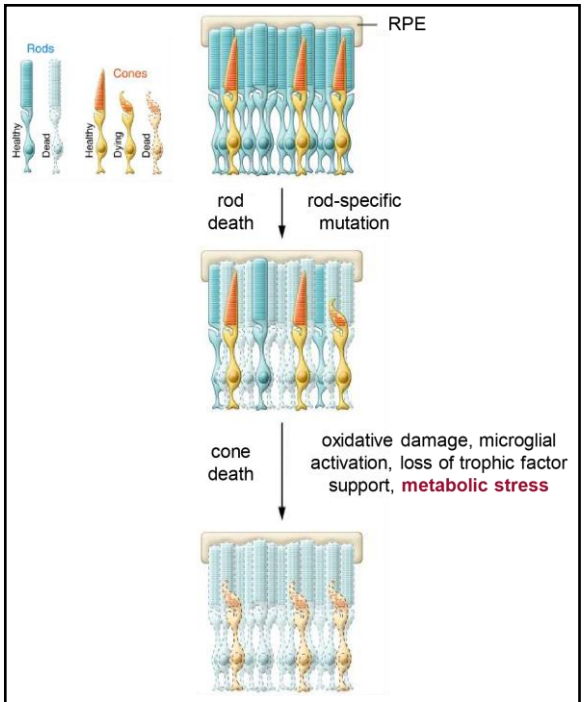


**Figure 3.4. Mechanisms of secondary cone degeneration in RP.** Many RP subtypes are driven by mutations within genes that specifically affect rod function or homeostasis but are not expressed in cones. Several mechanisms are implicated to play a role in degeneration of cones in later stage disease. Figure adapted from Ramachandran et al., 2015.

peroxidation and other markers of oxidative stress compared to healthy controls. In addition, aqueous humor isolated from these patients also demonstrated reduced superoxide dismutase activity and protein concentration (Martinez-Fernandez de la Camara et al., 2013). Administration of pharmacological reagents with antioxidant properties has shown therapeutic efficacy in slowing photoreceptor degeneration in RP models (Komeima et al., 2006; Komeima et al., 2007). Gene augmentation approaches utilizing antioxidant proteins have been shown to slow the course of photoreceptor degeneration in RP models. Overexpression of ROS scavenging enzymes, such as SOD2 or catalase, slowed the course of cone degeneration in RP models (Lu et al., 2009; Usui et al., 2009). Xiong et al. (2015) demonstrated increased cone survival, photoreceptor structure, functional preservation, and reduced markers of oxidative stress across several RP mouse models by overexpressing the antioxidant transcription factor, NRF2. Interestingly, overexpression of PGC-1α, another transcription factor with critical functions associated with oxidative metabolism and mitochondrial function, exacerbated photoreceptor degeneration in these models (Xiong et al., 2015).

*Microglial activation*

Microglial cells (MGCs) are resident macrophages of the nervous system that remain quiescent until activated in response to environmental stimuli such as inflammation and tissue damage. Once active, they serve two primary functions including phagocytosis of neighboring cellular debris and secretion of pro-inflammatory molecules to combat potential infectious agents (Saijo et al., 2011). While this response is intended to be protective in nature, chronic MGC activation can cause unintended cytotoxicity in the context of many neurodegenerative disease states (Cai et al., 2014; Gupta et al., 2003; Lucin et al., 2009; Wang et al., 2013; . Chronic microglial activation is found in many ocular diseases including age-related macular degeneration and retinitis pigmentosa (Gupta et al., 2003). With respect to RP, a decrease in ONL thickness corresponded with increased MGC density and cell numbers consistent between four independent mouse strains (Zhang et al., 2018). Moreover, genetic rescue of rod photoreceptors

in related models successfully halted MGC activation, further highlighting the pathologic contribution of these cells in RP-associated photoreceptor degeneration (Zhang et al., 2018). Furthermore, this evidence also suggests MGC activation as another potential conserved target to delay photoreceptor degeneration.

*Loss of rod-mediated trophic signaling support*

Rod-derived cone viability factor (RdCVF) is encoded by the *Nxnl1* gene and expressed exclusively by rod photoreceptors and bipolar cells in the retina. The pre-mRNA transcript is subject to alternative splicing, yielding two protein isoforms with distinct functions. The longer isoform (RdCVFL) is restricted to the rod cell body and contains an additional thioredoxin-like fold with putative enzymatic function associated with antioxidant capacities (Byrne et al., 2015; Elachouri et al., 2015; Mei et al., 2016). The shorter isoform (RdCVFS) is a secreted protein that exhibits neurotrophic activity upon neighboring cone cells. Direct protein administration or AAV-mediated expression of both isoforms have been evaluated in mouse models of RP. In each system, the short isoform promotes cone viability despite the emergence of physiological insults mediated by rod clearance (Ait-Ali et al., 2015; Byrne et al., 2015). Recent studies identified the mechanism by which RdCVFS exhibits this trophic activity. Ait-ali et al. (2015) identified basigin-1 (BSG1), a transmembrane protein specifically expressed on the surface of photoreceptors, as the receptor for RdCVFS. Using a combination of mass spectrometry and fluorescence resonance energy transfer, these components were shown to form a complex with glucose transporter 1 (GLUT1) on the cone surface. GLUT1 is transmembrane protein associated with insulin-independent, facilitated diffusion of glucose into cells. Interaction between these components theoretically induces a conformational change in GLUT1, thereby enhancing glucose transport into the cone cell (Ait-Ali et al., 2015). The increased glucose uptake and utilization likely provides partial relief from ROS-mediated degeneration and other components of metabolic stress observed in secondary cone degeneration, as described below.

*Nutrient shortage and metabolic stress*

Photoreceptors are among the highest energy consuming cells in the human body (Ames, 2000). Similar to other neuronal populations, they require extensive quantities of ATP to stabilize membrane potential. Unlike other neurons, photoreceptors are constantly growing and recycling a significant portion of their cellular structure. This daily shedding and renewal of the outer segment places a substantial energetic and biosynthetic burden upon the cell. Therefore, photoreceptors must strike a delicate balance in the utilization of nutrients for oxidative phosphorylation to achieve optimal energy production as well as anabolic metabolism to maintain outer segment re-synthesis. Photoreceptors utilize a process known as aerobic glycolysis (or the Warburg effect) to meet these diverse metabolic demands. Aerobic glycolysis is typically observed in highly proliferative cell types, such as cancer cells, and is characterized by the conversion of glucose to lactate in the presence of oxygen (Jones et al., 2015). Under these circumstances, the photoreceptor can transfer glycolytic intermediates into the pentose phosphate pathway to generate precursor molecules for biosynthesis and NADPH, which is an important cofactor in other biosynthetic reactions and antioxidant defense (Jiang et al., 2014). Petit et al. (2018) investigated the importance of aerobic glycolysis within rod and cone cells through cre-mediated depletion of hexokinase 2 (HK2). This enzyme is highly expressed within photoreceptors (Ait-Ali et al., 2015) and is responsible for the conversion of glucose to glucose-6-phosphate as the initial step in glycolysis. Previous investigations suggest HK2 functions as a critical “gatekeeper” of aerobic glycolysis (Wolf et al., 2011). Loss of HK2 did not impact the overall survival and health of rod cells but impaired their function as demonstrated by a ~30% reduction in scotopic a- and b-wave ERG responses compared to control animals. In addition, HK2 ablation exacerbated cone death kinetics in the *Pde6b*$^{rd1}$ mouse of retinitis pigmentosa, thus underlining the critical nature of aerobic glycolysis in cone survival (Petit et al., 2018).

A more recently characterized mechanism of photoreceptor degeneration in RP involves metabolic stress stemming from insufficient nutrient uptake. A seminal report by Punzo et al.

(2009) investigated changes in cone metabolism following rod loss in a panel of RP mouse models varying in their kinetics of photoreceptor degeneration. Irrespective of the mouse strain, cones displayed a global switch in metabolic pathways critical to anabolic metabolism toward mechanisms associated with catabolism and other recycling pathways. Components associated with the insulin/mTOR pathway were particularly downregulated at the onset of cone death. Moreover, these transcriptional changes corresponded with an upregulation in features associated with starvation-induced mechanisms such as chaperone-mediated autophagy and increased expression of glucose transporters and HIF1α. Systemic administration of insulin alleviated cone atrophy in a transient manner, suggesting stimulation of the insulin/mTOR pathway may provide an effective means to improve cone survival in this disease context (Punzo et al., 2009) **(Figure 3.5)**. The exact mechanism by which cones become nutrient deprived is unknown. However, it is hypothesized that loss of rod structural support disrupts nutrient flow from the RPE to the cone cells thus implementing this phenotype (Punzo et al., 2012).

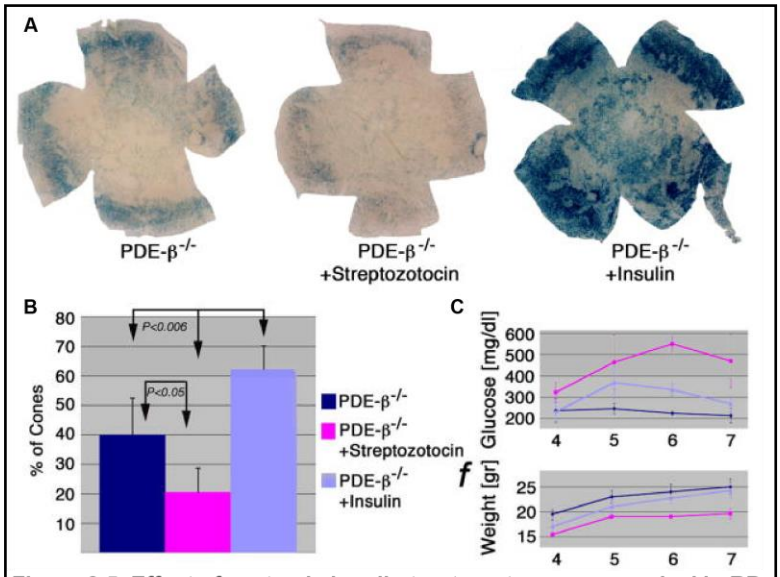


**Figure 3.5. Effect of systemic insulin treatment on cone survival in RP mice. (A)** Representative *Rd1* retinal flat mounts displaying cones stained blue for beta-galactosidase activity following daily injection with streptozotocin (pancreatic beta cell toxin) (middle) or insulin (right) compared to untreated (left). **(B)** Quantification of cone survival between treatment groups. **(C)** Measurement of blood glucose levels and weight performed over the course of the experiment. Figure adapted from Punzo et al., 2009.

*The insulin/AKT/mTOR pathway in ocular health and disease*

The mechanistic target of rapamycin (mTOR) is a serine/threonine kinase that influences numerous aspects of cellular metabolism in response to extracellular signaling events, intracellular energy status, and nutrient availability. It carries out several functions within two distinct complexes. mTOR complex 1 (mTORC1) is composed of five subunits including mTOR, RAPTOR, mLST8, PRAS40, and DEPTOR (Saxton et al. 2017). RAPTOR plays a pivotal role in the recruitment of target proteins through recognition of TOR signaling (TOS) motifs found within downstream substrates (Nojima et al., 2003; Saxton et al., 2017). mLST8 provides structural stabilization and support to the mTOR kinase domain allowing it to effectively phosphorylate target proteins (Saxton et al., 2017; Yang et al., 2013). PRAS40 and DEPTOR promote functions inhibitory to substrate binding and complex activation (Sancak et al., 2007; Saxton et al., 2017; Wang et al., 2007; Peterson et al., 2009). Once active, mTORC1 phosphorylates a variety of protein targets essential for macromolecular synthesis. It enhances protein synthesis through inhibition of eukaryotic translation initiation factor 4E binding protein 1 (4E-BP1) and activation of S6 kinase 1 (S6K1) (Blommaart et al., 1995; Hara et al., 1998). Moreover, mTORC1 also increases lipid biosynthesis through several mechanisms

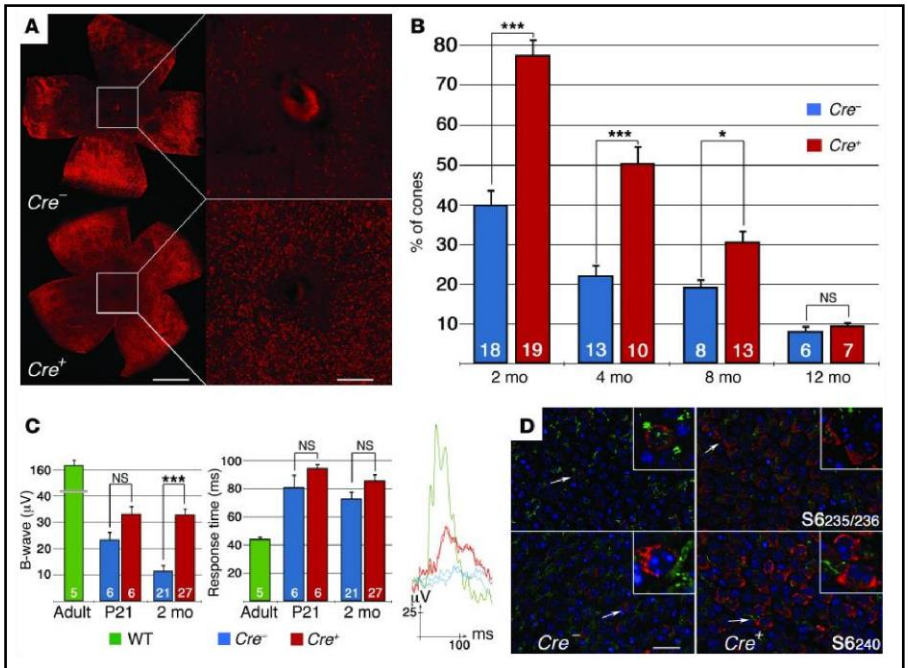


**Figure 3.6. Loss of *Tsc1* (hamartin) improves cone survival and function in RP mice. (A)** Representative *Rd1* retinal flat mounts stained with a cone marker. **(B)** Quantification of cone survival following cre-mediated ablation of *Tsc1* compared to controls. **(C)** Loss of *Tsc1* improves cone-specific ERG responses. **(D)** *Tsc1* ablation activates mTORC1 in RP cones. Figure adapted from Venkatesh et al., 2015.

that converge upon activation of sterol regulatory element binding proteins (SREBPs), which are transcription factors that control lipogenic gene expression (Bakan et al., 2012). Such processes are likely critical for photoreceptor homeostasis as daily shedding and re-synthesis of outer segment membranes requires extensive protein and lipid turnover. mTOR complex 2 (mTORC2) contains six components including mTOR, mLST8, RICTOR, DEPTOR, Proctor1/2, and mSIN1 (Saxton et al., 2017). RICTOR serves a comparable role to RAPTOR in recruitment of mTOR substrates (Sarbassov et al., 2004). DEPTOR serves a regulatory role by inhibiting kinase activity in response to various stimuli. mSIN1 promotes assembly of the complex and mTOR kinase activity (Frias et al., 2006). mTORC2 controls processes associated with cell proliferation and survival. It phosphorylates various members of the protein kinase C (PKC) family which are involved in cytoskeletal remodeling and cell migration (Jacinto et al., 2004; Sarbassov et al., 2004). In addition, mTORC2 regulates cell survival and proliferation through downstream activation of AKT (Saxton et al., 2017).

Downstream investigations provide a more detailed elucidation of the contribution of mTOR in photoreceptor disease and neuroprotection. Venkatesh et al. (2015) utilized a cre-dependent system to conditionally delete upstream suppressors in the mTOR signaling cascade to interrogate the effects upon cone metabolism, survival, and function in various RP mouse lines **(Figure 3.6)**. Similarly, Zhang et al. (2016) investigated the effects of *Tsc1* ablation in the *Pde6b*$^{H620Q/H620Q}$ mouse retina and observed similar neuroprotective features corresponding with mTOR activation. Interestingly, this investigation described beneficial effects upon both cone and rod photoreceptor subtypes, suggesting the putative neuroprotective effects of mTOR stimulation are not limited to cone photoreceptors in RP disease progression. An additional investigation demonstrated enhanced cone survival in the

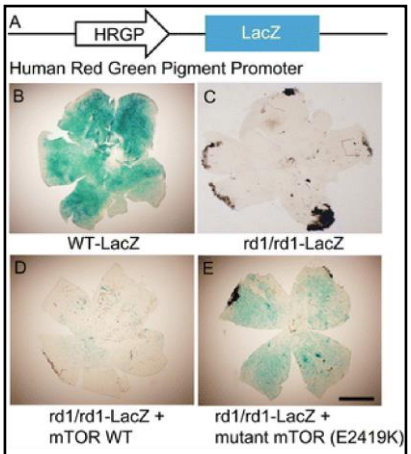


**Figure 3.7. Expression of mutant mTOR increases cone survival in RP mice.** Electroporation of plasmid encoding a constitutively active version of mTOR improves cone survival in Rd1 mice. Cone-specific expression of LacZ labels surviving cells. Figure adapted from Rajala et al., 2018.

*Pde6b*$^{rd1}$ mouse retina following electroporation of a plasmid expressing a constitutively active mTOR mutant (Rajala et al., 2018) **(Figure 3.7)**. Notably, the mTOR cDNA sequence is approximately 7.7 kilobases and thus exceeds the packaging capacity of AAV vectors. Therefore, alternative means are necessary to stimulate mTOR activation with clinically relevant vector systems.

*Approaches to stimulating mTOR signaling activity with AAV-mediated gene augmentation*

I hypothesized that AAV-mediated delivery and augmentation of critical components involved in stimulation of the canonical mTOR signaling cascade could effectively reprogram cellular metabolism and refute cone photoreceptor degeneration in pre-clinical models of RP **(Figure 3.8)**. Prior investigations highlight the therapeutic potential of reprogramming cell metabolism in neurodegenerative disease models by direct stimulation of AKT activity via pharmacological induction or gene augmentation (Isiegas et al., 2016; Ries et al., 2006). Ries et al. (2006) observed neuroprotective value upon dopaminergic neurons in a mouse model of Parkinson's disease following AAV-mediated augmentation of AKT. Downstream studies examined the contribution of AKT overexpression in promoting mTOR activity within retinal cell types.

The AKT family is composed of three isoforms encoded by separate genes including AKT1/PKBα, AKT2/PKBβ, and AKT3/PKBγ. Mice deficient in AKT1 display an impaired growth phenotype, and animals devoid of AKT2 succumb to metabolic disease associated with insulin intolerance (Chen et al., 2001; Cho et al., 2001; Cho & Thorvaldsen et al., 2001) . The role of AKT3 has been much more elusive, but various reports suggest this isoform plays a critical role in neurodevelopment and neuronal homeostasis. Murine knockouts of AKT3 but not AKT1 or AKT2 demonstrate reduced brain and neuron size. Furthermore, AKT3 inactivation decreases downstream stimulation of mTOR signaling components such as p70 S6 kinase in brain tissues suggesting a critical role in controlling this pathway within neurons (Easton et al., 2005). Given the collective evidence supporting the role of AKT3 in stimulation of mTOR signaling within

neurons, I selected this gene as a candidate to reprogram photoreceptor metabolism in retinitis pigmentosa models.

Ras homolog enriched in brain (Rheb) is a small GTPase associated with various cellular activities including protein synthesis, growth, and regeneration. From a mechanistic perspective, many of these processes are driven by the role of Rheb in stimulating mTOR complex 1 (mTORC1). When cellular nutrients and energy are abundant, mTORC1 is recruited to the lysosomal membrane by RAPTOR where it interacts with Rheb (Groenewoud et al., 2013). The exact mechanism in which Rheb activates mTORC1 is not fully understand. However, evidence suggests GTP-bound Rheb induces a conformational change within mTORC1 that activates it allosterically (Yang et al., 2017). Moreover, Rheb demonstrates specific activity to mTORC1 and does not influence the activation of mTORC2 (Sato et al., 2009). Upstream of this process, Rheb activity is predominantly regulated by the tuberous sclerosis complex (TSC1/2). Specifically, tuberin (TSC2) functions as a GTPase activating protein (GAP) towards Rheb, thereby stimulating Rheb to hydrolyze its GTP cargo to GDP (Inoki et al., 2003). Once bound to GDP, Rheb enters an inactive state thereby inhibiting its capacity to stimulate mTORC1.

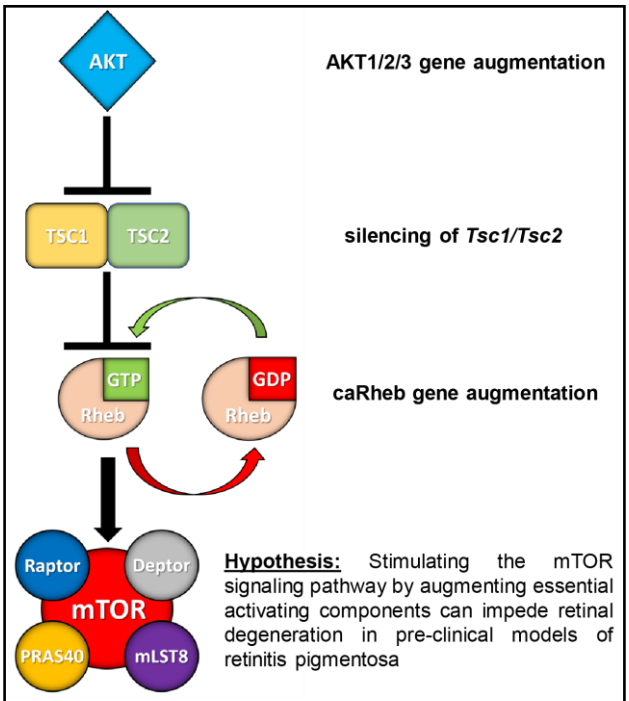


**Figure 3.8. Strategies to stimulate mTOR activation with AAV-mediated gene transfer.** I hypothesized that targeting critical points of the mTOR signaling pathway with a gene transfer approach can delay cone photoreceptor degeneration in animal models of retinitis pigmentosa.

Stimulating mTORC1 activity via caRheb overexpression has demonstrated therapeutic promise in several neurodegenerative disease models. Reinstating mTORC1 activity via this

approach rescues neuropathology and cardiac phenotypes in mouse models of Huntington's disease (Child et al., 2018; Lee et al., 2015). In the context of retinal degenerative disease models, Jeong et al. (2015) reported the ability of Rheb gene transfer to upregulate expression of ciliary neurotrophic factor (CNTF) and its primary cell-surface receptor (CNTFRα) in dopaminergic neurons. Previous studies utilizing AAV-mediated gene augmentation of CNTF demonstrate trophic effects in retinal degenerative disease models (Liang & Aleman et al., 2001; Liang & Dejneka et al., 2001). Therefore, one could surmise the potential of Rheb augmentation to promote photoreceptor neuroprotection via multiple outlets including mTORC1 stimulation and the activation of other pro-survival mechanisms such as those mediated by CNTF/CNTFRα. Based on this collective data, I hypothesized that Rheb gene augmentation would effectively stimulate mTOR activity thereby promoting photoreceptor survival in models of retinitis pigmentosa.

In this study, I investigated the effects of AKT3 or caRheb overexpression in the *Pde6b*$^{rd10}$ mouse model of retinitis pigmentosa. Disease in the *Pde6b*$^{rd10}$ mouse is similar to that in the *Pde6b*$^{rd1}$ mouse model **(Figures 3.5 and 3.7)** except that the progression is slightly delayed (Chang et al., 2002). It contains a missense mutation in exon 13 of the *Pde6b* gene that generates a premature stop codon. This gene encodes the β subunit of the cGMP phosphodiesterase (PDE6) complex, which is an essential component of the rod photo-transduction cascade and which is the same gene responsible for the *Pde6b*$^{rd1}$ phenotype. Under normal circumstances, photon capture by rhodopsin triggers a conformational change in its protein structure allowing it to bind and stimulate the G-protein, transducin. Afterwards, transducin binds the γ-subunit PDE6 downstream signaling cascade in which PDE is responsible for the conversion of cGMP to 5'-GMP. The rapid hydrolysis of cGMP leads to the closure of cGMP-gated cation channels and hyperpolarization of the rod cell. In the case of the *Pde6b*$^{rd10}$ mouse, loss of β subunit activity leads to insufficient closure of these channels and constitutive influx of cations leading to activation of cell death signaling cascades (Wang et al., 2017). Light driven responses measured with electroretinogram (ERG) are severely reduced in these animals and

essentially absent by two months of age. Rod degeneration typically begins around PN16-18 with peak death occurring near PN25 (Gargini et al., 2007).

I assessed the neuroprotective potential of these approaches on visual function, structural morphology, and preservation of photoreceptors. Potential mechanisms of this neuroprotective effect by examining the expression of markers indicative of mTOR activation. In addition, I investigated the long-term safety of these approaches with respect to the potential for oncogenic proliferation of retinal neurons and effects upon other retinal cell types.

## Results

*Design and characterization of mTOR activation vectors*

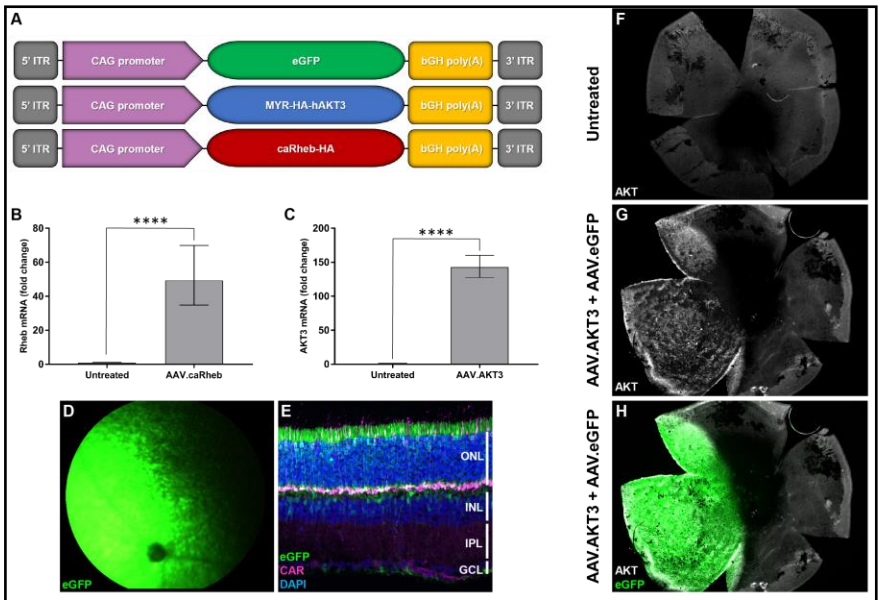


**Figure 3.9. Design and characterization of AAV7m8 vectors. (A)** Outline of vector expression cassettes. Quantification of **(B)** Rheb mRNA and **(C)** AKT3 mRNA expression following vector transduction in 84-31 cells compared to untreated controls. Data represented as mean ± SD (N=3). ****P < 0.0001. **(D)** Representative fundus image of mouse retina following subretinal delivery of AAV7m8.eGFP. **(E)** Retinal tropism of AAV7m8 following subretinal injection. **(F)** AKT expression in untreated *Pde6b*$^{rd10}$ retina. **(G-H)** Co-localization of AKT and eGFP expression from AAV vectors following subretinal delivery.

AAV7m8 is a variant of AAV2 generated through *in vivo* selection and displays enhanced retinal and cellular transduction properties (Dalkara 2013, Khabou 2016). We generated AAV7m8 vectors encoding an enhanced green fluorescent protein reporter (AAV.eGFP), a hyperactive versions of human AKT3 (AAV.AKT3), and a constitutively active Rheb mutant (AAV.caRheb) **(Figure 3.9A)**. The AKT3 transgene contains an N-terminal myristoylation (MYR) sequence, thereby enhancing membrane targeting and localization (McIlhinney, 1998). The Rheb transgene contains the canonical S16H mutation which confers resistance to TSC-mediated GAP activity (Yan et al., 2006). Transduction of 84-31 cells with the AAV.caRheb or AAV.AKT3 vectors displays robust expression of target gene mRNA compared to untreated controls **(Figures 3.9B-C)**. Subretinal delivery of AAV7m8 displays robust labeling of retinal neurons occupying the outer nuclear layer, including photoreceptors and retinal pigment epithelia (RPE) in wild-type animals **(Figures 3.9D-E)**. Likewise, this vector exerts similar effects when administered to the *Pde6b*$^{rd10}$ retina **(Figures 3.9G-H)**. Co-injection with a reporter vector localize specifically to the area of subretinal delivery **(Figures 3.9F-H)** allowing adequate tracing of the treated retinal region.

*caRheb gene transfer fails to attenuate retinal degeneration in the Pde6b$^{rd10}$ mouse*

I investigated the effect of caRheb gene augmentation in the *Pde6b*$^{rd10}$ retina. Animals received subretinal injection of AAV vectors at PN13-14. Visual function was measured with electroretinogram (ERG) and optokinetic response (OKR). Retinal histology was examined at PN45 to determine the effects of AAV.caRheb on photoreceptor survival **(Figure 3.10A-C)**. Quantification of total ONL thickness per retina displayed insignificant preservation of photoreceptors following treatment with AAV.caRheb compared to untreated controls or animals treated with the AAV.eGFP reporter alone **(Figure 3.10B)**. In addition to total ONL thickness, I measured the number of GFP$^{+}$ ONL cells per 200 µm sections of transduced regions in rd10

retina treated with AAV.eGFP alone or in combination with AAV.caRheb. Once again, I did not observe statistically different changes in ONL cell numbers between these treatments **(Figure 3.10C)**. Furthermore, AAV.caRheb did not preserve visual function compared to control treatments as measured with ERG **(Figures 3.10D-F)** and OKR **(Figure 3.10G)**. Collectively, these data suggest caRheb gene transfer does not promote photoreceptor neuroprotection in the *Pde6b*$^{rd10}$ mouse retina.

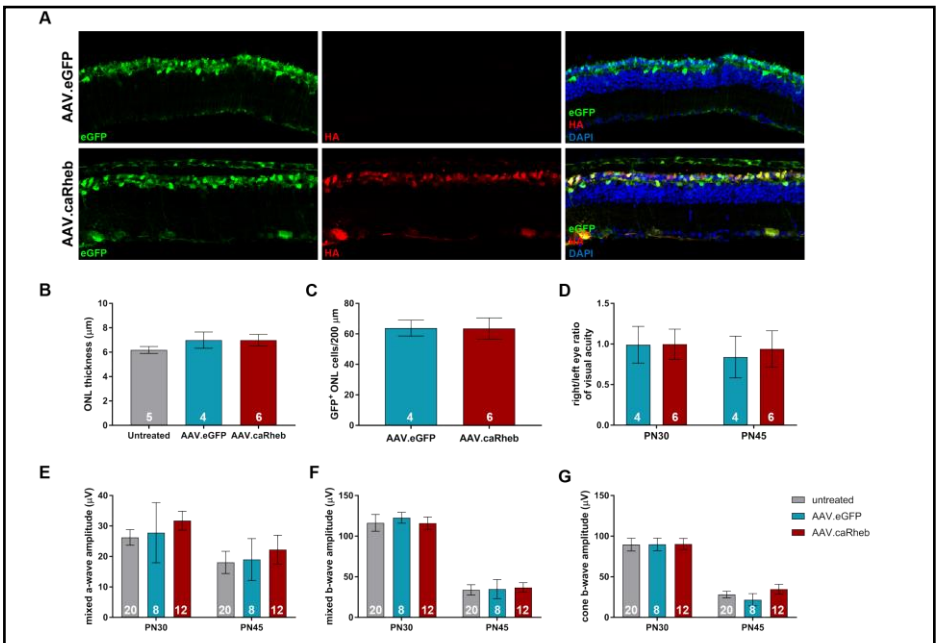


**Figure 3.10. caRheb augmentation fails to attenuate photoreceptor degeneration.** **(A)** Panels depicting *Pde6b*$^{rd10}$ retinal cross-sections at PN45 treated with AAV.eGFP or AAV.caRheb. **(B)** Quantification of total ONL thickness of *Pde6b*$^{rd10}$ retina treated with AAV.eGFP, AAV.caRheb, or remained untreated. **(C)** Quantification of GFP+ ONL cells per 200 μm from eyes treated with AAV.eGFP or AAV.caRheb. **(D)** OKR right/left ratio to assess visual acuity. Electroretinogram (ERG) measurements of the **(E)** mixed rod-cone A-wave amplitude, **(F)** mixed rod-cone B-wave amplitude, and **(G)** cone B-wave amplitude between treatments. Data represent mean ± SEM. Index indicated as the numerical values within the data bars.

Interestingly, the AAV.caRheb vector displays differential effects with respect to mTORC1 activation within a cell-based setting and *in vivo* **(Figure 3.11)**. Transduction of 84-31 cells with the AAV.caRheb vector promotes robust activation of mTORC1 as measured with western blot analysis. Specifically, protein samples derived from cells treated with AAV.caRheb demonstrate enhanced presence of the canonical mTORC1 marker, phosphorylated ribosomal protein S6

(pS6$^{Ser240/244}$) whereas AAV.eGFP and untreated cells do not show such levels. However, following subretinal delivery the AAV.caRheb vector did not display activation of mTORC1 within photoreceptors or other retinal cell types as assayed by immunohistochemical staining for pS6$^{Ser240/244}$ activation marker. These results suggest retinal or photoreceptor-intrinsic mechanisms may inhibit or deter caRheb from activating mTORC1.

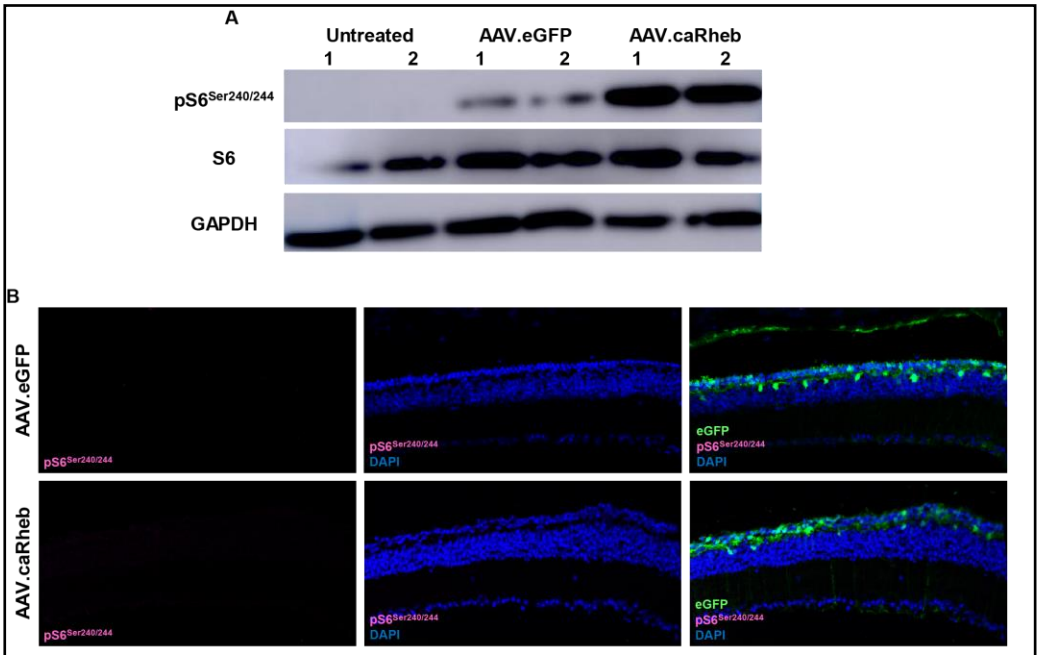


**Figure 3.11. AAV.caRheb stimulates mTORC1 activity in vitro but not in photoreceptors. (A)** Western blot depicting expression of pS6$^{Ser240/244}$, S6, and GAPDH loading control from untreated 84-31 cells or treated with AAV.eGFP or AAV.caRheb. Numerical values indicate biological replicates for each treatment condition. **(B)** Representative micrographs of retinal sections injected with AAV.eGFP alone (top panels) or in combination with AAV.caRheb (bottom panels) and stained with antibodies directed against pS6$^{Ser240/244}$.

*AKT3 gene augmentation promotes photoreceptor survival and structural preservation in the Pde6b$^{rd10}$ retina*

I examined the effect of AKT3 gene augmentation on photoreceptor survival and structural integrity in the *Pde6b$^{rd10}$* retina. Histological analysis of retinal architecture at PN30 and

PN45 revealed a potent neuroprotective effect upon outer nuclear layer cells localized specifically to regions of vector transduction co-labeled with reporter vector fluorescence **(Figures 3.12A-J)**. I observed similar measurements for total ONL thickness in untreated and AAV.GFP injected eyes at PN30. Co-injection of AAV.GFP with AAV.AKT3 provided statistically significant preservation of total ONL thickness compared to control eyes **(Figure 3.12L)**. Furthermore, this neuroprotective effect was sustained in retinal samples harvested at later points in the degenerative process (PN45) **(Figures 3.12K-L)**. In addition to attenuation of cellular numbers, immunostaining with a canonical marker of the cone cell body (CAR) displayed morphological preservation compared to non-transduced retinal regions and control eyes **(Figures 3.12F-J)**. Remarkably, immunostaining for rhodopsin revealed enhanced preservation of rod outer segments at the PN30 harvest point compared to age-matched controls suggesting the importance of this pathway in mediating survival and maintenance of both photoreceptor subtypes **(Figures 3.12A-E)**.

*Effect of AKT3 gene transfer on retinal and visual function in the Pde6b$^{rd10}$ retina.*

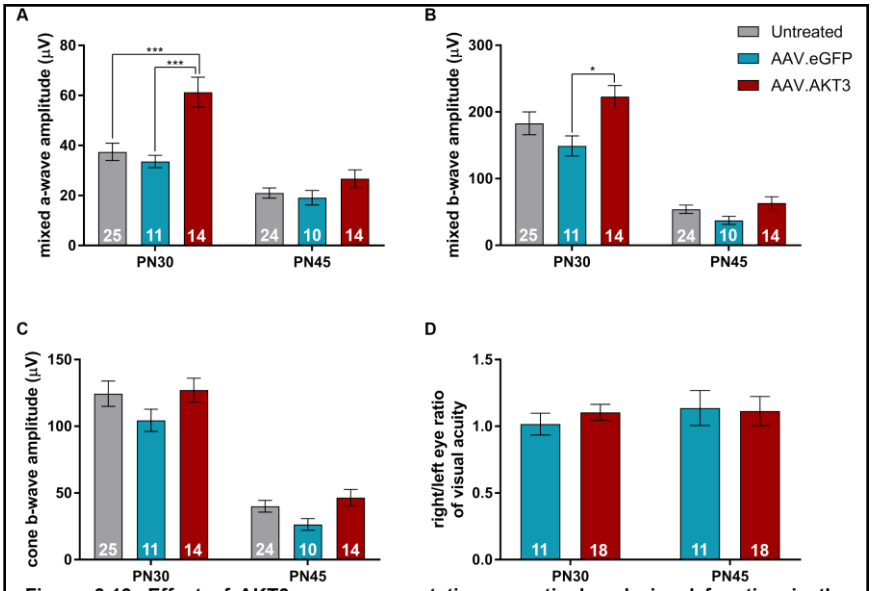


**Figure 3.13. Effect of AKT3 gene augmentation on retinal and visual function in the *Pde6b$^{rd10}$* retina. (A)** Evaluation of mixed rod-cone a-wave amplitudes between untreated, AAV.eGFP, and AAV.AKT3 treated retina. **(B)** Assessment of mixed rod-cone b-wave amplitudes between treatments. **(C)** Photopic (cone) b-wave amplitudes between treatment groups. **(D)** Right/left eye ratio of visual acuity examined by optokinetic response (OKR). Right eyes were treated with AAV.eGFP alone or in combination with AAV.AKT3 while left eyes remained untreated. Data represent mean ± SEM. *$P$ < 0.05; ***$P$ < 0.001. Index indicated by numerical values within bars.

I assessed retinal and visual function at the PN30 and PN45 time points with electroretinography (ERG) and optokinetic response (OKR) measurements, respectively. Combined rod-cone responses from eyes treated subretinally with AAV.AKT3 displayed improved a-wave **(Figure 3.13A)** amplitudes compared to both untreated and AAV.eGFP treated controls at PN30. In addition, eyes treated with AAV.AKT3 also elicited increased mixed b-wave responses **(Figure 3.13B)** compared to the AAV.eGFP treated eyes but not untreated eyes at this time point. However, there were no significant differences between treatment groups at PN45 **(Figures 3.13B)**. We also measured the cone-specific b-wave response but did not observe statistically significant differences between treatment groups at neither time point **(Figure 3.13C)**. We examined visual acuity in response to gene transfer by measuring the optokinetic response (OKR). Data represent the right/left eye ratio of these recordings in which untreated left eyes served as within-animal controls while right eyes were treated with AAV.eGFP alone or in combination with AAV.AKT3. Treatment with AAV.AKT3 did not maintain visual acuity compared to the AAV.eGFP control at PN30 or PN45 **(Figure 3.13D)**. Collectively, this data suggests AKT3 gene augmentation provides some degree of visual preservation during early-mid stage disease but does not retain visual function in later stage degeneration.

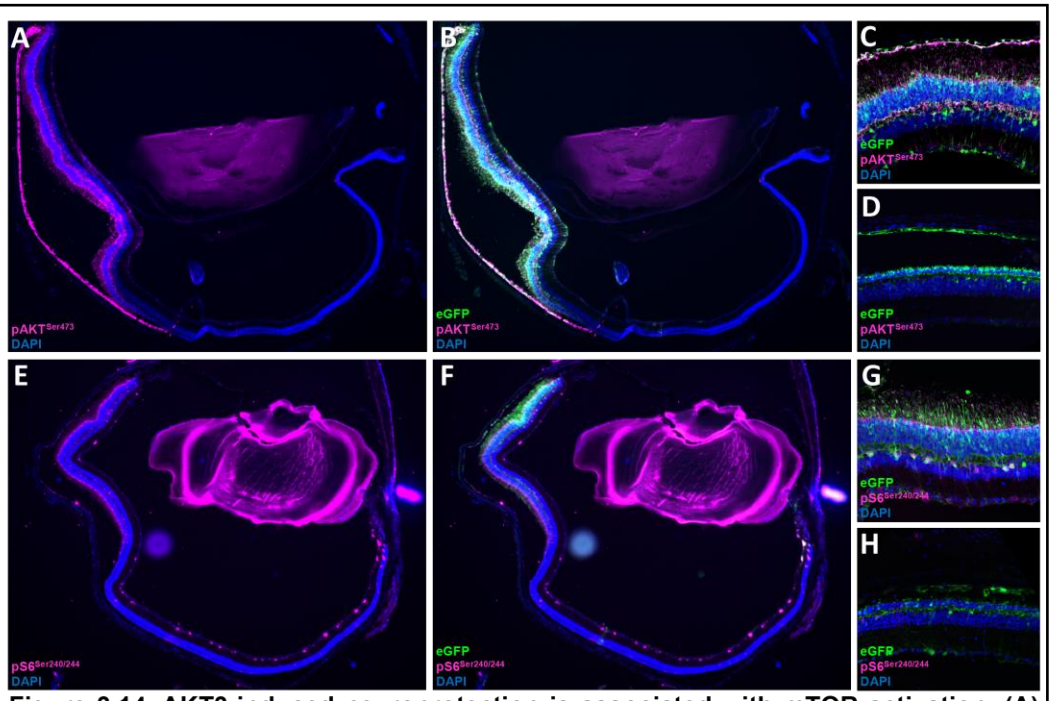


**Figure 3.14. AKT3-induced neuroprotection is associated with mTOR activation. (A)** Representative image of an *Rd10* retina treated with AAV.AKT3 and stained with antibodies directed against the mTORC2 activation marker, phospho-AKT$^{Ser473}$ (pink). **(B)** Co-localization with the eGFP tracer marking the region of subretinal delivery. **(C)** Higher magnification of AAV.AKT3 transduced section stained with mTORC2 marker. **(D)** *Pde6b*$^{rd10}$ retina treated with AAV.eGFP alone and stained with the mTORC2 marker. **(E)** Representative image of a *Pde6b*$^{rd10}$ retina treated with AAV.AKT3 and stained for the canonical mTORC1 activation marker, phospho-S6$^{Ser240/244}$ (pink). **(F)** Co-localization with the eGFP tracer. **(G)** Higher magnification of AAV.AKT3 transduced section stained with mTORC1 marker. **(H)** *Pde6b*$^{rd10}$ retina treated with AAV.eGFP alone and stained with the mTORC1 marker.

Prior investigations underscore the contribution of mTOR in mediating photoreceptor neuroprotection in RP models (Tsang et al., 2014; Venkatesh et al., 2015; Zhang et al., 2016). Likewise, I hypothesized that the AKT3-induced neuroprotective response was affiliated with activation of pathways associated with anabolism and cell survival by immunostaining retinal sections with antibodies directed against canonical downstream markers indicative of mTOR activation **(Figure 3.14)**. Regions of the retina transduced specifically with AAV.AKT3 demonstrate enhanced expression of phosphorylated ribosomal protein S6 (pS6) compared to non-transduced areas and control treatments **(Figures 3.14E-H)**. This finding builds upon previous evidence suggesting the importance of mTORC1 in maintaining photoreceptor

homeostasis in the degenerative retina (Venkatesh et al., 2015; Zhang et al., 2016). Interestingly, I also observed increased expression of an mTORC2 marker (pAKT-S473) within regions specifically exposed to AKT3 gene augmentation, suggesting stimulation of additional functions associated with cell survival and stress resistance **(Figures 3.14A-D)**. Retinal sections obtained from untreated and AAV.GFP control groups did not display enhanced expression of these markers implying the AKT3-induced neuroprotection is, at least, partially driven by such mechanisms **(Figures 3.14D, H)**.

*AKT3 does not breach photoreceptor quiescence but activates müller glia*

Dysregulated AKT signaling is a common hallmark of many human cancers (Altomare et al., 2005). I examined the effect of AKT3 augmentation on retinal quiescence by immunostaining with canonical markers of cellular proliferation. Expression of Ki67 was restricted to cells occupying the ganglion cell layer in untreated *Pde6b*$^{rd10}$ retinas and those treated with AAV.eGFP. Co-staining with antibodies directed against GFAP identified these Ki67$^{+}$ cells as müller glia, which provide support to other retinal cell types through mediating neurotrophic factor release, regulation of extracellular ion balance, and debris scavenging (Goldman, 2014; Reichenbach et al., 2013). Importantly, cells occupying the ONL did not display positive immunoreactivity for the Ki67 marker suggesting the AKT3-induced protective response was not a byproduct of quiescent escape **(Figures 3.15H-I)**. Interestingly, müller cells within regions of the retina specifically transduced with AAV.AKT3 demonstrate morphological changes representative of astrogliosis such as upregulation of GFAP expression and spreading of their processes throughout different cellular layers **(Figures 3.15G-I)**. Immunostaining against PCNA, an additional marker of cell proliferation, did not display reactivity in any of the aforementioned treatment groups (data not shown) providing additional support that AKT3-induced neuroprotective effects are preservative rather than proliferative with respect to photoreceptors.

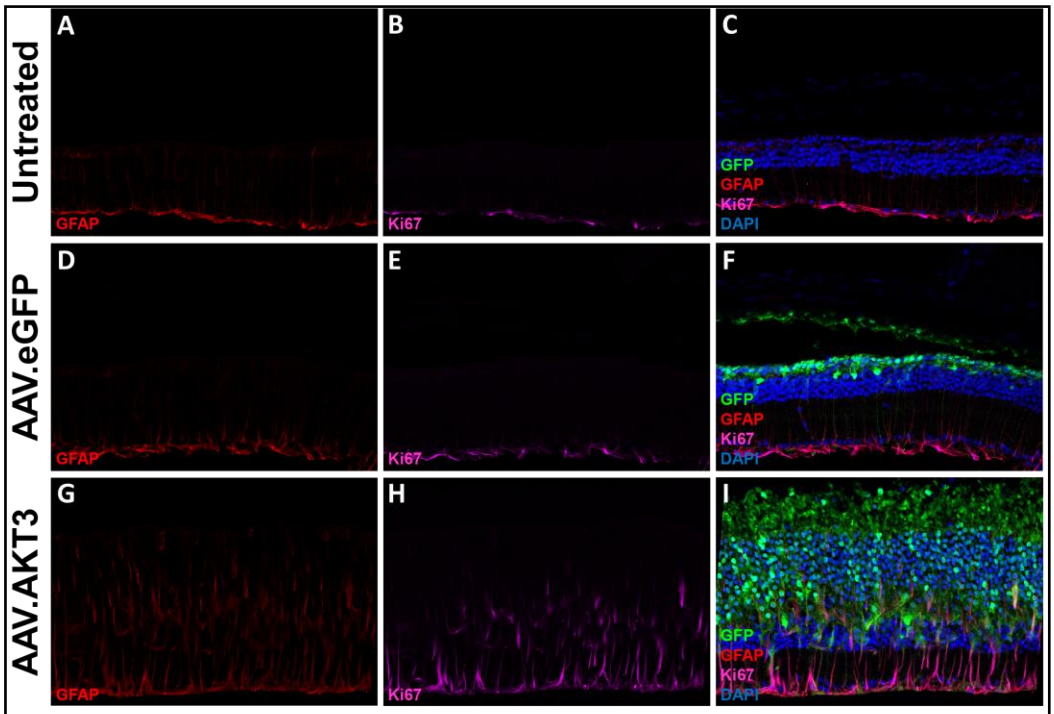


**Figure 3.15. AKT3 overexpression does not breach photoreceptor quiescence but activates muller cells.** Representative images of *Pde6b*$^{rd10}$ retinal cross-sections that are **(A-C)** untreated, **(D-F)** treatment with AAV.eGFP alone, or **(G-I)** co-treatment with AAV.AKT3. Sections are stained with antibodies directed against GFAP (muller cell marker; red) and Ki67 (cell proliferation marker; pink).

*Long-term constitutive AKT3 overexpression leads to retinal disorganization in wild-type animals*.

I examined the effects of long-term AAV.AKT3 overexpression in the C57BL/6 (wild-type) retina. Animals received subretinal injections of AAV.AKT3/AAV.eGFP in one eye and AAV.eGFP in the contralateral eye. Eyes were harvested for histological analysis at PN125. Retinal regions exposed to AAV.AKT3 transduction demonstrate profound disorganization of retinal layers and loss of photoreceptor structure **(Figure 3.16)**. Moreover, these regions once again display an increase in histological markers of reactive gliosis previously observed in *Pde6b*$^{rd10}$ retinal samples **(Figure 3.16G-I)**. Non-transduced regions within the wild-type samples appear phenotypically normal **(Figure 3.16A-C)**. Moreover, eyes that were administered AAV.eGFP alone also show no histological findings suggestive of retinal disorganization or cellular loss **(Figure 3.16D-F, J)**. These results suggest long-term stimulation of anabolic metabolism via

AKT3 overexpression and/or widespread expression through incorporation of a constitutive promoter lead to aberrant changes in retinal structure and homeostasis.

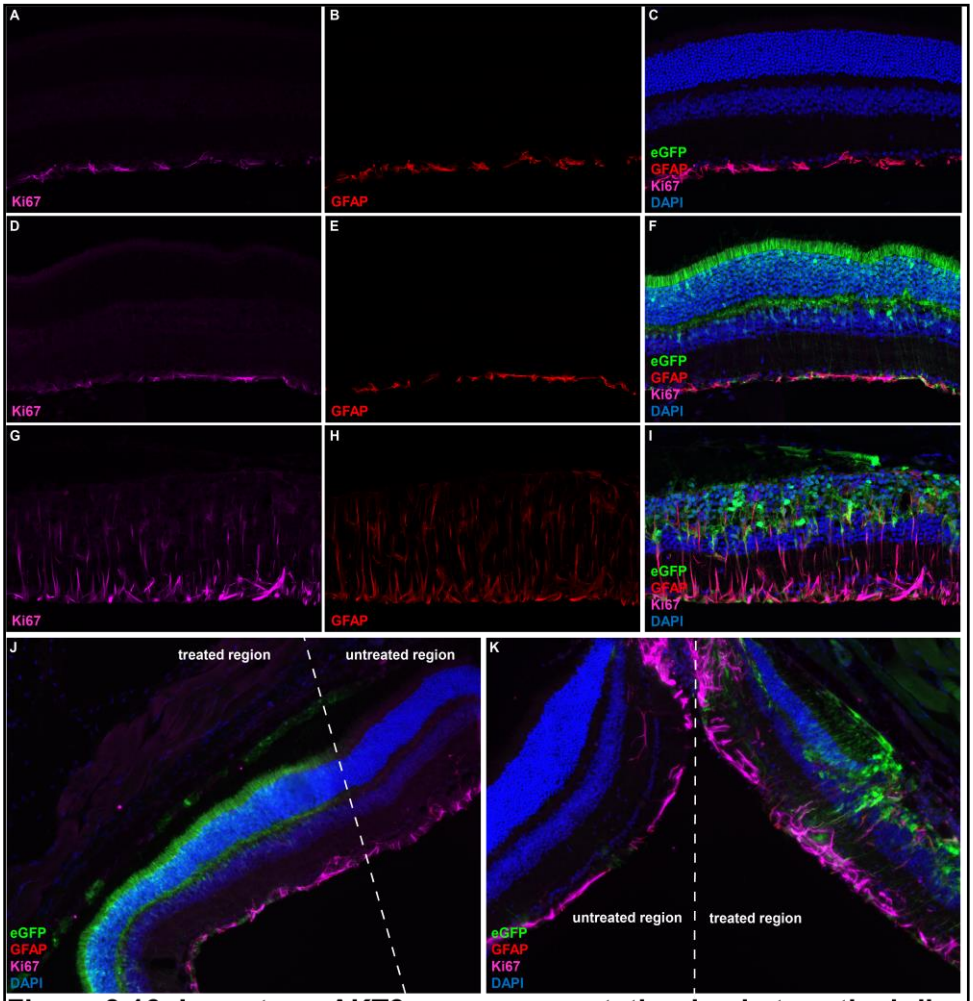


**Figure 3.16. Long-term AKT3 gene augmentation leads to retinal disorganization in wild-type animals.** Representative micrographs of a wild-type retina **(A-C)** untreated, **(D-F)** treated with AAV.eGFP, and **(G-I)** treated with AAV.AKT3/AAV.eGFP at PN125. Sections are stained with antibodies directed against Ki67 (pink) and GFAP (red). **(J)** Transitional zone between untreated and AAV.eGFP treated retinal section. **(K)** Transitional zone between untreated and AAV.AKT3/AAV.eGFP retinal regions.

*Photoreceptor-restricted AKT3 gene augmentation promotes neuroprotection in the Pde6b$^{rd10}$ retina but does not stimulate reactive gliosis*

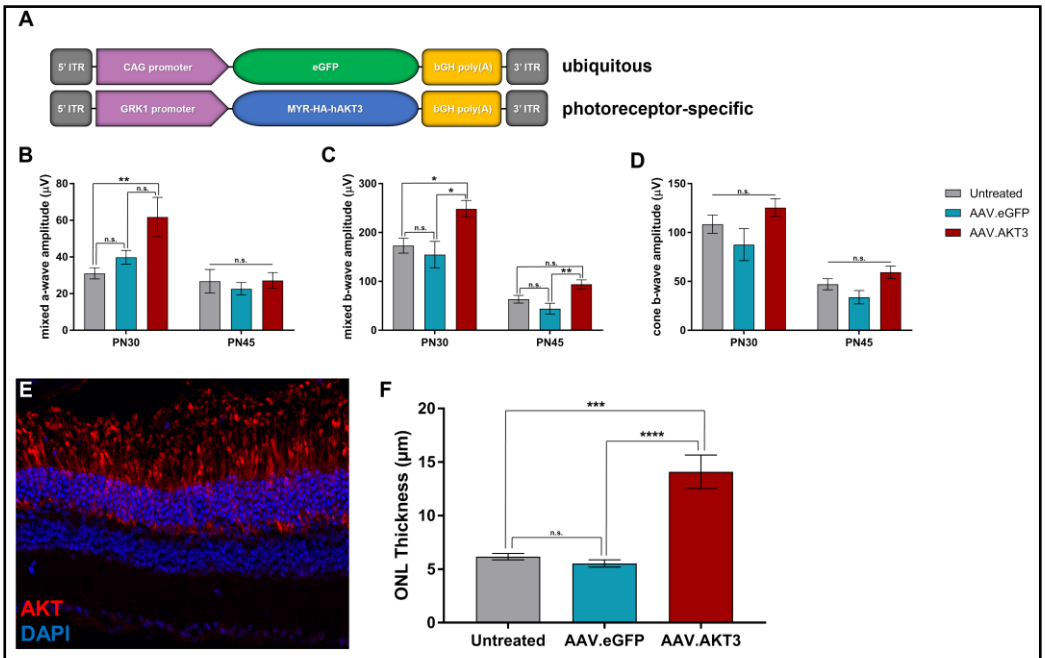


**Figure 3.17. Photoreceptor-specific expression of AKT3 mediates similar neuroprotective effects in the *Pde6b*$^{rd10}$ retina**. **(A)** Outline of vector transgene cassettes used in the experiment. The AKT3 transgene is regulated by the photoreceptor-specific GKR1 promoter. Quantification of ERG responses for the **(B)** mixed a-wave, **(C)** mixed b-wave, and **(D)** cone b-wave between treatment groups. **(E)** Representative cross section of an PN45 Rd10 retina treated with AAV.GRK1.AKT3. Photoreceptor-specific expression of AKT in red. **(F)** Quantification of ONL thickness between treatment groups. Data represented as mean ± SEM. **P*<0.05, ***P*<0.01, ****P*<0.001, *****P*<0.0001.

I hypothesized that photoreceptor-specific augmentation of AKT3 could mediate similar neuroprotective effects as the ubiquitously expressed vector without adverse effects on other retinal cell types. I generated an additional AAV7m8 vector that drives AKT3 transgene expression regulated by the photoreceptor-specific rhodopsin kinase 1 (GRK1) promoter **(Figure 3.17A)**. Subretinal delivery to *Pde6b*$^{rd10}$ animals mediates neuroprotective effects upon photoreceptor structure and function. Immunolabeling retinal sections with antibodies directed against AKT demonstrate specific expression within the photoreceptor layer **(Figure 3.17E)**. Moreover, photoreceptor-specific AKT3 expression led to increased ONL thickness compared to untreated or AAV.eGFP administration alone **(Figure 3.17F)**. Similar to previous findings with the ubiquitous AKT3 vector, photoreceptor-specific AKT3 overexpression mediated preservation of mixed a- and b-wave responses at the PN30 time point. Moreover, this vector was able to

preserve mixed b-wave responses at the PN45 timepoint compared to eyes that received the AAV.eGFP control vector **(Figure 3.17C)**. Similar to the ubiquitous vector, cone-specific responses remained similar between treatment groups **(Figure 3.17D)**. I hypothesized that reactive gliosis stimulated by AKT3 overexpression was attributed to off target gene expression within muller glia and photoreceptor-selective transgene expression of AKT3 would not stimulate glial activation and deter this cellular phenotype. *Pde6b*$^{rd10}$ retinas treated with AAV.GRK1.AKT3 were stained with antibodies directed against GFAP (muller cell marker) and Ki67 (proliferative marker). Untreated and AAV.GRK1.AKT3 regions of the retina display similar qualitative findings with respect to muller glial activity, supporting the role of ubiquitous AKT3 gene transfer in stimulating reactive gliosis. Thus, incorporation of the photoreceptor-specific promoter confers both safety and efficacy, at least through the 45 day time point **(Figure 3.18)**.

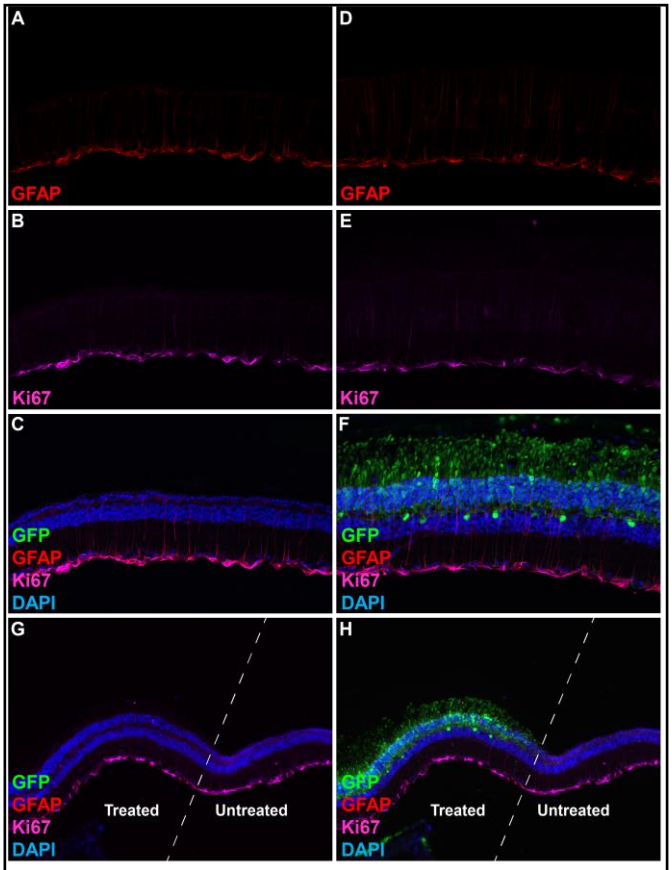


**Figure 3.18. AAV.GRK1.AKT3 does not stimulate reactive gliosis in the *Pde6b*$^{rd10}$ retina.** **(A-C)** Representative images of an untreated mouse retina at PN45 stained with canonical markers for muller cells (GFAP) and proliferation (Ki67). **(D-F)** Micrographs of a PN45 *Rd10* retina treated with AAV.GRK1.AKT3. **(G)** Transitional region between untreated and treated portions of the *Rd10* retina and **(H)** co-localized with the eGFP tracer.

## Methods

### *Animals*

C57Bl/6 and *Pde6b*$^{rd10}$ mice were obtained from the Jackson Laboratory and raised in a 12-hour light/dark cycle. Animals were housed at the University of Pennsylvania vivarium in compliance with ARVO guidelines on the care and use of laboratory animals as well as with institutional and federal regulations.

### *AAV vectors*

A plasmid encoding the human *AKT3* cDNA sequence containing N-terminal myristoylation (MYR) and HA tags was kindly provided by William Sellers (addgene plasmid #9017). The MYR-HA-hAKT3 sequence was amplified and cloned into an AAV proviral expression plasmid using the In-Fusion HD cloning system (Clonetech). The human Rheb cDNA clone was obtained from Origene. Inverse PCR mutagenesis was employed to create the S16H mutation with the following primer sequences: 5' [phospho] CACGTGGGGAAATCCTCATTGAC 3' (S16H Forward) and 5' CCGGTAGCCCAGGAT 3'. For production of viral vectors, the helper plasmid expressing AAV7m8 *Cap* was kindly provided by John Flannery and David Schaffer (addgene plasmid #64839). AAV7m8-AKT3 and AAV7m8-eGFP vectors were generated using previously described methods (Ramachandran et al., 2017) and purified with CsCl gradient by the Center for Advanced Retinal and Ocular Therapeutics (CAROT) research vector core (University of Pennsylvania, PA, USA).

### *Cell culture*

84-31 cells were kindly provided by Dr. James Wilson (University of Pennsylvania) and were cultured in DMEM-GlutaMax supplemented with 10% FBS and 1% penicillin-streptomycin. For AAV transductions, 84-31 cells were plated at a density of $2.5x10^5$ cells/well in a 6-well dish.

Afterwards, cells were immediately transduced with AAV7m8 vectors at $1x10^6$ multiplicity of infection (MOI). Cells were maintained at 37°C with 5% $CO_2$.

*RNA isolation and RT-qPCR*

RNA was isolated from 84-31 cells using the Macherey-Nagel Nucleospin RNA kit. First-strand cDNA synthesis was performed using 500 ng of total RNA with the SuperScript III first-strand synthesis system according to manufacturer's protocol. Real-time PCR was performed with the Applied Biosystems 7500 Fast system using the Power SYBR green PCR master mix (Invitrogen). The following primer sequences were used: 5' CCACTCCTCCACCTTTGAC 3' (human *GAPDH* Forward), 5' ACCCTGTTGCTGTAGCCA 3' (human *GAPDH* Reverse), 5' ACTCCTACGATCCAACCATAGA 3' (human *Rheb* Forward), 5' TGGAGTATGTCTGAGGAAAGATAGA 3' (human *Rheb* Reverse), 5' AGGATGGTATGGACTGCATGG 3' (human *AKT3* Forward), and 5' GTCCACTTGCAGAGTAGGAAAA 3' (human *AKT3* Reverse). Relative gene expression was quantified with the $\Delta\Delta C_T$ method and normalized to *GAPDH*.

*Subretinal Injections*

Subretinal injections were performed as previously described (Dooley et al., 2018). Each retina received 1 uL of vector preparation. Eyes injected with AAV.eGFP received $2x10^9$ total vector genomes. Eyes that were co-injected with AAV.eGFP plus AAV.AKT3 or AAV.caRheb were dosed with $1x10^9$ vector genomes per vector to achieve $2x10^9$ total vector genomes.

*Electroretinogram*

Mice were anesthetized and maintained as previously described. Pupils were dilated with 1% tropicamide (Alcon Laboratories, Fort Worth, TX). Clear plastic contact lenses with embedded platinum wires were used to record light responses, and a platinum wire loop was placed into the animal's mouth to serve as a reference electrode. ERGs were recorded with the Espion E2

system (Diagnosys, Lowell, MA). Three ERG responses were recorded with the following parameters: scotopic response (dark adaption, 0.01 scot cd s $m^{-2}$ stimulus), maximum rod-cone response (dark adaptation, 500 scot cd s $m^{-2}$ stimulus), maximum cone response (30 scot cd $m^{-2}$ adapting steady background light, 500 scot cd s $m^{-2}$ stimulus).

*Optokinetic Response*

Visual acuity was assessed by measuring the optokinetic response (OKR) using the OptoMotry software and apparatus (Cerebral Mechanics, Inc, Medicine Hat, AB, Canada) as previously described (Prusky et al., 2004). Recordings were performed by an investigator blinded to the ocular treatments.

*Immunohistochemistry*

Eyes were enucleated, harvested, and prepared as frozen sections as previously described (Dooley et al., 2018). Sections were incubated in blocking buffer containing PBS, 10% normal goat serum (CST), and 2% Triton X-100 for one hour at room temperature. Afterwards, sections were incubated in primary antibody solution overnight in a humidified chamber containing the previously described components and combinations of the following antibodies: rabbit anti-cone arrestin (1:400; Millipore #ab15282), rabbit anti-phospho-S6-Ser240/244 (1:100; CST #5364), rabbit anti-phospho-AKT-Ser273 (1:100; CST #4060), mouse anti-rhodopsin (1:400; Abcam #ab5417), rabbit anti-HA (1:100; CST #3724), rabbit anti-Ki67 (1:400; Abcam #ab15580), mouse anti-PCNA (1:400; Abcam #ab29), chicken anti-GFAP (1:400; Abcam #ab4674), rabbit anti-AKT (1:100; CST #4691). Following primary antibody incubation, sections were washed three times with PBS and incubated in secondary antibody solution for 2 hours at room temperature in a humidified chamber containing PBS, 10% normal goat serum, 2% Triton X-100, and combination of the following secondary antibodies: alexa fluor-594 goat anti-chicken (1:500; Abcam #ab150176), alexa fluor-594 goat anti-mouse (1:500; #ab150116), alexa fluor-594 goat anti-rabbit (1:500; Abcam #ab150080), Cy5-conjugated goat anti-rabbit (1:500; KPL #072-02-15-

16). Sections were removed from secondary antibody incubation and washed three times with PBS. Sections stained for the presence of phosphorylated antigens were incubated and washed in solutions containing TBS instead of PBS.

*ONL measurements*

Whole retinal sections were tiled using a 40X objective with the EVOS FL Auto 2 cell imaging system. In each image, ONL thickness was measured at three equidistant points spaced 75-100 µm apart. These measurements were averaged between all images to represent the average ONL thickness of the section. Three retinal sections were averaged per sample. ONL numbers from specific regions of the retina transduced with vector were quantified by counting the number of $GFP^+$ ONL cells per a 200 µm area. Once again, three retinal sections were averaged per sample to acquire these measurements.

*Western blotting*

Protein samples were separated with the NuPage electrophoresis system (Thermo Fisher). Samples were heated at 70$^o$C and loaded onto 4-12% Bis-Tris protein gels (Thermo Fisher). Separated proteins were then transferred to a PVDF membrane with the XCell II blot module (Thermo Fisher) at 35 volts for 1.5 hours. Following protein transfer, membranes were incubated in tris-buffered saline containing 0.1% (v/v) Tween 20 (BioRad) (TBST) and 5% (w/v) bovine serum albumin (BSA; Sigma-Aldrich) for 1 hour at room temperature. Afterwards, blots were incubated in the previously described solution containing the following primary antibodies: rabbit anti-phospho-S6-Ser240/244 (1:1000; CST #5364), rabbit anti-S6 (1:1000; CST #2217), rabbit anti-GAPDH (1:1000; CST #5174). Primary antibody incubation occurred overnight at 4$^o$C. Blots were removed from primary antibody solution and washed three times in TBST for 5 minutes each. Afterwards, they were placed in secondary antibody solution composed of TBST, 5% BSA, and HRP-conjugated anti-rabbit ECL (1:10,000; GE Healthcare) for 1 hour at room temperature. Membranes were washed three times in TBST followed by incubation with ECL2

(Thermo Fisher) according to manufacturer's instructions for 5 minutes. Finally, membranes were imaged using the Amersham Imager 600 (GE Healthcare) with chemiluminescence settings.

*Statistics*

All data are represented as means ± SEM unless otherwise indicated. Differences between two treatment groups were compared using an unpaired student's t-test. Differences between three or more experimental groups were compared using a one-way ANOVA followed by Turkey's honest significant difference test. Calculations for statistical significance were determined using GraphPad Prism 7.0. Differences were considered statistically significant at $P < 0.05$

# CHAPTER 4 CRISPR/Cas9 activation enhances *in vitro* potency of AAV vectors regulated by tissue-specific promoters

*Cell-based potency assays for drug development and approval*

Potency of a drug product is defined as the biological activity directly related to a clinical endpoint. The US Food and Drug Administration (FDA) requires a validated potency assay prior to the release of a new drug to ensure its identity, purity, and stability (. Furthermore, potency assays should encompass features that enable a quantitative measurement of biological activity that is specific to the intended function of the product. Assay parameters can be designed to interrogate functional features of the product within animal models or cell-based systems. However, cell-based potency assays are highly preferred due to the greater time, resources, variability, and ethical considerations often associated with animal use (FDA).

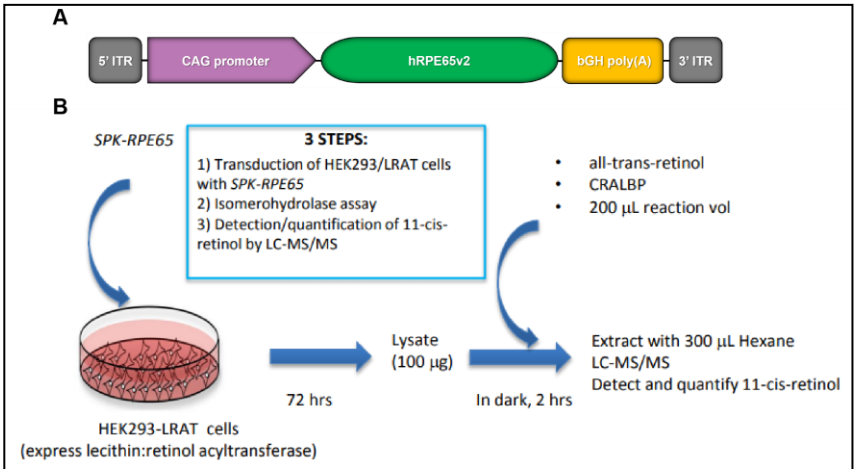


**Figure 4.1. Cell-based potency assay for SPK-RPE65 (Luxturna). (A)** SPK-RPE65 expression cassette packaged within AAV2. **(B)** Outline of potency assay in HEK-293-LRAT cells to detect and quantify the outcome measure, 11-cis-retinol. Figure adapted from Couto et al., 2016.

Viral vectors occupy a unique space in drug development as these are highly sophisticated biological particles composed of protein and nucleic acid components. Their structural and functional complexity presents a variety of challenges in the design and implementation of potency assays for specific disease targets. **Figure 4.1** depicts the cell-based potency assay developed for Luxturna, which is an AAV2-based therapy for vision loss associated with *RPE65* mutations. The vector expression cassette encodes a codon-optimized version of the human *RPE65* cDNA driven by

the ubiquitous CAG promoter **(Figure 4.1A)**. Cell lysates are derived from transduction of HEK293 cells that constitutively express LRAT (lecithin retinol acyltransferase). Afterwards, lysates are incubated in the presence of all-trans-retinol and CRALBP to reconstitute a portion of the visual cycle and generate of the desired outcome measure, 11-cis-retinol. Constitutively expressed LRAT converts the all-trans-retinol substrate to all-trans-retinyl-ester. Afterwards, the RPE65 protein provided *in trans* by the AAV expression cassette stimulate the conversion of all-trans-retinyl-ester to 11-cis-retinol, which is detected by liquid chromatography with tandem mass spectrometry (LC-MS/MS) **(Figure 4.1B)**. Features associated with the AAV serotype and expression cassette are favorable. Foremost, HEK293 cells are readily infected by the AAV2 capsid. In addition, transgene expression is driven by a highly active ubiquitous promoter, thereby providing substantial levels of RPE65 protein to carry out the desired enzymatic activities of the

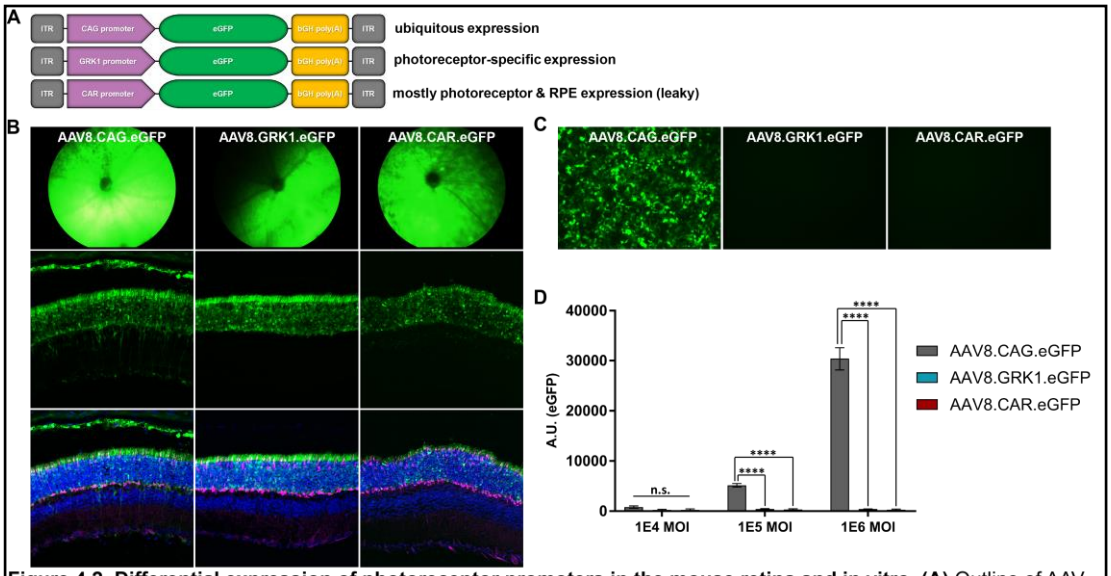


**Figure 4.2. Differential expression of photoreceptor promoters in the mouse retina and in vitro. (A)** Outline of AAV reporter cassettes driven by ubiquitous or photoreceptor promoters. **(B)** Representative fundus and retinal cross-section images of wild-type mouse retina following subretinal injection of AAV8 reporter vectors. **(C)** Representative micrographs of 84-31 cells transduced with different AAV8 vectors at 1E6 multiplicity of infection (MOI). **(D)** AAV8 reporter expression quantified after treatment with three different MOIs 48 hours post-transduction. Data represent mean ± SEM (N=3). ****$P$<0.0001.

functional assay.

In addition to capsid limitations, another a major challenge concerns the selection of tissue or cell-specific regulatory elements to control transgene expression. In many cases, these promoters provide specificity and robust levels of expression *in vivo* but display relatively poor

activity when applied to *in vitro* systems. In the context of retinal gene transfer, several promoter sequences enable selective and stable gene expression patterns in specific neuronal populations such as photoreceptors (Chaffiol et al., 2017; Flannery et al., 1997; Hanlon et al., 2017; Khani et al., 2017). AAV vectors driven by such regulatory elements are expected to demonstrate robust safety and efficacy profiles in pre-clinical models of inherited retinal degeneration, underscoring their translational potential and continued development for clinical application (Boye et al., 2013; Boye et al., 2015; Petersen-Jones et al., 2018). However, these elements display exceptionally poor and often times undetectable activity when applied to *in vitro* systems **(Figure 4.2C-D)** thereby impeding their use in cell-based potency assays.

*CRISPR/Cas9 and genome editing*

Recent developments surrounding gene editing technologies such as CRISPR/Cas9 provide a powerful means to create simple, rapid, and precise modifications to genomic DNA sequences (Cong et al., 2013; Jinek et al., 2013). The canonical system is composed of two components. Cas9 is an RNA-guided DNA endonuclease derived from various bacterial species with *Streptococcus pyogenes* Cas9 (SpCas9) being the most well characterized and extensively utilized variant to date **(Figure 4.3)**. The guide RNA (sgRNA) is a small RNA molecule composed of a conserved scaffold sequence important for binding to Cas9 and another approximately 20 basepair sequence that contains homology to the genomic target sequence of interest. The target sequence must contain a trinucleotide sequence, 5'-NGG-3', termed the protospacer adjacent motif (PAM). The presence of the PAM sequence allows Cas9 to destabilize the double-stranded DNA helix and promote binding of the sgRNA to its homologous genomic

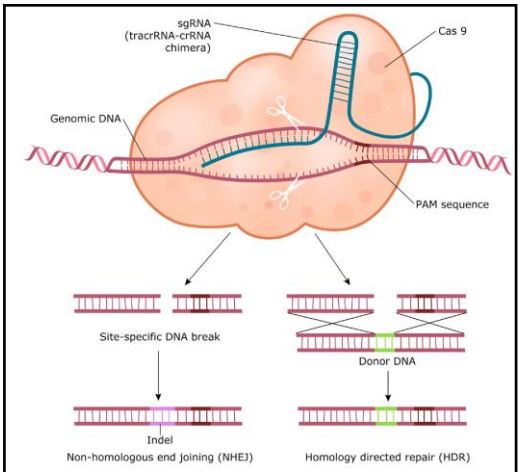


**Figure 4.3. Overview of CRISPR/Cas9 genome engineering.** Canonical systems utilize *S. pyogenes* Cas9 and an sgRNA sequence to induce double-stranded DNA breaks at target loci. Faulty DNA repair via NHEJ can lead to the formation of indels with the possibility of disrupting the open reading frame. Inclusion of a donor template with homologous sites flanking the DNA break to lead to gene knock-in via HDR. Figure adapted from Savic et al., 2016.

sequence. If these sequences form a successful RNA:DNA duplex, the nuclease domain of the Cas9 will mediate a double-stranded cut in the target sequence a few basepairs upstream of the PAM recognition site. The presence of a double-stranded break (DSB) elicits components of the DNA damage response. Breaks are typically resolved through the nonhomologous end joining (NHEJ) repair pathway. This process does not retain sequence fidelity and leads to the random insertions or deletions of nucleotides (indels) at the break site, thereby potentially generating a termination codon within the open reading frame and disrupting gene function (Brinkman et al., 2018). This mechanism is used extensively to generate gene-specific knockouts within human cells for numerous biological applications including disease modeling, pathway interrogation, and screening of drug targets (Dow, 2015; Kurata et al., 2017; Shalem et al., 2014). Beyond NHEJ, site-directed knock-in of a donor template can be achieved utilizing the homology directed repair (HDR) pathway. This requires inclusion of a donor template sequence flanked by sites that are homologous to the DSB region (Brinkman et al., 2018). Gene transfer strategies utilizing HDR-associated gene knock-in were shown to improve phenotypic outcomes in a mouse model of ornithine transcarbamylase (OTC) deficiency (Yang et al., 2016).

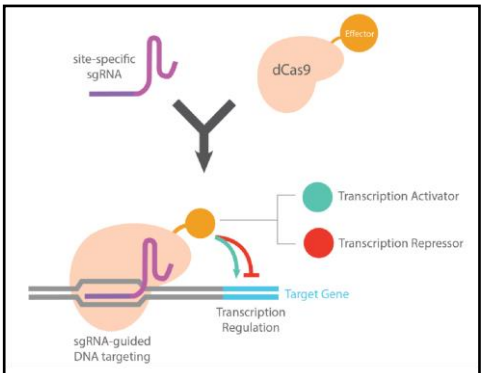


**Figure 4.4. Targeted transcriptional regulation with dCas9.** Mutation of key residues within Cas9 can render it catalytically inactive (dCas9) but retain DNA binding capacity. Fusion of transcriptional effectors to the C-terminus of dCas9 allows precise modulation of gene expression at target loci. Various effector domains allow activation, repression, or epigenetic remodeling of gene activity. Figure adapted from abmgood.com.

*Genome engineering with targeted transcriptional effectors*

In addition to gene editing, more recently described systems have employed catalytically inactive variants of Cas9 (dCas9) tethered to effector domains for enabling selective regulation of transcriptional activity **(Figure 4.4)**. Inactivation of Cas9 catalytic activity is achieved by mutating two amino acids critical to endonuclease function (Qi et al., 2013). While these mutations successfully ablate nuclease activity, Cas9 still retains all functions with respect to DNA binding

and recognition. Based on this core platform, numerous approaches have been described to achieve various modalities of gene regulation including activation, repression, or epigenetic remodeling (Kabadi et al., 2014; Perez-Pinera et al., 2013; Qi et al., 2013). Qi et al. (2013) were the first to report the utility of dCas9-mediated transcriptional regulation and elucidated the ability of dCas9 to repress gene expression by blocking RNA polymerase (RNAP) binding during transcriptional elongation. Perez-Pinera et al. (2013) developed an approach to stimulate gene expression from target genes by fusing dCas9 to the canonical VP64 transactivation domain derived from Herpes simplex virus. Such systems have improved our fundamental understanding of gene function through incredibly rapid, specific, and high-throughput genetic screening methods that utilize dCas9-mediated gene repression (Bak et al., 2017; Zheng et al., 2018). Furthermore, CRISPR-based gene activation has demonstrated therapeutic utility in pre-clinical models of type 1 diabetes, kidney disease, and muscular dystrophy (Liao et al., 2017). Building upon these canonical systems, Chavez et al. (2015) engineered a synthetic transactivation complex, termed VPR, which combines activities of the VP64, p65, and Rta activation domains **(Figure 4.5A)**. VPR was shown to stimulate higher levels of gene expression compared to dCas9 fused to the canonical VP64 transactivation domain **(Figure 4.5B-C)**. I hypothesized that such an approach could provide an effective means to activate tissue-specific promoters from AAV expression cassettes in cell-based functional and potency assays.

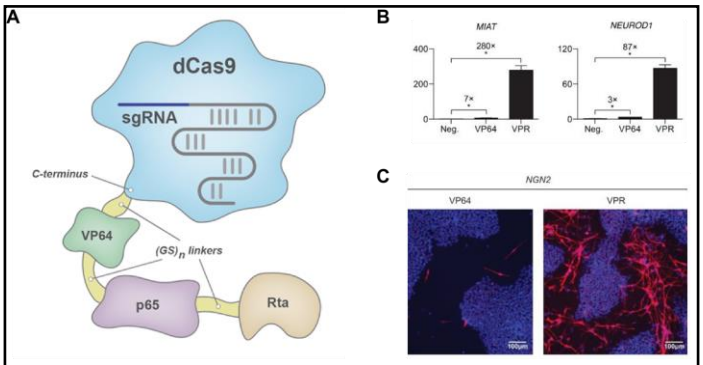


**Figure 4.5. Synthetic transactivation complexes promote robust gene activation. (A)** Outline of dCas9 fused to the synthetic VPR transactivation complex. **(B)** dCas9.VPR stimulates potent gene activation compared dCas9 fused to the canonical VP64 transactivation domain. **(C)** dCas9.VPR promotes enhanced protein expression compared to dCas9.VP64. Figure adapted from Chavez et al., 2015.

**Results**

*Rhodopsine kinase 1 (GRK1) and cone arrestin (CAR) promoters display robust activity in photoreceptors but poor activity in cell-based systems*

I generated AAV8 reporter vectors driven by the cytomegalovirus enhancer/chicken beta actin (CAG) hybrid promoter, human rhodopsin kinase (GRK1) promoter, or human cone arrestin (CAR) promoter **(Figure 4.2A)**. Subretinal administration of vectors demonstrates robust activity *in vivo* with fundoscopic analysis and immunohistochemistry of retinal sections **(Figure 4.2B)**. Vectors regulated by the ubiquitous CAG promoter display expression in multiple retinal cell types in the outer and inner nuclear layers. AAV8.GRK1.eGFP activity was restricted specifically to photoreceptors, while AAV8.CAR.eGFP vectors display leaky expression within photoreceptors and RPE. AAV transduction with these photoreceptor promoters *in vitro* reveals exceptionally poor activity when compared to CAG driven vectors as demonstrated by microscopy and fluorescence intensity **(Figure 4.2C-D)**. These results underscore the major discrepancy in vector activity *in vivo* versus cell-based systems when transgene expression is regulated by a tissue-specific promoter. Moreover, the results highlight the major limitation of building a cell-based potency assay for gene transfer vectors regulated by tissue or cell-specific promoters.

*In vitro activation of photoreceptor promoters with dCas9 transcriptional activation*

I hypothesized that recently characterized dCas9-based transcriptional activators would allow stimulation of photoreceptor promoters in the context of an *in vitro* system. I screened twenty unique guide RNAs targeting the GRK1 or CAR promoter sequences using a fluorescence-based reporter assay. Guide RNAs were cloned into expression plasmids encoding enhanced green fluorescent protein (eGFP) driven by either the GRK1 or CAR promoters **(Figure 4.6A)**. These constructs were transfected into 84-31 cells that stably express dCas9 fused to the VPR transactivation complex (84-31.VPR). Fluorescence readings 48 hours post-transfection revealed differential effects upon reporter expression driven by photoreceptor promoters **(Figure 4.6B-C)**. Most guide sequences provided a modest increase in reporter expression compared to cells transfected with plasmids harboring an empty sgRNA cassette (NG). Guide RNA candidate

#9 demonstrated the most potent stimulation of GRK1 driven reporter expression, while sgRNA candidates #4 and #10 stimulated similar and robust levels of reporter activity **(Figure 4.6B-C)**. Likewise, fluorescent microscopy revealed robust induction of eGFP protein expression in 84-

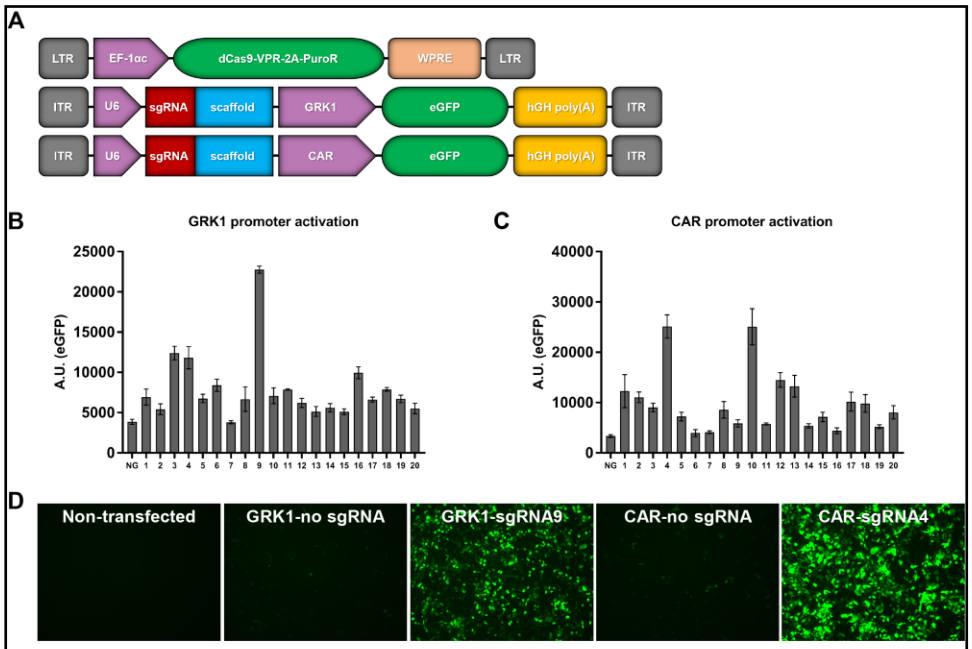


**Figure 4.6. *In vitro* stimulation of photoreceptor promoters with CRISPR/Cas9 activation.** **(A)** Outline of lentiviral vector cassette used to generate 84-31-VPR cells (top), GRK1 sgRNA/reporter construct (middle), and CAR sgRNA/reporter construct (bottom). **(B)** GRK1 promoter activation screen. **(C)** CAR promoter activation screen. X-axes denote the activity of 20 unique sgRNAs targeting each promoter. NG = "no guide" control. Data represented as mean ± SEM. **(D)** Representative micrographs of 84-31.VPR cells transfected with empty guide/reporter or sgRNA/reporter plasmids.

31.VPR cells transfected with these top performing sgRNA/reporter plasmids compared to empty guide control plasmids **(Figure 4.6D)**.

*dCas9-mediated transcriptional activation stimulates tissue-specific promoter expression from AAV vectors*

I generated a panel of stable cell lines that co-express dCas9.VPR and a top performing sgRNA candidate targeting the GKR1 promoter (84-31.GRK1.9) or CAR promoter (84-31.CAR.4) from a single lentiviral expression cassette **(Figure 4.7A)**. Transduction with two different AAV serotypes demonstrated robust activation of transgene expression specifically within 84-31 cell lines co-expressing the sgRNA and dCas9.VPR **(Figure 4.7B-C)**. Moreover, photoreceptor

promoter expression was shown to increase in a dose-dependent manner **(Figure 4.7C)**. To determine whether this approach could be broadly applied to other cell lines, I examined vector expression in ARPE-19 cells, which display morphological and biochemical features of retinal pigment epithelia (RPE). Transduction of ARPE-19 cells selected to stably co-express dCas9.VPR and sgRNA9 (ARPE-19.GRK1.9) resulted in enhanced levels of reporter expression compared to control cells **(Figure 4.7D)**. Collectively, these results demonstrate the potent and broad applicability of this system for activating tissue specific promoters from AAV expression cassettes irrespective of cell line.

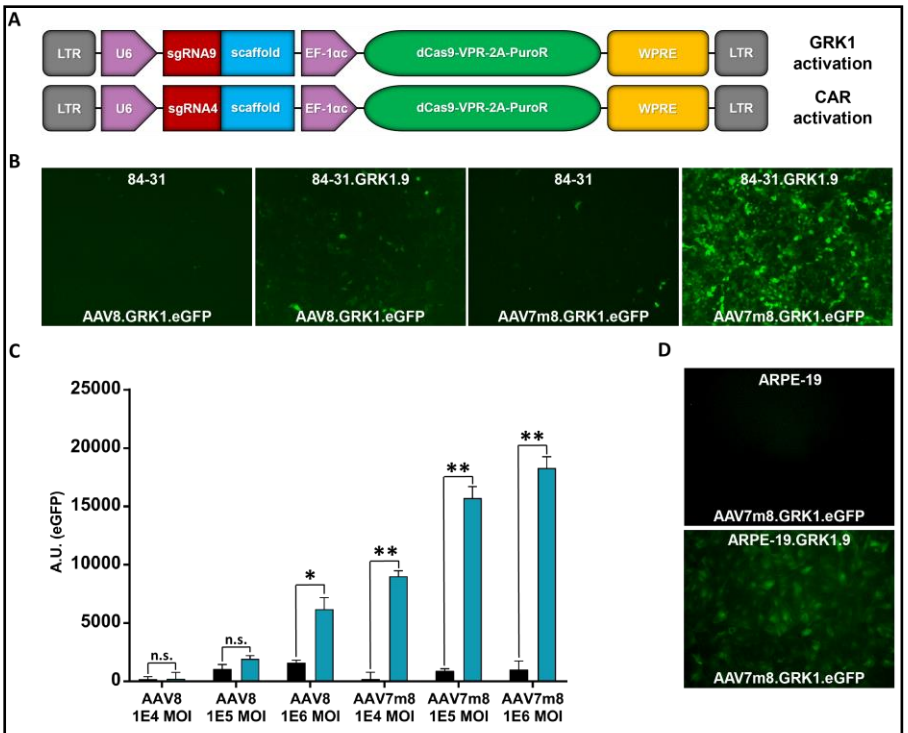


**Figure 4.7. CRISPR activation stimulates tissue-specific transgene expression from AAV vectors. (A)** Outline of lentiviral constructs used to generate cell lines that co-express dCas9.VPR and sgRNAs targeting the GKR1 (top) or CAR (bottom) promoter sequences. **(B)** Micrographs of wild-type or cells containing the GRK1.9 promoter activation system following treatment with AAV8 or AAV7m8 vectors. **(C)** Quantification of fluorescence intensity in wild-type or cells containing the GKR1.9 promoter activation system following AAV8 or AAV7m8 transduction at three MOIs. **(D)** AAV7m8 activity in ARPE-19 cells with or without the GRK1.9 promoter activation system. Data represented as mean ± SEM (N=3). **P* < 0.05, ***P* < 0.01.

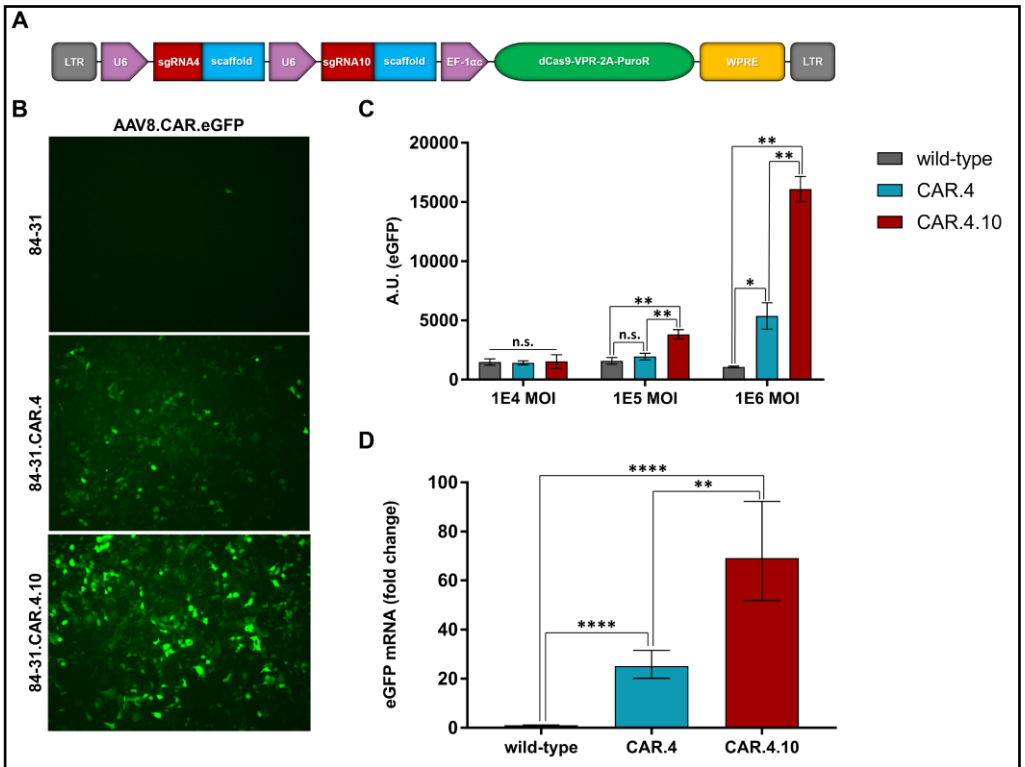


**Figure 4.8. Multiplex sgRNA targeting of a single promoter enhances AAV expression. (A)** Lentiviral cassette co-expressing dCas9.VPR with sgRNA4 and sgRNA10 targeting the CAR promoter. Lentiviral vectors were used to generate 84-31.CAR.4.10 cell line. **(B)** Representative micrographs different cell lines transduced with AAV8.CAR.eGFP at 1E6 MOI. **(C)** Quantification of fluorescence intensity in different cell lines following transduction with AAV8.CAR.eGFP at different MOIs (N=4). Data represent mean ± SEM. **P*<0.05, ***P*<0.01. **(D)** Quantification of eGFP gene expression in cell lines following transduction with AAV8.CAR.eGFP at 1E6 MOI (N=3). Data represent mean ± SD. ***P*<0.01, *****P*<0.0001.

Prior reports suggest co-expression of multiple guide RNA sequences (multiplexing) targeting a single promoter region may vastly improve dCas9-mediated gene activation. Likewise, I hypothesized that inclusion of a second guide RNA could enhance the activation of photoreceptor promoters from AAV genomes. We engineered a lentiviral vector encoding dCas9-VPR and the two top performing guide RNA sequences targeting the CAR promoter **(Figure 4.8A)**. Similar to previous experiments, I generated a stable cell line (84-31-CAR.4.10) and selected positively transduced clones with puromycin incubation. These cells display greater levels of reporter gene expression as assayed by microscopy, fluorescence intensity readings,

and gene expression analysis **(Figure 4.8B-D)**. Similar to previous experiments, the degree of reporter gene expression increased in a dose-dependent manner suggesting the importance of AAV genome copies as the rate limiting determinant of promoter activation.

*AAVR co-expression mediates a synergistic effect upon AAV promoter activation*

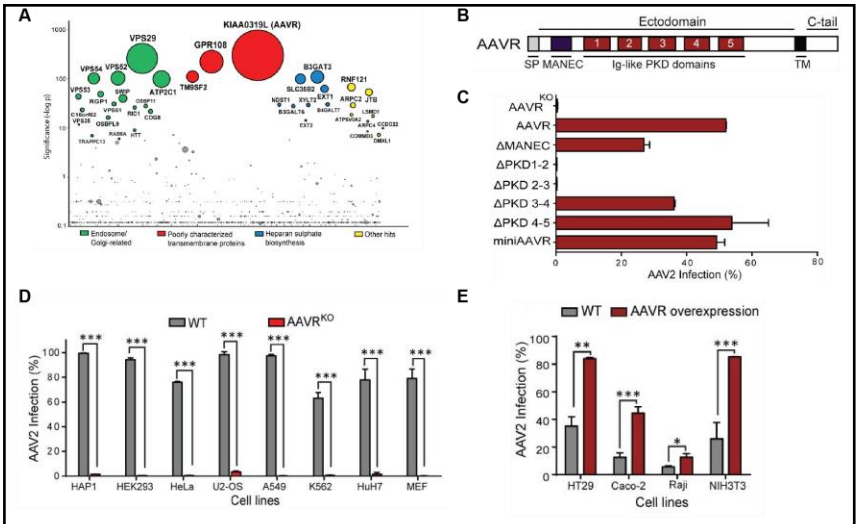


**Figure 4.9. AAVR: a "universal" receptor for AAV infection. (A)** An unbiased, haploid genetic screen was used to identify a previously uncharacterized transmembrane receptor, KIAA0319L (AAVR). **(B)** Structural map of AAVR protein domains. **(C)** PKD1-3 are essential for AAVR interaction with AAV2. **(D)** AAVR knockout diminshes AAV2 infection efficiency across cell lines. **(E)** AAVR overexpression enhances AAV2 infecion efficiency across cell lines. Figures adapted from Pillay et al., 2016.

Recent studies identified and characterized a "universal" transmembrane receptor for AAV infection denoted as AAVR (Pillay et al., 2016; Pillay et al., 2017; Dudek et al., 2018) **(Figure 4.9)**. I generated 84-31 cells that stably express AAVR with a lentiviral vector **(Figure 4.10A)**. Transduction of 84-31 cells that stably overexpress AAVR display differential effects upon reporter gene expression compared to control cells **(Figure 4.10B-C)**. Surprisingly, transduction with many serotypes was inhibited compared to 84-31 control cells suggesting a discrepancy between AAVR activity and capsid or cell line dependent properties. Importantly, the transduction efficiency of some clinically relevant capsids, including AAV8 and AAV8BP2, was enhanced with AAVR supplementation. Based on these findings, I hypothesized that enhanced vector uptake through the AAVR pathway would provide additional substrate for the dCas9 activating components and subsequently improve vector transgene expression. 84-31 and 84-31-CAR.4.10

cells were similarly transduced with a lentiviral vector driving AAVR overexpression, and positive clones were selected with blasticidin. Transduction of 84-31-CAR4.10.AAVR cells with AAV8.CAR.eGFP demonstrates superior transgene expression compared to control cell lines as detected by microscopy and RT-qPCR **(Figure 4.10D-E)**. Collectively, these results highlight the synergistic value of enhancing AAV. Furthermore, they once again suggest vector genome copies as the limiting factor in achieving substantial tissue-specific promoter activation from AAV transgene cassettes.

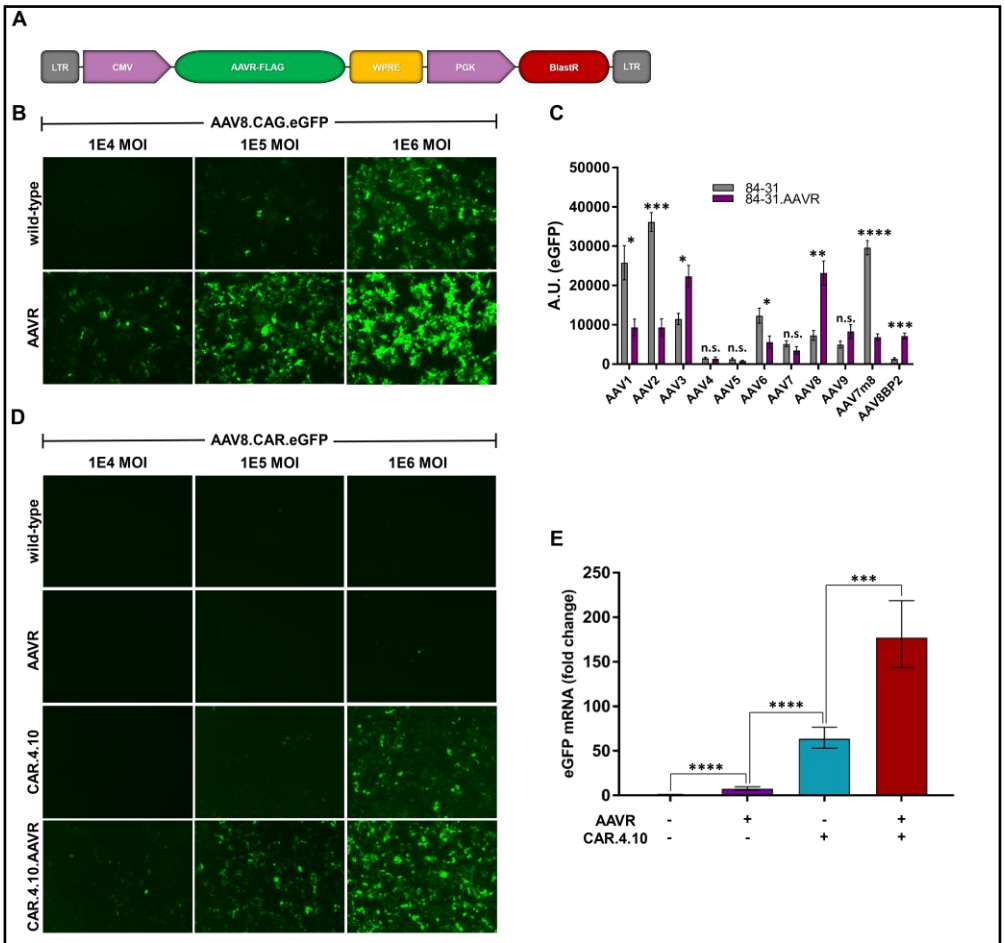


**Figure 4.10. AAVR co-expression mediates a synergistic effect upon promoter activity. (A)** Outline of lentiviral vector used to generate AAVR overexpression cell lines. **(B)** Representative micrographs displaying the effect of AAVR overexpression in 84-31 cells following AAV8.CAG.eGFP transduction at three different MOIs. **(C)** Quantification of eGFP fluorescence intensity in wild-type 84-31 and 84-31.AAVR cells with a panel of AAV serotypes at 5E5 MOI. Data represent mean intensity ± SEM (N=4). **(D)** Representative micrographs of different cell lines transduced with AAV8.CAR.eGFP at differing MOIs. **(E)** Quantification of eGFP expression with RT-qPCR following transduction with AAV8.CAR.eGFP at 1E6 MOI. Data represent mean ± SD (N=3).*$P$<0.05, **$P$<0.01, ***$P$<0.001, ****$P$<0.0001.

## Methods

*Plasmid generation*

The pAAV-U6-sgRNA-CMV-eGFP-KASH plasmid was kindly supplied by Hetian Lei (Addgene #85451). The eGFP-KASH coding sequence was removed by digestion with AgeI-HF and EcoRI-HIF (NEB), and the wild-type eGFP sequence was amplified and restored between these sites. In addition, the CMV promoter cassette was removed by digestion with NheI-HF and SpeI-HF (NEB) and replaced with the GRK1 or CAR promoter sequences. Guide RNA sequences targeting either promoter were cloned between the SapI sites between the U6 promoter and guide scaffold. The pLenti-EF1α-dCas9-VPR-2A-Puro plasmid was a kind gift from Kristen Brennand (Addgene #99373). pLentiCRISPRv2 was kindly provided by Feng Zhang (Addgene #52961). Top performing candidate guide RNAs were cloned between the BsmBI (NEB) sites of pLentiCRISPRv2. Afterwards, the SpCas9-2A sequence was removed by digestion with XbaI-HF and BamHI-HF (NEB). The dCas9-VPR-2A sequence was amplified and cloned into the XbaI/BamHI digested pLentiCRISPRv2 with the In-Fusion HD cloning system (Clonetech) to create lentiviral expression plasmids that co-express a single guide RNA and dCas9-VPR-2A-Puro. A plasmid encoding AAVR-FLAG was a kind gift from Jan Carette (Stanford University). The AAVR-FLAG sequence was amplified and cloned into a lentiviral expression vector containing a downstream blasticidin resistance cassette. All plasmids were propagated in One Shot Stbl3 competent cells (Invitrogen).

*Cell culture*

HEK293T and ARPE-19 cells were supplied by ATCC (Manassas, VA, USA). HEK293T cells were cultured in DMEM-GlutaMax (Gibco) supplemented with 10% FBS and 1% penicillin-streptomycin. ARPE-19 cells were maintained in Dulbecco's modified eagle medium: nutrient mixture F-12 (DMEM/F12; Gibco) and supplemented with 10% fetal bovine serum (FBS) and 1% penicillin-streptomycin. 84-31 cells were provided by James M. Wilson (University of

Pennsylvania) and were cultured in DMEM-GlutaMax supplemented with 10% FBS and 1% penicillin-streptomycin. All cell lines were grown at 37°C with 5% $CO_2$. Cell lines stably transduced with lentiviral vectors were selected and maintained in medium containing 1 µg/mL puromycin or 10 µg/mL blasticidin-S.

*Guide RNA selection*

Candidate guide RNA sequences were identified with web-based design tools including CRISPR Design (crispr.mit.edu) and CRISPR-ERA (crispr-era.stanford.edu).

*Lentiviral vector production*

$2x10^6$ HEK293T cells were plated in 10cm dishes. The following day cells were transfected with 6 ug of the appropriate lentiviral expression plasmid, 4 ug psPAX2 (supplied by Didier Trono; Addgene #12260), and 2 ug pMDG.2 (supplied by Didier Trono; Addgene #12259) combined with 16 uL of Lipofectamine 2000 (Invitrogen) according to manufacturer's protocol. Cells were refed with fresh media the following day. Media containing lentiviral particles was harvested 48 and 72 hours post-transfection, pooled, and stored at -80C until use.

*AAV vector production*

AAV vectors were generated using previously described methods (McDougald et al., 2018) and purified with CsCl gradient by the CAROT research vector core at the University of Pennsylvania.

*In vitro AAV transduction and fluorescence intensity measurements*

$5x10^4$ cells were plated into individual wells of 96-well black bottom dishes. Afterwards, cells were immediately transduced with AAV vectors at the MOIs indicated. eGFP fluorescence was quantified at 48 hours post-transduction. Data represent mean arbitrary units (A.U.) in eGFP fluorescence between three technical replicates per experiment. Data from each treatment group

were normalized to the mean of three non-transduced control wells. Experiments were performed at least three times.

*Promoter activation screen*

$5x10^4$ 84-31.VPR cells were plated into individual wells of 96-well black bottom dishes. The following day cells were transfected with 200 ng of sgRNA/reporter plasmid and 1 uL of Lipofectamine 2000 (Invitrogen). eGFP fluorescence was quantified at 48 hours post-transfection. Data represent the mean arbitrary units (A.U.) of eGFP fluorescence between three technical replicates. The screens were performed a total of three times (N=3), and the data from each treatment were normalized to the mean of three non-transfected control wells.

*In vivo studies*

C57Bl/6 mice were obtained from the Jackson Laboratory and housed at the University of Pennsylvania vivarium and maintained in compliance with the ARVO statement for the Use of Animals in Ophthalmic and Vision Research and institutional and federal guidelines under IACUC #805890. Subretinal injections were performed as previously described (Dooley et al., 2018). Each retina received $1x10^9$ vector genomes in a total volume of 1 uL.

*Immunohistochemistry*

Eyes were enucleated, fixed, and processed as frozen retinal sections as described previously. Sections were incubated in blocking buffer consisting of 10% normal goat serum (CST) and 2% Triton X-100 (Sigma) and 1xDPBS for 1 hour at room temperature. Next, sections were incubated in blocking solution containing rabbit anti-cone arrestin (1:400; Millipore) overnight in a humidified chamber at room temperature. Sections were washed three times in 1xDPBS and incubated in secondary antibody solution consisting of blocking buffer and Cy5-labeled goat anti-rabbit IgG (1:400; KPL) for 1 hour at room temperature. Sections were washed

in 1xDPBS three times and slides were mounted with Fluoromount-G (Southern Biotech) containing DAPI.

*RNA isolation and RT-qPCR*

RNA was isolated using the Macherey-Nagel Nucleospin RNA kit. First-strand cDNA synthesis was performed using 1000 ng of total RNA with the SuperScript III first-strand synthesis system according to manufacturer's protocol. Real-time PCR was performed with the Applied Biosystems 7500 Fast system using the Power SYBR green PCR master mix (Invitrogen). The following primer sequences were used: CCACTCCTCCACCTTTGAC (human *GAPDH* forward), ACCCTGTTGCTGTAGCCA (human *GAPDH* reverse), CGACAACCACTACCTGAGCA (*eGFP* forward), CTTGTACAGCTCGTCCATGC (*eGFP* reverse). Relative gene expression was quantified with the $\Delta\Delta C_T$ method and normalized to *GAPDH*.

*Statistics*

Statistical analyses between two groups were performed using the unpaired student's *t* test. Comparison of three or more groups were determined to be statistically significant using a one-way ANOVA with Turkey's HSD post-test. A *P* value of less than 0.05 was considered statistically significant.

# Chapter 5 Discussion

## *RGC-directed gene transfer attenuates functional and cellular pathology in experimental optic neuritis*

Chapter 2 explored the effects of *SIRT1* or *NRF2* gene transfer in experimental optic neuritis. Under cellular conditions of redox equilibrium, NRF2 is sequestered within the cytoplasm and subject to proteasomal-mediated degradation (Dinkova-Kastova et al., 2002; Itoh et al., 2003; McMahon et al., 2003). During oxidative challenge, modifications to critical binding proteins free NRF2 to translocate into the nucleus, recruit transcriptional machinery to antioxidant response elements (AREs), and stimulate transcription of target genes associated with antioxidant defense and cellular detoxification (Johnson et al., 2015). SIRT1 is recruited to the nucleus and other cellular compartments where it modulates the activity of various protein targets. SIRT1 is known to deacetylate and inhibit the transcription factor, p53, thereby downregulating apoptotic gene expression and thus improving cell viability (Luo et al., 2001). SIRT1 promotes mitochondrial function and antioxidant metabolism by activating PGC-1α, a master transcriptional regulator of these responses (Nemoto et al., 2005). While SIRT1 and NRF2 are typically believed to function via separate pathways, recent evidence suggests SIRT1 involvement in regulating the expression and activation of NRF2 (Ding et al., 2016). In addition, treatment with pharmacological agents such as resveratrol, a known activator of SIRT1, was shown to enhance NRF2 expression and activity of its downstream effectors (Zhang et al., 2016; Xia et al., 2017). We hypothesized that gene augmentation of NRF2 or SIRT1 within RGCs could ameliorate pathological features of experimental optic neuritis. Our data demonstrates distinct effects upon RGC survival and function following AAV2-mediated overexpression of NRF2 or SIRT1, suggesting these candidate factors promote neuroprotective mechanisms that may modify MS pathogenesis.

RGC-directed gene therapy with SIRT1 and NRF2 vectors revealed differential effects upon visual acuity during EAE. Visual acuity was not affected prior to EAE development with any of the vectors tested, suggesting vector delivery or transgene overexpression did not mediate

unintended toxicity on retinal function. We observed a statistically significant decline in visual acuity beginning at day 21 post-immunization with all AAV2 and vehicle treated animals subjected to EAE, whereas sham-induced cohorts presented robust responses throughout the experimental timeline. While Larabee et al. (2016) reported that *NRF2* knockout mice exhibit increased visual decline compared to wild-type cohorts during EAE, augmenting NRF2 activity with AAV2 gene transfer was unable to preserve visual acuity in the current study. Failure to reverse effects of knockout studies may be due to the limited number of RGCs (21%) infected with the AAV2 vectors in this study. However, interestingly, overexpression of SIRT1 mediated a trending increase in functional recovery beginning at day 28 post-induction compared to vehicle and AAV2.eGFP control groups subjected to EAE. This protective effect achieved statistical significance compared to the AAV2.eGFP control group at 35 and 42 days post-induction, which is remarkable given that only a subset of RGCs were infected. This finding also correlates with prior investigations utilizing compounds that stimulate SIRT1 activity and demonstrate varying degrees of OKR preservation in the context of experimental optic neuritis as well as optic nerve crush (Shindler et al., 2007; Fonseca-Kelly et al., 2012; Zuo et al., 2013).

RGC numbers were significantly reduced in all animal groups sensitized to EAE. However, we observed increased RGC numbers with SIRT1 and NRF2 gene augmentation compared to the AAV2.eGFP and vehicle treatment groups. SIRT1 gene transfer did not mediate a statistically significant increase in RGC numbers but only a positive trend in survival compared to EAE-induced controls. NRF2 gene transfer provided the most robust protective response with respect to total and regional RGC survival. This outcome is particularly interesting as NRF2 augmentation did not correlate with an improvement in retinal function as shown by OKR recordings. However, disparities between OKR and RGC survival have been previously documented in this model (Fonseca-Kelly et al., 2012). Another explanation for this finding could be that NRF2 overexpression is simply supporting survival of the RGC cells bodies but unable to sustain function. This finding coincides with the inability of NRF2 gene augmentation to ameliorate ongoing inflammation and demyelination of the optic nerve, thus providing another

explanation for the discrepancy between functional and cellular preservation. This interpretation is also consistent with findings by Xiong et al. (2015) where NRF2 gene transfer mediated transient yet significant preservation of RGCs following optic nerve crush without promoting axonal regeneration required for functional retention. Importantly, as indicated above, we only achieved approximately 21% RGC transduction with the AAV2 vector and previously described dose. Regarding the discrepancy between OKR preservation and RGC survival following AAV2.SIRT1 treatment, it is also possible that SIRT1 augmentation may influence the survival of ON direction-selective ganglion cells, which is the subset of cells that contribute to the OKR, but not mediate a statistically significant effect upon total RGC survival (Sugita et al., 2013). Moreover, selection of a vector platform with enhanced capabilities for RGC transduction may provide a more potent means of cellular protection and functional preservation in this model. Recent developments utilizing rational design and *in vivo* selection have generated novel AAV capsids with improved potency and tropism for retinal cell types compared to naturally isolated serotypes such as AAV2 (Cronin et al., 2014; Choudhury et al., 2016; Zinn et al., 2015; Deverman et al., 2016). Further investigation into SIRT1 or NRF2-mediated neuroprotection in this model with an improved vector system is certainly warranted. The differential effects observed here also suggest a potential role for combined therapy with overexpression of both SIRT1 and NRF2. Due to limitations of the current transduction efficiency and the total volume that can be injected in the eye, co-injection of both vectors is not feasible, but future development of improved vector systems may allow investigation of a dual therapy.

While we did observe evidence of neuroprotection upon RGC function and viability, overexpression of neither NRF2 nor SIRT1 was able to suppress the inflammatory and demyelinating phenotype associated with optic neuritis. RGC directed gene therapy did not influence immune recruitment to the optic nerve as shown by H&E histological analysis. This observation correlates with previous studies that examined small molecule-mediated neuroprotection during EAE. Specifically, pharmacological activators of SIRT1, including resveratrol and related compounds, did not suppress inflammation in the spinal cord or optic

nerve when administered at various doses in the same EAE model (Fonseca-Kelly et al., 2012) used in the current study. Interestingly, transgenic overexpression of human SIRT1 within neurons was able to reduce inflammation within spinal cord lesions (Nimmagadda et al., 2013). Similar to the effects on immunomodulation, AAV2-mediated expression of NRF2 or SIRT1 did not alleviate optic nerve demyelination. While these approaches did not attenuate demyelination, other studies that examined antioxidant or mitochondrial-directed gene therapy strategies during EAE have shown preserved myelin in the optic nerve (Qi et al., 2007; Qi & Lewin et al., 2007; Talla et al., 2013; Talla et al., 2014; Talla et al., 2015). However, discrepancies in animal models, EAE immunization protocols, and other components of study design limit a direct comparison with these reports. In addition, our findings with respect to inflammation and myelination may once again reflect the limited transduction efficiency of the AAV2 vector.

Collectively, this study demonstrates at least partial neuroprotective effects of NRF2 and SIRT1 gene augmentation in the context of experimental optic neuritis, and suggests an important role of these signals in MS pathogenesis. Moreover, the results underscore the therapeutic potential of targeting conserved cell survival pathways or mechanisms to impede progression of complex neurodegenerative disease. Downstream investigations will determine the optimal combinations of promoter elements (ex. CAG, SNCG, CMV, CBh), AAV capsids (ex. AAV2, AAV7m8, AAV2 tyrosine mutants), and transgenes (native versus codon-optimized) to improve RGC targeting efficiency.

*Stimulation of the mTOR signaling pathway with AAV-mediated gene augmentation promotes divergent effects upon photoreceptor neuroprotection in a pre-clinical model of retinitis pigmentosa*

Chapter 3 examined the therapeutic potential of reprogramming cell metabolism in a pre-clinical model of inherited vision loss following stimulation of the mTOR pathway with AAV-mediated gene augmentation. The exact role of mTOR signaling in the context of neurodegenerative disease remains an intense topic of debate. Several lines of evidence suggest

that downregulation of mTOR activity via treatment with the canonical mTOR inhibitor, rapamycin, can attenuate pathological mechanisms in several models of neurodegeneration including Parkinson's disease, Huntington's disease, and Alzheimer's disease (Ravikumar et al., 2004; Malagelada et al., 2010; Spilman et al., 2010; Bove et al., 2011). Conversely, other investigations suggest stimulation of the insulin/AKT/mTOR axis can mediate beneficial outcomes in related neurodegenerative disease models (Ries et al., 2006; Kim et al., 2012; Lee et al., 2015). In the present study, targeting the mTOR pathway at two separate points of regulation led to divergent effects upon photoreceptor survival, structural integrity, and visual function, thus emphasizing the complex nature of re-wiring cell metabolism for therapeutic intent.

Several studies highlight the protective potential of targeting Rheb activation to improve therapeutic outcomes in the context of neurodegenerative disease models (Kim et al., 2012; Lee et al., 2015; Lim et al., 2016; Wu 2016, Wu 2017). Stimulating the mTOR pathway at this downstream point of regulation with caRheb gene augmentation did not mediate a notable protective effect in the *Pde6b*$^{rd10}$ retina. Interestingly, AAV.caRheb vectors demonstrated potent stimulation of mTORC1 activity *in vitro* showing enhanced expression of the canonical mTORC1 activation marker, pS6. However, this activity did not translate *in vivo* as shown by negative immunostaining for the pS6 in retinal sections overexpressing the caRheb transgene. This suggests the presence of mechanisms in place to inhibit caRheb's capacity to stimulate mTORC1 within photoreceptors or limited ability to detect increased expression of this marker *in vivo*. These observations diverge from previous studies in which caRheb gene transfer sufficiently stimulated mTORC1 activity within various neuronal populations and conferred stress resistance in models of Parkinson's disease, Huntingtin's disease, and optic nerve trauma (Kim et al., 2012; Lee et al., 2015; Lim et al., 2016). Other lines of evidence suggest Rheb may play a competing role in promoting cell death signaling programs in response to different forms of cellular stress (Potheraveedu et al., 2017). UV or TNFα-induced cellular stress combined with Rheb overexpression enhanced apoptotic signaling *in vitro*, whereas Rheb knockdown or treatment with rapamycin provided partial protection from these cytotoxic agents (Karassek et al., 2010). In

the context of retinal degeneration, light-induced damage of retinal ganglion cells (RGCs) led to upregulation in Rheb expression that associated with an increase in markers of apoptosis prior to degeneration (Shu et al., 2014). Taken together, the protective or pro-apoptotic functions of Rheb are likely determined by mechanisms elicited through the specific pathology in question. Moreover, amplifying Rheb activity with gene transfer likely modulates divergent effects upon cell biology depending on the particular disease context.

AKT3 was selected based on a previous report demonstrating its increased capacity to stimulate mTORC1 activity compared to other AKT variants within retinal cell types (Miao et al., 2016). In addition, targeted ablation of AKT3, but not AKT1 or AKT2, leads to severe neurodevelopmental defects including reduced brain and neuron size suggesting a unique role for this variant in neuronal homeostasis (Easton et al., 2005). AKT3 augmentation with AAV vectors stimulated a potent neuroprotective effect upon photoreceptor survival and morphological preservation. This protective effect was associated with stimulation of mTORC1 and mTORC2 in regions of the retina specifically transduced with the AAV.AKT3 vector. While the role of mTORC1 has been extensively evaluated in RP disease models (Venkatesh et al., 2015; Zhang et al., 2016), our findings are the first to report upregulation in mTORC2 signaling activity associated with photoreceptor neuroprotection. This data deviates from previous observations by Venkatesh et al. (2015) in which mTORC2 activity was decreased following transgenic ablation of *Pten* and increased cone survival in the *Pde6b*$^{rd1}$ mouse retina. Downstream investigations to delineate the specific contributions of mTORC1 and mTORC2 in mediating photoreceptor survival in pre-clinical models of IRD will be necessary.

Despite the dramatic cellular preservation mediated by AKT3 gene augmentation, we observed differential effects upon functional preservation following evaluation with electroretinography and OKR. We observed statistically significant preservation of the mixed rod-cone a-wave and b-wave responses in eyes treated with AAV.AKT3 at the PN30 measurement but not during later stage degeneration. Despite the morphological preservation of cone structure

with AAV.AKT3 treatment, we did not observe an improvement in cone-specific light responses compared to controls at any of the time points tested. This finding deviates from prior investigations that examined strategies of cone photoreceptor neuroprotection in similar disease models. These differences may be explained by variations in study design with respect not only to the transgene cassette but vector dose, injection route, kinetics of degeneration, and timing of vector delivery. In the present study, vectors were injected at a time point just prior to the onset of photoreceptor death, whereas previous investigations administered the experimental intervention immediately after birth and prior to retinal maturation and onset of disease mechanisms (Xiong et al., 2015). These differences in experimental design likely have important downstream implications relevant to retinal coverage, kinetics of vector recruitment and expression in relation to onset of neurodegenerative mechanisms, and ultimately therapeutic outcome measures.

Interestingly, we observed histological features that suggest enhanced müller cell activation within regions of the *Pde6b*$^{rd10}$ retina specifically transduced with the AAV.AKT3 vector. Reactive gliosis is a response typically associated with tissue injury where these cells become activated and proliferate to mediate various functions including tissue remodeling, neurotrophic factor release, scavenging of cellular debris (Bringmann et al., 2009; Goldman, 2014; Reichenbach et al., 2013). While this response is intended to suppress further retinal damage, chronic activation may be detrimental to neighboring cells and disrupt retinal homeostasis. For example, activated müller cells have been observed to upregulate expression and secretion various pro-inflammatory molecules including tumor necrosis factor (TNF) and monocyte chemoattractant protein (MCP-1). Furthermore, they are known to secrete excess amounts of nitric oxide (NO) which generates free radicals that may be damaging to neighboring cells (Bringmann et al., 2009). Long-term expression of AAV.AKT3 in the wild-type mouse retina was accompanied with extensive retinal disorganization and loss of cellular structures in regions specific to the subretinal bleb. Conversely, animals injected with the reporter vector alone demonstrate normal retinal architecture. Moreover, wild-type animals treated with AAV.AKT3 also demonstrate enhanced histological markers indicative of chronic reactive gliosis. Interestingly, I

did not observe histological hallmarks of reactive gliosis in *Pde6b*$^{rd10}$ retinal samples treated with GRK1-driven AKT3 vectors. This finding suggests the chronic muller cell activation was a byproduct of off target transgene expression within these cells types when exposed to vectors driven by the ubiquitous CAG promoter. Overall, these findings caution detailed investigation to accurately define how other retinal cell types respond to neuroprotective reagents beyond examination of the primary cellular targets exhibiting pathology.

Advancement of gene therapies based on strategies to reprogram cell metabolism must be met with highly stringent safety criteria prior to clinical translation. While we did not observe evidence of tumor formation, long-term overexpression of AKT3 in wild-type animals led to extensive retinal disorganization and loss of photoreceptor structure. This finding is unsurprising as cells require a delicate balance in these metabolic components to accommodate their precise physiological demands. Determining and achieving this balance with gene augmentation or silencing strategies will be an enormous challenge in translating these approaches to the clinic. Additional regulatory elements, such as stress-responsive promoters or inducible systems, will likely play critical roles in the clinical development of neuroprotective gene transfer strategies based on cellular reprogramming. For example, Fujita et al. (2017) developed an AAV vector that combined NRF2 gene augmentation with the stress-inducible Mcp-1 promoter to provide spatial and temporal regulation of transgene expression. Other inducible systems built upon features of the *Lac* or *Tet* operon have been incorporated within AAV expression cassettes for regulation of vector expression via small molecule induction (Santiago et al., 2018; Sochor et al., 2015; Zhong et al., 2016). Coupling such elements with AKT gene expression may allow “fine tuning” of downstream metabolic pathways and, importantly, provide a molecular safety switch in the event of genotoxicity or oncogenic transformation.

Collectively, this investigation demonstrates a broadly protective effect upon photoreceptor viability and structure following gene augmentation in a model of inherited retinal degeneration. These findings underscore the importance of AKT activity and downstream

pathways associated with anabolic metabolism in photoreceptor survival and maintenance. Furthermore, it emphasizes the complex and delicate nature of reprogramming cell metabolism as well as important safety concerns in arresting progression of complex neurodegenerative disease with “generic” gene therapy strategies.

*CRISPR/Cas9 transcriptional activation stimulates tissue-specific promoter activity from AAV vectors*

Various commercial reagents are available to enhance plasmid transfection or AAV transduction within non-permissive primary cells and stem cells. While these tools are valuable to increase overall levels of gene transfer efficiency, these reagents will likely provide minimal advantages if the transgene is controlled by a tissue or cell-specific regulatory element. Other investigations highlight the use of pharmacological reagents to stimulate endogenous promoter activity, which may provide a possible avenue to improve *in vitro* potency of tissue-restricted vectors. For example, Li et al. (2002) identified a region of the cone arrestin promoter sequence that is responsive to retinoic acid. However, effects upon transgene expression are likely transient due to the limited half-life of the compound. In addition, it is unclear what impact different pharmacological reagents may exert upon cell biology. It may also be possible to amplify transgenic promoter activity by overexpressing transcription factors known to act upon the DNA sequence of interest. However, transcription factors typically act upon networks of associated genetic elements, thereby imposing a non-specific response. Similar to pharmacological induction, it is unclear how transcriptional reprogramming will affect underlying cell biology and other downstream parameters of the potency assay. The present approach utilizing dCas9-based gene activation provides a highly potent, stable, and precise platform to stimulate cell-specific promoters from AAV vectors.

Supplementing dCas9 activation with AAVR co-expression provided a highly effective means to improve vector performance and thereby increase levels of tissue-specific promoter transgene expression. Specifically, AAVR overexpression dramatically enhanced AAV8 uptake in cell lines harboring both GRK1 or CAR promoter activation systems. Interestingly, we observed differential effects upon capsid uptake with AAVR overexpression using a panel of eleven distinct serotypes suggesting capsid or cell-type dependent effects upon AAV entry. For example, AAVR overexpression within 84-31 cells greatly reduced expression of vectors such as AAV7m8 and AAV3. However, expression of these vectors was greatly enhanced in ARPE-19.AAVR cells compared to control cell lines (data not shown). While AAVR is certainly a major determinant of AAV entry, other distinct mechanisms likely influence the process of viral transduction at various steps. It is possible that AAVR overexpression could perturb such mechanisms in a cell line dependent fashion thus disrupting certain molecular events relevant to capsid binding to cellular receptors/co-receptors, endocytosis, or nuclear transport.

Altogether, this study outlines a broadly applicable approach for engineering cell lines to express AAV vectors regulated by tissue-specific promoters. While our data demonstrate the utility of this approach in the context of retinal-specific regulatory elements, this strategy may be applied broadly to other promoter sequences that display specific activity within a tissue or cell population of interest. Furthermore, continued identification and engineering of Cas proteins with broader PAM recognition features and enhanced DNA binding specificity will allow the continued improvement of such systems. Current and future directions of this investigation involve utilizing these cell lines for the design and implementation of gene therapy vector potency assays that address numerous inherited retinal disease targets.

# BIBLIOGRAPHY


Abed DA, Goldstein M, Albanyan H, Jin H, Hu L. (2015). Discovery of direct inhibitors of Keap1-Nrf2 protein-protein interaction as possible therapeutic and preventive agents. *Acta Pharm Sin B*, 5(4): 285-99.

Acland GM, Aguirre GD, Bennett J, Aleman TS, Cideciyan AV, Bennicelli J, Dejneka NS, Pearce-Kelling SE, Maguire AM, Palczewski K, Hauswirth WW, Jacobson SG. (2005). Long-term restoration of rod and cone vision by single dose rAAV-mediated gene transfer to the retina in a canine model of childhood blindness. *Mol Ther,* 12(6): 1072-82.

Acland GM, Aguirre GD, Ray J, Zhang Q, Aleman TS, Cideciyan AV, Pearce-Kelling SE, Anand V, Zeng Y, Maguire AM, Jacobson SG, Hauswirth WW, Bennett J. (2001). Gene therapy restores vision in a canine model of childhood blindness. *Nat Genet*, 28(1): 92-5.

Ait-Ali N, Fridlich R, Millet-Puel G, Clerin E, Delalande F, Jaillard C, Blond F, Perrocheau L, Reichman S, Byrne LC, Olivier-Bandini A, Bellalou J, Moyse E, Bouillaud F, Nicol X, Dalkara D, van Dorsselaer A, Sahel JA, Leveillard T. (2015). Rod-derived cone viability factor promotes cone survival by stimulating aerobic glycolysis. *Cell*, 161(4): 817-32.

Amat R, Planavila A, Chen SL, Iglesias R, Giralt M, Villarroya F. (2009). SIRT1 controls the transcription of the peroxisome proliferator-activated receptor-gamma co-activator-1alpha (PGC-1alpha) gene in skeletal muscle through the PGC-1alpha autoregulatory loop and interaction with MyoD. *J Biol Chem*, 284(33): 21872-80.

Ambati J, Fowler BJ. (2012). Mechanisms of age-related macular degeneration. *Neuron*, 75(1): 26-39.

Ames A 3rd. (2000). CNS energy metabolism as related to function. *Brain Res Brain Res Rev*, 34(1-2): 42-68.

Ashtari M, Cyckowski LL, Monroe JF, Marshall KA, Chung DC, Auricchio A, Simonelli F, Leroy BP, Maguire AM, Shindler KS, Bennett J. (2011). The human visual cortex responds to gene therapy-mediated recovery of retinal function. *J Clin Invest*, 121(6): 2160-8.

Ashtari M, Zhang H, Cook PA, Cyckowski LL, Shindler KS, Marshall KA, Aravand P, Vossough A, Gee JC, Maguire AM, Baker CI, Bennett J. (2015). Plasticity of the human visual system after retinal gene therapy in patients with Leber's congenital amaurosis. *Sci Transl Med*, 7(296): 296ra110.

Atchison RW, Casto BC, Hammon WM. (1965). Adenovirus-associated defective virus particles. *Science*, 149(3685): 754-6.

Bainbridge JW, Smith AJ, Barker SS, Robbie S, Henderson R, Balaggan K, Viswanathan A, Holder GE, Stockman A, Tyler N, Petersen-Jones S, Bhattacharya SS, Thrasher AJ, Fitzke FW, Carter BJ, Rubin GS, Moore AT, Ali RR. (2008). Effect of gene therapy on visual function in Leber's congenital amaurosis. *N Engl J Med*, 358(21): 2231-9.

Bak RO, Dever DP, Reinisch A, Cruz Hernandez D, Majeti R, Porteus MH. (2017). Multiplexed genetic engineering of human hematopoietic stem and progenitor cells using CRISPR/Cas9 and AAV6. *Elife*, e27873.

Bakan I, Laplante M. (2012). Connecting mTORC1 signaling to SREBP-1 activation. *Curr Opin Lipidol*, 23(3): 226-34.

Baker SA, Kerov V. (2013). Photoreceptor inner and outer segments. *Curr Top Membr*, 72: 231-65.

Basner-Tschakarjan E, Mingozzi F. (2014). Cell-mediated immunity to AAV vectors, evolving concepts and potential solutions. *Front Immunol*, 5: 350.

Beck RW, Cleary PA, Anderson MM Jr, et al. (1992). A randomized controlled trial of corticosteroids in the treatment of acute optic neuritis. The optic neuritis study group. *N Eng J Med,* 326(9): 581-588.

Bennett J. (2017). Taking stock of retinal gene therapy: looking back and moving forward. *Mol Ther*, 25(5): 1076-1094.

Bennett J, Duan D, Engelhardt JF, Maguire AM. (1997). Real-time, noninvasive in vivo assessment of adeno-associated virus-mediated retinal transduction. *Invest Ophthalmol Vis Sci*, 38(13): 2857-63.

Bennett J, Wellman J, Marshall KA, McCague S, Ashtari M, DiStefano-Pappas J, Elci OU, Chung DC, Sun J, Wright JF, Cross DR, Aravand P, Cyckowski LL, Bennicelli JL, Mingozzi F, Auricchio A, Pierce EA, Ruggiero J, Leroy BP, Simonelli F, High KA, Maguire AM. (2016). *Lancet*, 388(10045): 661-72.

Bennicelli J, Wright JF, Komaromy A, Jacobs JB, Hauck B, Zelenaia O, Mingozzi F, Hui D, Chung D, Rex TS, Wei Z, Qu G, Zhou S, Zeiss C, Arruda VR, Acland GM, Dell'Osso LF, High KA, Maguire AM, Bennett J. (2008). Reversal of blindness in animal models of leber congenital amaurosis using optimized AAV2-mediated gene transfer. *Mol Ther*,16(3): 458-65.

Berger A, Lorain S, Josephine C, Desrosiers M, Peccate C, Voit T, Garcia L, Sahel JA, Bemelmans AP. (2015). Repair of rhodopsin mRNA by spliceosome-mediated RNA trans-splicing: a new approach for autosomal dominant retinitis pigmentosa. *Mol Ther*, 23(5): 918-930.

Berson EL, Rosner B, Sandberg MA, et al. (1993). A randomized trial of vitamin A and vitamin E supplementation for retinitis pigmentosa. *Arch Ophthalmol*, 111: 761-772.

Bhattacharya SS, Wright AF, Clayton JF, Price WH, Phillips CI, McKeown CM, Jay M, Bird AC, Pearson PL, Southern EM, et al. (1984). Close genetic linkage between X-linked retinitis pigmentosa and a restriction fragment length polymorphism identified by recombinant DNA probe L1.28. *Nature*, 309(5965): 253-5.

Blommaart EF, Luiken JJ, Blommaart PJ, van Woerkom GM, Meijer AJ. (1995). Phosphorylation of ribosomal protein S6 is inhibitory for autophagy in isolated rat hepatocytes. *J Biol Chem*, 270(5): 2320-6.

Bokhoven M, Stephen SL, Knight S, Gevers EF, Robinson IC, Takeuchi Y, Collins MK. (2009). Insertional gene activation by lentiviral and gammaretroviral vectors. *J Virol,* 83(1): 283-94.

Boughman JA, Vernon M, Shaver KA. (1983). Usher syndrome: definition and estimate of prevalence from two high-risk populations. *J Chronic Dis*, 36: 595-603.

Bove J, Martinez-Vicente M, Vila M. (2011). Fighting neurodegeneration with rapamycin: mechanistic insights. *Nat Rev Neuro*, 12: 437-452.

Boyd RF, Sledge DG, Boye SL, Boye SE, Hauswirth WW, Komaromy AM, Petersen-Jones SM, Bartoe JT. (2016). Photoreceptor-targeted gene delivery using intavitreally administered AAV vectors in dogs. *Gene Ther*, 23(4): 400.

Boye SL, Peshenko IV, Huang WC, Min SH, McDoom I, Kay CN, Liu X, Dyka FM, Foster TC, Umino Y, Karan S, Jacobson SG, Baehr W, Dizhoor A, Hauswirth WW, Boye SE. (2013). AAV-mediated gene therapy in the guanylate cyclase (RetGC1/RetGC2) double knockout mouse model of leber congenital amaurosis. *Human Gene Ther*, 24(2):189-202.

Boye SL, Peterson JJ, Choudhury S, Min SH, Ruan Q, McCullough KT, Zhang Z, Olshevskaya EV, Peshenko IV, Hauswirth WW, Ding XQ, Dizhoor AM, Boye SE. (2015). Gene therapy

fully restores vision to the all-cone Nrl(-/-) Gucy2e(-/-) mouse model of leber congenital amaurosis-1. *Hum Gene Ther*, 26(9):575-592.

Bringmann A, Iandiev I, Pannicke T, Wurm A, Hollborn M, Wiedemann P, Osborne NN, Reichenbach A. (2009). Cellular signaling and factors involved in muller cell gliosis: neuroprotective and detrimental effects. *Prog Retin Eye Res*, 28(6): 423-51.

Brinkman EK, Chen T, de Haas M, Holland HA, Akhtar W, van Steensel B. (2018). Kinetics and fidelity of the repair of Cas9-induced double-strand DNA breaks. *Mol Cell,* 70: 801-813.

Bryant L, Lozynska O, Maguire AM, Aleman TS, Bennett J. (2017). Prescreening whole exome sequencing results from patients with retinal degeneration for variants in genes associated with retinal degeneration. *Clin Ophthalmol*, 12: 49-63.

Byrne LC, Dalkara D, Luna G, Fisher SK, Clerin E, Sahel JA, Leveillard T, Flannery JG. (2015). Viral-mediated RdCVF and RdCVFL expression protects cone and rod photoreceptors in retinal degeneration. *J Clin Invest*,125(1): 105-116.

Cai Z, Hussain MD, Yan LJ. (2014). Microglia, neuroinflammation, and beta-amyloid protein in Alzheimer's disease. *Int J Neurosci*, 124: 307-321.

Campbell G, Mahad DJ. (2018). Mitochondrial dysfunction and axon degeneration in progressive multiple sclerosis. *FEBS Lett*, 592(7): 1113-1121.

Candiello J, Balasubramani M, Schrieber EM, Cole GJ, Mayer U, Halfter W, Lin H. (2007). Biomechanical properties of native basement membranes. *FEBS J*, 274(11): 2897-908.

Carvalho LS, Turunen HT, Wassmer SJ, Luna-Velez MV, Xiao R, Bennett J, Vandenberghe LH. (2017). Evaluating efficiencies of dual AAV approaches for retinal targeting. *Front Neurosci*, 11: 503.

Chaffiol A, Caplette R, Jaillard C, Brazhnikova E, Desrosiers M, Dubus E, Duhamel L, Mace E, Marre O, Benoit P, Hantraye P, Bemelmans AP, Bamberg E, Duebel J, Sahel JA, Picaud S, Dalkara D. (2017). A new promoter allows optogenetic vision restoration with enhanced sensitivity in macaque retina. *Mol Ther*, 25(11): 2546-2560.

Chang B, Hawes NL, Hurd RE, Davisson MT, Nusinowitz S, Heckenlively JR. (2002). Retinal degeneration mutants in the mouse. *Vision Res*, 42(4): 517-525.

Chavez A, Scheiman J, Vora S, Pruitt BW, Tuttle M, P R Iyer E, Lin S, Kiani S, Guzman CD, Wiegand DJ, Ter-Ovanesyan D, Braff JL, Davidsohn N, Housden BE, Perrimon N, Weiss R, Aach J, Collins JJ, Church GM. (2015). Highly efficient cas9-mediated transcriptional reprogramming. *Nat Methods.* 12(4): 326-8.

Chen WS, Xu PZ, Gottlob K, Chen ML, Sokol K, Shiyanova T, Roninson I, Weng W, Suzuki R, Tobe K, Kadowaki T, Hay N. (2001). Growth retardation and increased apoptosis in mice with homozygous disruption of the Akt1 gene. *Genes Dev*, 15(17): 2203-8.

Child DD, Lee JH, Pascua CJ, Chen YH, Mas Monteys A, Davidson BL. (2018). Cardiac mTORC1 dysregulation impacts stress adaptation and survival in Huntington's disease. *Cell Rep*, 23(4): 1020-1033.

Cho H, Mu J, Kim JK, Thorvaldsen JL, Chu Q, Crenshaw EB 3rd, Kaestner KH, Bartolomei MS, Shulman GI, Birnbaum MJ. (2001). Insulin resistance and a diabetes mellitus-like syndrome in mice lacking the protein kinase Akt2 (PKB beta). *Science,* 292(5522): 1728-31.

Cho H, Thorvaldsen JL, Chu Q, Feng F, Birnbaum MJ. (2001). Akt1/PKBalpha is required for normal growth but dispensable for maintenance of glucose homeostasis in mice. *J Biol Chem*, 276(42): 38349-52.

Choudhury SR, Fitzpatrick Z, Harris AF, et al. (2016). In vivo selection yields AAV-B1 capsid for central nervous system and muscle gene therapy. *Mol Ther.* 24(7):1247-1257.

Cong L, Ran FA, Cox D, Lin S, Barretto R, Habib N, Hsu PD, Wu X, Jiang W, Marraffini LA, Zhang F. (2013). Multiplex genome engineering using CRISPR/Cas9 systems. *Science*, 339(6121): 819-23.

Coo H, Aronson KJ. (2004). A systematic review of several potential non-genetic risk factors for multiple sclerosis. *Neuroepidemiology*, 23(1-2): 1-12.

Costello F, Coupland S, Hodge W, et al. (2006). Quantifying axonal loss after optic neuritis with optical coherence tomography. *Ann Neurol,* 59(6): 963-969.

Cronin T, Vandenberghe LH, Hantz P, et al. (2014). Efficient transduction and optogenetic stimulation of retinal bipolar cells by a synthetic adeno-associated virus capsid and promoter. *EMBO Mol Med,* 6(9):1175-1190.

Dalkara D, Byrne LC, Klimczak RR, Visel M, Yin L, Merigan WH, Flannery JG, Schaffer DV. (2013). In vivo-directed evolution of a new adeno-associated virus for therapeutic outer retinal gene delivery from the vitreous. *Sci Transl Med*, 5(189): 189ra76.

Dalkara D, Kolstad KD, Caporale N, Visel M, Klimczak RR, Schaffer DV, Flannery JG. (2009) Inner limiting membrane barriers to AAV-mediated retinal transduction from the vitreous. *Mol Ther*, 17(12): 2096-2102.

Davis BM, Crawley L, Pahlitzsch M, Javaid F, Cordeiro MF. (2016). Glaucoma: the retina and beyond. *Acta Neuropathol*, 132(6): 807-826.

Dejneka NS, Surace EM, Aleman TS, Cideciyan AV, Lyubarsky A, Savchenko A, Redmond TM, Tang W, Wei Z, Rex TS, Glover E, Maguire AM, Pugh EN Jr., Jacobson SG, Bennett J. (2004). In utero gene therapy rescues vision in a murine model of congenital blindness. *Mol Ther,* 9(2): 182-8.

Dendrou CA, Fugger L, Friese MA. (2015). Immunopathology of multiple sclerosis. *Nat Rev Immunol*, 15(9): 545-558.

Deverman BE, Pravdo PL, Simpson BP, et al. (2016). Cre-dependent selection yields AAV variants for widespread gene transfer to the adult brain. *Nat Biotechnol,* 34(2):204-209.

Deyle DR, Russell DW. (2009). Adeno-associated virus integration. *Curr Opin Mol Ther*, 11(4): 442-447.

Ding YW, Zhao GJ, Li XL, et al. (2016). SIRT1 exerts protective effects against paraquat-induced injury in mouse type II alveolar epithelial cells by deacetylating NRF2 in vitro. *Int J Mol Med*, 37(4): 1049-1058.

Dinkova-Kostova AT, Abramov AY. (2015). The emerging role of Nrf2 in mitochondrial function. *Free Radic Biol Med*, 88(Pt B): 179-188.

Dinkova-Kostova AT, Holtzclaw WD, Cole RN, et al. (2002). Direct evidence of sulfhydryl groups of KEAP1 are the sensors regulating induction of phase 2 enzymes that protect against carcinogens and oxidants. *Proc Natl Acad Sci U S A,* 99(18):11908-11913.

Dixon SJ, Stockwell BR. (2014). The role of iron and reactive oxygen species in cell death. *Nat Chem Biol*, 10(1): 9-17.

Dooley SJ, McDougald DS, Fisher KJ, Bennicelli JL, Mitchell LG, Bennett J. (2018). Spliceosome-mediated pre-mRNA trans-splicing can repair CEP290 mRNA. *Mol Ther Nucleic Acids*, 12: 294-308.

Doudna JA, Charpentier E. (2014). Genome editing. The new frontier of genome engineering with CRISPR-Cas9. *Science*, 346(6213): 1258096.

Dow LE. (2015). Modeling disease in vivo with CRISPR/Cas9. *Trends Mol Med*, 21(10): 609-621.

Dudek AM, Pillay S, Puschnik AS, Nagamine CM, Cheng F, Qiu J, Carette JE, Vandenberghe LH. (2018). An alternate route for adeno-associated virus (AAV) entry independent of AAV receptor. *J Virol,* 92(7):e02213-17.

Dudus L, Anand V, Acland GM, Chen SJ, Wilson JM, Fisher KJ, Maguire AM, Bennett J. (1999). Persistent transgene product in retina, optic nerve and brain after intraocular injection of rAAV. *Vision Res*, 39(15): 2545-53.

Easton RM, Cho H, Roovers K, Shineman DW, Mizrahi M, Forman MS, Lee VMY, Szabolcs M, de Jong R, Oltersdorf T, Ludwig T, Efstratiadis A, Birnbaum MJ. (2005). Role for AKT3/protein kinase Bγ in attainment of normal brain size. *Mol Cell Biol*, 25(5): 1869-1878.

Ebers GC, PRISMS. (1998). Randomised double-blind placebo-controlled study of interferon β-1a in relapsing/remitting multiple sclerosis. *Lancet*, 352(9139): 1498-504.

Elachouri G, Lee-Rivera I, Clerin E, Argentini M, Fridlich R, Blond F, Ferracane V, Yang Y, Raffelsberger W, Wan J, Bennett J, Sahel JA, Zack DJ, Leveillard T. (2015). Thioredoxin rod-derived cone viability factor protects against photooxidative retinal damage. *Free Radic Biol Med*, 81; 22-9.

Euler T, Haverkamp S, Schubert T, Baden T. (2014). Retinal bipolar cells: elementary building blocks of vision. *Nat Rev Neuro*, 15: 507-519.

Ferrari FK, Xiao X, McCarty D, Samulski RJ. (1997). New developments in the generation of Ad-free, high titer rAAV gene therapy vectors. *Nat Med*, 3(11): 1295-7.

Ferrari S, Di Lorio E, Barbaro V, Ponzin D, Sorrentino FS, Parmeggiani F. (2011). Retinitis pigmentosa: genes and disease mechanisms. *Curr Genomics*, 12(4): 238-249.

Finkel T. (2011). Signal transduction by reactive oxygen species. *J Cell Biol,* 194(1): 7-15.

Fisher JB, Jacobs DA, Markowitz CE, et al. (2006). Relation of visual function to retinal nerve fiber layer thickness in multiple sclerosis. *Ophthalmol,* 113(2): 324-332.

Flannery JG, Zolotukhin S, Vaquero MI, LaVail MM, Muzyczka N, Hauswirth WW. (1997). Efficient photoreceptor-targeted gene expression *in vivo* by recombinant adeno-associated virus. *Proc Natl Acad Sci U S A*, 94(13):6916-6921.

Fonseca-Kelly Z, Nassrallah M, Uribe J, et al. (2012). Resveratrol neuroprotection in a chronic mouse model of multiple sclerosis. *Front Neurol*, 3: 84.

Fontoura P. (2010). Monoclonal antibody therapy in multiple sclerosis. *MAbs*, 2(6): 670-681.

Forrester JV, Xu H. (2012). Good news-bad news: the yin and yang of immune privilege of the eye. *Front Immunol*, 3: 338.

Frias MA, Thoreen CC, Jaffe JD, Schroder W, Sculley T, Carr SA, Sabatini DM. (2006). mSin1 is necessary for AKT/PKB phosphorylation, and its isoforms define three distinct mTORC2s. *Curr Biol,* 16(18): 1865-70.

Friedmann T, Roblin R. (1972). Gene therapy for human genetic disease? *Science*, 175(4025): 949-55.

Fujita K, Nishiguchi KM, Shiga Y, Nakazawa T. (2017). Spatially and temporally regulated NRF2 gene therapy using Mcp-1 promoter in retinal ganglion cell injury. *Mol Ther Methods Clin Dev,* 5: 130-141.

Gal RL, Vedula SS, Beck R. (2015). Corticosteroids for treating optic neuritis. *Cochrane Database Syst Rev*, 8: CD001430.

Gao GP, Alvira MR, Wang L, Calcedo R, Johnston J, Wilson JM. (2002). Novel adeno-associated viruses from rhesus monkeys as vectors for human gene therapy. *Proc Natl Acad Sci USA*, 99(18): 11854-9.

Gargini C, Terzibasi E, Mazzoni F, Strettoi E. (2007). Retinal organization in the retinal degeneration 10 (rd10) mutant mouse: a morphological and ERG study. *J Comp Neurol*, 500(2): 222-228.

Goldman D. (2014). Muller glia cell reprogramming and retina regeneration. *Nat Rev Neurosci*, 15(7): 431-442.

Gorrini C, Harris IS, Mak TW. (2013). Modulation of oxidative stress as an anticancer strategy. *Nat Rev Drug Discov*, 12(12): 931-47.

Greenfield AL, Hauser SL. (2018). B-cell therapy for multiple sclerosis: entering an era. *Ann Neurol*, 83: 13-26.

Groenewoud MJ, Zwartkruis FJ. (2013). Rheb and rags come together at the lysosome to activate mTORC1. *Biochem Soc Trans,* 41(4): 951-5.

Gupta N, Brown KE, Milam AH. (2003). Activated microglia in human retinitis pigmentosa, late-onset retinal degeneration, and age-related macular degeneration. *Exp Eye Res*, 76: 463-471.

Guy J, Qi X, Hauswirth WW. (1998). Adeno-associated viral-mediated catalase expression suppresses optic neuritis in experimental allergic encephalomyelitis. *Proc Natl Acad Sci U S A,* 95(23): 13847-13852.

Haider L. (2015). Inflammation, iron, energy failure, and oxidative stress in the pathogenesis of multiple sclerosis. *Oxid Med Cell Longev*, 725370.

Hanlon KS, Chadderton N, Palfi A, Blanco Fernandez A, Humphries P, Kenna PF, Millington-Ward S, Farrar GJ. (2017). A novel retinal ganglion cell promoter for utility in AAV vectors. *Front Neurosci*, 11:521.

Hara K, Yonezawa K, Weng QP, Kozlowski MT, Belham C, Avruch J. (1998). Amino acid sufficiency and mTOR regulate p70 S6 kinase and eIF-4E BP1 through a common effector mechanism. *J Biol Chem,* 273(23): 14484-94.

Hartong DT, Berson EL, Dryja TP. (2006). Retinitis pigmentosa. *Lancet*, 368(9549): 1795-809.

Hauser SL, Bar-Or A, Comi G, Giovannoni G, Hartung HP, Hemmer B, Lublin F, Montalban X, Rammohan KW, Selmaj K, Traboulsee A, Wolinksy JS, et al. (2017). Ocrelizumab versus interferon beta-1a in relapsing multiple sclerosis. *N Eng J Med*, 376: 221-234.

Hauswirth WW, Aleman TS, Kaushal S, Cideciyan AV, Schwartz SB, Wang L, Conlon TJ, Boye SL, Flotte TR, Byrne BJ, Jacobson SG. (2008). Treatment of leber congenital amaurosis due to RPE65 mutations by ocular subretinal injection of adeno-associated virus gene vector: short-term results of a phase I trial. *Hum Gene Ther*, 19(10): 979-90.

Heppner FL, Greter M, Marino D, Falsig J, Raivich G, Hovelmeyer N, Waisman A, Rulicke T, Prinz M, Priller J, Becher B, Aguzzi A. (2005). Experimental autoimmune encephalomyelitis repressed by microglia paralysis. *Nat Med*, 11(2): 146-52.

Hickman SJ, Kapoor R, Jones SJ, Altmann DR, Plant GT, Miller DH. (2003). Corticosteroids do not prevent optic nerve atrophy following optic neuritis. *J Neurol Neurosurg Psychiatry*, 74(8): 1139-41.

Higashi C, Kawaji A, Tsuda N, Hayashi M, Saito R, Yagishita Y, Suzuki T, Uruno A, Nakamura M, Nakao K, Furusako S, Yamamoto M. (2017). The novel NRF2 inducer TFM-735 ameliorates experimental autoimmune encephalomyelitis in mice. *Eur J Pharmacol*, 802: 76-84.

Hirsch ML, Wolf SJ, Samulski RJ. (2016). Delivering transgenic DNA exceeding the carrying capacity of AAV vectors. *Methods Mol Biol*, 1382: 21-39.

Hoang QV, Linsenmeier RA, Chung CK, Curcio CA. (2002). Photoreceptor inner segments in monkey and human retina: mitochondrial density, optics, and regional variation. *Vis Neurosci*,19(4): 395-407.

Hunter MI, Nlemadim BC, Davidson DL. (1985). Lipid peroxidation products and antioxidant proteins in plasma and cerebrospinal fluid from multiple sclerosis patients. *Neurochem Res*, 10(12): 1645-52.

Huseby ES, Liggitt D, Brabb T, Schnabel B, Ohlen C, Goverman J. (2001). A pathogenic role for myelin-specific CD8(+) T cells in a model for multiple sclerosis. *J Exp Med*, 194(5): 669-76.

Huser D, Heilbronn R. (2003). Adeno-associated virus integrates site-specifically into human chromosome 19 in either orientation and with equal kinetics and frequency. *J Gen Virol*, 84(Pt 1): 133-7.

Inoki K, Li Y, Xu T, Guan KL. (2003). Rheb GTPase is a direct target of TSC2 GAP activity and regulates mTOR signaling. *Genes Dev*, 17(15): 1829-34.

International Human Genome Sequencing Consortium. (2001). Initial sequencing and análysis of the human genome. *Nature*, 409: 860-921.

Isiegas C, Marinich-Madzarevich JA, Machena M, Ruiz JM, Cano MJ, de la Villa P, Hernandez-Sanchez C, de la Rosa EJ, de Pablo F. (2016). Intravitreal injection of proinsulin-loaded microspheres delays photoreceptor cell death and vision loss in the rd10 mouse model of retinitis pigmentosa. *Invest Ophthalmol Vis Sci,* 57(8):3610-8.

Itoh K, Wakabayashi N, Katoh Y, Ishii T, Igarashi K, Engel JD, Yamamoto M. (1999). Keap1 represses nuclear activation of antioxidant response elements by Nrf2 through binding to the amino-terminal Neh2 domain. *Genes Dev*, 13(1): 76-86.

Itoh K, Wakabayashi N, Katoh Y, et al. (2003). Keap1 regulates both cytoplasmic-nuclear shuttling and degradation of NRF2 in response to electrophiles. *Genes Cells,* 8(4):379-391.

Jacinto E, Loewith R, Schmidt A, Lin S, Ruegg MA, Hall A, Hall MN. (2004). Mammalian TOR complex 2 controls the actin cytoskeleton and is rapamycin insensitive. *Nat Cell Biol*, 6: 1122-1128.

Jacobs LD et al. (1996). Intramuscular interferon beta-1a for disease progression in relapsing multiple sclerosis. The multiple sclerosis collaborative research group (MSCRG). *Ann Neurol*, 39(3): 285-294.

Jacobson SG, Acland GM, Aguirre GD, Aleman TS, Schwartz SB, Cideciyan AV, Zeiss CJ, Komaromy AM, Kaushal S, Roman AJ, Windsor EA, Sumaroka A, Pearce-Kelling SE, Conlon TJ, Chiodo VA, Boye SL, Flotte TR, Maguire AM, Bennett J, Hauswirth WW. (2006). Safety of recombinant adeno-associated virus type 2-RPE65 vector delivered by ocular subretinal injection. *Mol Ther*, 13(6): 1074-84.

Jeong H, Cohen DE, Cui L, et al. (2011). SIRT1 mediates neuroprotection from mutant huntingtin by activation of the TORC1 and CREB transcriptional pathway. *Nat Med*, 18(1):159-165.

Jeong J, Juhn K, Lee H, Kim SH, Min BH, Lee KM, Cho MH, Park GH, Lee KH. (2007). SIRT1 promotes DNA repair activity and deacetylation of Ku70. *Exp Mol Med*, 39(1): 8-13.

Jeong KH, Nam JH, Jin BK, Kim SR. (2015). Activation of CNTF/CNTFRα signaling pathway by hRheb(S16H) transduction of dopaminergic neurons in vivo. *PLOS One*, 10(3):e0121803.

Jiang P, Du W, Wu M. (2014). Regulation of the pentose phosphate pathway in cancer. *Protein Cell*, 5(8): 592-602.

Jinek M, East A, Cheng A, Lin S, Ma E, Doudna J. (2013). RNA-programmed genome editing in human cells. *Elife,* 2:e00471.

Johnson DA, Johnson JA. (2015). NRF2—a therapeutic target for the treatment of neurodegenerative diseases. *Free Radic Biol Med,* 88(Pt B):253-267.

Johnson DA, Amirahmadi S, Ward C, et al. (2010). The absence of the pro-antioxidant transcription factor NRF2 exacerbates experimental autoimmune encephalomyelitis. *Toxicol Sci,* 114(2):237-246.

Jones W, Bianchi K. (2015). Aerobic glycolysis: beyond proliferation. *Front Immunol*, 6: 227.

Jorgensen A, Wiencke AK, La Cour M, Kaestel CG, Madsen HO, Hamann S, Lui GM, Scherfig E, Prause JU, Svejgaard A, Odum N, Nissen MH, Ropke C. (1998). Human retinal pigment epithelial cell-induced apoptosis in activated T cells. *Invest Ophthalmol Vis Sci*, 39(9): 1590-9.

Kabadi AM, Ousterout DG, Hilton IB, Gersbach CA. (2014). Multiplex CRISPR/Cas9-based genome engineering from a single lentiviral vector. *Nucleic Acids Res*, 42(19): e147.

Kale N. (2016). Optic neuritis as an early sign of multiple sclerosis. *Eye Brain,* 8:195-202.

Kansanen E, Kivela AM, Levonen AL. (2009). Regulation of NRF2-dependent gene expression by 15-deoxy-$\Delta^{12,14}$-prostaglandin $J_2$. *Free Radic Biol Med*, 47(9): 1310-7.

Karassek S, Berghaus C, Schwarten M, Goemans CG, Ohse N, Kock G, Jockers K, Neumann S, Gottfried S, Herrmann C, Heumann R, Stoll R. (2010). Ras homolog enriched in brain (rheb) enhances apoptotic signaling. *J Biol Chem*, 285(44): 33979-91.

Karg E, Klivenyi P, Nemeth I, Bencsik K, Pinter S, Vecsei L. (1999). Nonenzymatic antioxidants of blood in multiple sclerosis. *J Neurol*, 246(7): 533-9.

Katoh Y, Iida K, Kang MI, Kobayashi A, Mizukami M, Tong KI, McMahon M, Hayes JD, Itoh K, Yamamoto M. (2005). Evolutionary conserved N-terminal domain of Nrf2 is essential for

the Keap1-mediated degradation of the protein by proteasome. *Arch Biochem Biophys*, 433(2): 342-50.

Katoh Y, Itoh K, Yoshida E, Miyagishi M, Fukamizu A, Yamamoto M. (2001). Two domains of Nrf2 cooperatively bind CBP, a CREB binding protein, and synergistically activate transcription. *Genes Cells*, 6(10): 857-868.

Kay CN, Ryals RC, Aslanidi GV, Min SH, Ruan Q, Sun J, Dyka FM, Kasuga D, Ayala AE, Van Vilet K, Agbandje-McKenna M, Hauswirth WW, Boye SL, Boye SE. (2013). Targeting photoreceptors via intravitreal delivery using novel, capsid-mutated AAV vectors. *PLOS One*, 8(4): e62097.

Khan RS, Dine K, Das Sarma J, et al. (2014). SIRT1 activating compounds reduce oxidative stress mediated neuronal loss in viral induced CNS demyelinating disease. *Acta Neuropathol Commun*, 2: 3.

Khan RS, Fonseca-Kelly Z, Callinan C, et al. (2012). SIRT1 activating compounds reduce oxidative stress and prevent cell death in neuronal cells. *Front Cell Neurosci*, 6: 63.

Khani SC, Pawlyk BS, Bulgakov OV, Kasperek E, Young JE, Adamian M, Sun X, Smith AJ, Ali RR, Li T. (2017). AAV-mediated expression targeting of rod and cone photoreceptors with a human rhodopsin kinase promoter. *Invest Ophthalmol Vis Sci,* 48(9):3954-61.

Kim D, Nguyen MD, Dobbin MM, et al. (2007). SIRT1 deacetylase protects against neurodegeneration in models for alzheimer's disease and amyotrophic lateral sclerosis. *EMBO J,* 26(13): 3169-79.

Kim SR, Kareva T, Yarygina O, Kholodilov N, Burke RE. (2012). AAV transduction of dopamine neurons with constitutively active rheb protects from neurodegeneration and mediates axon regrowth. *Mol Ther*, 20(2):275-86.

Kimbrel EA, Lanza R. (2015). Current status of pluripotent stem cells: moving the first therapies to the clinic. *Nat Rev Drug Discov*, 14(10): 681-92.

Kolb H. (2003). How the retina works. *American Scientist*, 91: 28-35.

Kolb H, Fernandez E, Nelson R [editors]. (2007). WebVision: the organization of the retina and visual system. Retrieved from https://webvision.med.utah.edu/.

Komeima K, Rogers BS, Lu L, Campochiaro PA. (2006). Antioxidants reduce cone cell death in a model of retinitis pigmentosa, 103(30): 11300-5.

Komeima K, Rogers BS, Campochiaro PA. (2007). Antioxidants slow photoreceptor cell death in mouse models of retinitis pigmentosa. *J Cell Physiol*, 213(3): 809-15.

Kovac S, Angelova PR, Holmstrom KM, Zhang Y, Dinkova-Kastova AT, Abramov AY. (2015). Nrf2 regulates ROS production by mitochondria and NADPH oxidase. *Biochim Biophys Acta*, 1850(4): 794-801.

Kurata M, Yamamoto K, Moriarity BS, Kitagawa M, Largaespada DA. (2018). CRISPR/Cas9 library screening for drug target discovery. *J Hum Genet*, 63(2): 179-186.

La Mantia L, Vacchi L, Di Pietrantonj C, Ebers G, Rovaris M, Fredrikson S, Filippini G. (2012). Interferon beta for secondary progressive multiple sclerosis. *Cochrane Database Syst Rev*, CD005181.

Langemann H, Kabiersch A, Newcombe J. (1992). Measurement of low-molecular-weight antioxidants, uric acid, trysine, and tryptophan in plaques and white matter from patients with multiple sclerosis. *Eur Neurol*, 32(5): 248-52.

Larabee CM, Desai S, Agasing A, et al. (2016). Loss of Nrf2 exacerbates the visual deficits and optic neuritis elicited by experimental autoimmune encephalomyelitis. *Mol Vis,* 22:1503-1513.

Lassmann H, van Horssen J. (2016). Oxidative stress and its impact on neurons and glia in multiple sclerosis. *Biochimica et Biophysica Acta*, 1862: 506-510.

Lassmann H, van Horseen J, Mahad D. (2012). Progressive multiple sclerosis: pathology and pathogenesis. *Nat Rev Neuro*, 8: 647-656.

Lebherz C, Maguire A, Tang W, Bennett J, Wilson JM. (2008). Novel AAV serotypes for improved ocular gene transfer. *J Gene Med*, 10(4): 375-82.

Lee JH, Tecedor L, Chen YH, Monteys AM, Sowada MJ, Thompson ML, Davidson BL. (2015). Reinstating aberrant mTORC1 activity in Huntington's disease mice improves disease phenotypes. *Neuron*, 85(2): 303-15.

Leonard KC, Petrin D, Coupland SG, Baker AN, Leonard BC, LaCasse EC, Hauswirth WW, Korneluk RG, Tsilfidis C. (2007). XIAP protection of photoreceptors in animal models of retinitis pigmentosa. *PLOS One*, 2(3): e314.

Li A, Zhu X, Craft CM. (2002). Retinoic acid upregulates cone arrestin expression in retinoblastoma cells through a cis element in the distal promoter region. *Invest Ophthalmol Vis Sci*, 43(5):1375-83.

Liang FQ, Aleman TS, Dejneka NS, Dudus L, Fisher KJ, Maguire AM, Jacobson SG, Bennett J. (2001). Long-term protection of retinal structure but not function using RAAV.CNTF in animal models of retinitis pigmentosa. *Mol Ther*, 4(5): 461-72.

Liang FQ, Dejneka NS, Cohen DR, Krasnoperova NV, Lem J, Maguire AM, Dudus L, Fisher KJ, Bennett J. (2001). AAV-mediated delivery of ciliary neurotrophic factor prolongs photoreceptor survival in the rhodopsin knockout mouse. *Mol Ther,* 3(2): 241-8.

Liang KJ, Woodart KT, Weaver MA, Gaylor JP, Weiss ER, Samulski RJ. (2017). AAV-Nrf2 promotes protection and recovery in animal models of oxidative stress. *Mol Ther,* 25(3): 765-779.

Liao HK, Hatanaka F, Araoka T, Reddy P, Wu MZ, Sui Y, Yamauchi T, Sakurai M, O'Keefe DD, Nunez-Delicado E, Guillen P, Campistol JM, Wu CJ, Lu LF, Estaban CR, Izpisua Belmonte JC. (2017). In vivo target gene activation via CRISPR/Cas9-mediated trans-epigenetic modulation. *Cell*, 171(7): 1495-1507.

Lim JH, Stafford BK, Nguyen PL, Lien BV, Wang C, Zukor K, He Z, Huberman AD. (2016). Neural activity promotes long-distance, target-specific regeneration of adult retinal axons. *Nat Neurosci*, 19(8):1073-84.

Linington C, Bradl M, Lassmann H, Brunner C, Vass K. (1988). Augmentation of demyelination in rat acute allergic encephalomyelitis by circulating mouse monoclonal antibodies against a myelin/oligodendrocyte glycoprotein. *Am J Pathol*, 130(3): 443-454.

Long T, Yang Y, Peng L, Li Z. (2018). Neuroprotective effects of melatonin on experimental allergic encephalomyelitis mice via anti-oxidative stress activity. *J Mol Neurosci*, 64(2): 233-241.

Lotery AJ, Yang GS, Mullins RF, Russell SR, Schmidt M, Stone EM, Lindbloom JD, Chiorini JA, Kotin RM, Davidson BL. (2003). Adeno-associated virus type 5: transduction efficiency and cell-type specificity in the primate retina. *Hum Gene Ther*, 14(17): 1663-71.

Louis Jeune V, Joergensen JA, Hajjar RJ, Weber T. (2013). Pre-existing anti-adeno-associated virus antibodies as a challenge in a AAV gene therapy. *Hum Gene Ther Methods*, 24(2): 59-67.

Lu L, Oveson BC, Jo YJ, Lauer TW, Usui S, Komeima K, Xie B, Campochiaro PA. (2009). Increased expression of glutathione peroxidase 4 strongly protects retina from oxidative damage. *Antioxid Redox Signal,* 11(4): 715-24.

Lu Q, Ganjawala TH, Ivanova E, Cheng JG, Troilo D, Pan ZH. (2016). AAV-mediated transduction and targeting of retinal bipolar cells with improved mGluR6 promoters in rodents and primates. *Gene Ther,* 23(8-9): 680-9.

Lucin KM, Wyss-Coray T. (2009). Immune activation in brain aging and neurodegeneration: too much or too little? *Neuron*, 64: 110-122.

Lublin FD. (1984). Role of myelin antigens in murine relapsing experimental allergic encephalomyelitis. *J Clin Lab Immunol*, 13:179–182.

Luo J, Nikolaev AY, Imai S, Chen D, Su F, Shiloh A, Guarente L, Gu W. (2001). Negative control of p53 by sir2alpha promotes cell survival under stress. *Cell*, 107(2):137-48.

Maguire AM, High KA, Auricchio A, Wright JF, Pierce EA, Testa F, Mingozzi F, Bennicelli JL, Ying GS, Rossi S, Fulton A, Marshall KA, Banfi S, Chung DC, Morgan JI, Hauck B, Zelenaia O, Zhu X, Raffini L, Coppieters F, De Baere E, Shindler KS, Volpe NJ, Surace EM, Acerra C, Lybarsky A, Redmond TM, Stone E, Sun J, McDonnell JW, Leroy BP, Simonelli F, Bennett J. (2009). Age-dependent effects of RPE65 gene therapy for Leber's congenital amaurosis: a phase 1 dose-escalation trial. *Lancet,* 374(9701): 1597-605.

Maguire AM, Simonelli F, Pierce EA, Pugh EN Jr., Mingozzi F, Bennicelli J, Banfi S, Marshall KA, Testa F, Surace EM, Rossi S, Lyubarsky A, Arruda VR, Konkle B, Stone E, Sun J, Jacobs J, Dell'Osso L, Hertle R, Ma JX, Redmond TM, Zhu X, Hauck B, Zelenaia O, Shindler KS, Maguire MG, Wright JF, Volpe NJ, McDonnell JW, Auricchio A, High KA, Bennett J. (2008). Safety and efficacy of gene transfer for Leber's congenital amaurosis. *N Engl J Med*, 358(21): 2240-8.

Mahad DH, Trapp BD, Lassmann H. (2015). Pathological mechanisms in progressive multiple sclerosis. *Lancet Neurol*, 14: 183-93.

Maier K, Rau CR, Storch MK, Sattler MB, Demmer I, Weissert R, Taheri N, Kuhnert AV, Bahr M, Diem R. (2004). Ciliary neurotrophic factor protects retinal ganglion cells from secondary cell death during acute autoimmune optic neuritis in rats. *Brain Pathol*, 14(4): 378-387.

Malagelada C, Jin ZH, Jackson-Lewis V, Przedborski S, Greene LA. (2010). Rapamycin protects against neuron death in in vitro and in vivo models of Parkinson's disease. *J Neurosci*, 30(3): 1166-75.

Mali P, et al. (2013). Cas9 transcriptional activators for target specificity screening and paired nickases for cooperative genome engineering. *Nat Biotechnol,* 31:833–838.

Martin A, Tegla CA, Cudrici CD, et al. (2015). Role of SIRT1 in autoimmune demyelination and neurodegeneration. *Immunol Res,* 61(3):187-197.

Martinez-Fernandez de la Camara C, Salom D, Dolores Sequedo M, Hervas D, Marin-Lambies C, Aller E, Jaijo T, Diaz-Llopis M, Maria Milan J, Rodrigo R. (2013). Altered antioxidant-oxidant status in the aqueous humor and peripheral blood of patients with retinitis pigmentosa. *PLOS One*, 8(9): e74223.

Massof RW, Finkelstein D. (1993). Supplemental vitamin A retards loss of ERG amplitudes in retinitis pigmentosa. *Arch Ophthalmol*, 111: 751-754.

Maver A, Lavtar P, Ristic S, Stopinsek S, Simcic S, Hocever K, Sepcic J, Drulovic J, Pekmezovic T, Novakovic I, Alenka H, Rudolf G, Sega S, Starcevic-Cizmarevic N, Palandacic A, Zamolo G, Kapovic M, Likar T, Peterlin B. (2017). Identification of rare genetic variation of NLRP1 gene in familial multiple sclerosis. *Sci Rep*, 7(1): 3715.

Mays LE, Wang L, Lin J, Bell P, Crawford A, Wherry EJ, Wilson JM. (2014). AAV8 induces tolerance in murine muscle as a result of poor APC transduction, T cell exhaustion, and minimal MHCI upregulation on target cells. *Mol Ther,* 22(1): 28-41.

McCarty DM, Young SM Jr, Samulski RJ. (2004). Integration of adeno-associated virus (AAV) and recombinant vectors. *Annu Rev Genet*, 38: 819-45.

McDougald DS, Dine KE, Zezulin AU, Bennett J, Shindler KS. (2018). SIRT1 and NRF2 gene transfer mediate distinct neuroprotective effects upon retinal ganglion cell survival and function in experimental optic neuritis. *Invest Ophthalmol Vis Sci,* 59(3): 1212-1220.

McIlhinney RA. (1998). Membrane targeting via protein N-myristoylation. *Methods Mol Biol*. 88: 211-25.

McMahon M, Itoh K, Yamamoto M, et al. (2003). Keap1-dependent proteasomal degradation of transcription factor NRF2 contributes to negative regulation of antioxidant response element-driven gene expression. *J Biol Chem,* 278(24):21592-21600.

Mei X, Chaffiol A, Kole C, Yang Y, Millet-Puel G, Clerin E, Ait-ali N, Bennett J, Dalkara D, Sahel JA, Duebel J, Leveillard T. (2016). The thioredoxin encoded by the rod-derived cone viability factor gene protects cone photoreceptors against oxidative stress. *Antioxid Redox Signal*, 24(16): 909-23.

Merry TL, Ristow M. (2016). Nuclear factor erythroid-derived 2-like 2 (NFE2L2, Nrf2) mediates exercise-induced mitochondrial biogenesis and the anti-oxidant response in mice. *J Physiol*, 594(18): 5195-207.

Miao L, Yang L, Huang H, Liang F, Ling C, Hu Y. (2016). mTORC1 is necessary but mTORC2 and GSK3B are inhibitory for AKT3-induced axonal regeneration in the central nervous system. *Elife,* 5:e14908.

Michan S, Sinclair D. (2007). Sirtuins in mammals: insights into their biological function. *Biochem J*, 404(1): 1-13.

Mingozzi F, High KA. (2011). Therapeutic in vivo gene transfer for genetic disease using AAV: progress and challenges. *Nat Rev Genet*, 12(5): 341-55.

Mingozzi F, High KA. (2013). Immune responses to AAV vectors: overcoming barriers to successful gene therapy. *Blood,* 122(1): 23-36.

Mitsuishi Y, Motohashi H, Yamamoto M. (2012). The Keap1-NRF2 system in cancers: stress response and anabolic metabolism. *Front Oncol*, 2:200.

Moi P, Chan K, Asunis I, Cao A, Kan YW. (1994). Isolation of NF-E2-related factor 2 (Nrf2), a NF-E2-like basic leucine zipper transcriptional activator that binds to the tandem NF-E2/AP1 repeat of the beta-globin locus control region. *Proc Natl Acad Sci U S A*, 91(21): 9926-9930.

Montalban X, Hauser SL, Kappos L, Arnold DL, Bar-Or A, Comi G, de Seze J, Giovannoni G, Hartung HP, Hemmer B, Lublin F, Rammohan KW, Selmaj K, Traboulsee A, Sauter A, Masterman D, Fontoura P, Belachew S, Garren H, Mairon N, Chin P, Wolinsky JS. (2017). Ocrelizumab versus placebo in primary progressive multiple sclerosis. *N Eng J Med*. 376: 209-220.

Mowat FM, Gornik KR, Dinculescu A, Boye SL, Hauswirth WW, Petersen-Jones SM, Bartoe JT. (2014). Tyrosine capsid-mutant AAV vectors for gene delivery to the canine retina from a subretinal or intravitreal approach. *Gene Ther*, 21(1): 96-105.

Na SY, Cao Y, Toben C, Nitschke L, Stadelmann C, Gold R, Schimpl A, Hunig T. (2008). Naïve CD8 T-cells initiate spontaneous autoimmunity to a sequestered model antigen of the central nervous system. *Brain*, 131(Pt 9): 2353-65.

Naidoo R, Knapp ML. (1992). Studies of lipid peroxidation products in cerebrospinal fluid and serum in multiple sclerosis and other conditions. *Clin Chem*, 38(12): 2449-54.

Navarro E, Gonzalez-Lafuente L, Perez-Liebana I, Buendia I, Lopez-Bernardo E, Sanchez-Ramos C, Prieto I, Cuadrado A, Satrustegui J, Cadenas S, Monsalve M, Lopez MG. (2017). Heme-oxygenase I and PGC-1a regulate mitochondrial biogenesis via microglial

activation of alpha7 nicotinic acetylcholine receptors using PNU282987. *Antioxid Redox Signal*, 27(2): 93-105.

Nemoto S, Fergusson MM, Finkel T. (2005). SIRT1 functionally interacts with the metabolic regulator and transcriptional coactivator PGC-1α. *J Biol Chem,* 280(16): 16456-16460.

Nimmagadda VK, Bever CT, Vattikunta NR, et al. (2013). Overexpression of SIRT1 protein in neurons protects against experimental autoimmune encephalomyelitis through activation of multiple SIRT1 targets. *J Immunol,* 190(9): 4595-4607.

Nioi P, Nguyen T, Sherratt PJ, Pickett CB. (2005). The carboxy-terminal Neh3 domain of Nrf2 is required for transcriptional activation. *Mol Cell Biol*, 25(24): 10895-10906.

Nojima H, Tokunaga C, Eguchi S, Oshiro N, Hidayat S, Yoshino K, Hara K, Tanaka N, Avruch J, Yonezawa K. (2003). The mammalian target of rapamycin (mTOR) partner, raptor, binds the mTOR substrates p70 S6 kinase and 4E-BP1 through their TOR signaling (TOS) motif. *J Biol Chem*, 278(18): 15461-4.

Paty DW, Li DK. (1993). Interferon beta-1b is effective in relapsing-remitting multiple sclerosis. II. MRI analysis results of a multicenter, randomized, double-blind, placebo-controlled trial. UBC MS/MRI study group and IFNB multiple sclerosis study group. *Neurology*, 43(4): 662-7.

Perez-Pinera P, Kocak DD, Vockley CM, Adler AF, Kabadi AM, Polstein LR, Thakore PI, Glass KA, Ousterout DG, Leong KW, Guilak F, Crawford GE, Reddy TE, Gersbach CA. (2013). RNA-guided gene activation by CRISPR-Cas9-based transcription factors. *Nat Methods,* 10(10): 973-976.

Perkins GA, Ellisman MH, Fox DA. (2003). Three-dimensional analysis of mouse rod and cone mitochondrial cristae architecture: bioenergetics and functional implications. *Mol Vis*, 9: 60-73.

Peterson TR, Laplante M, Thoreen CC, Sancak Y, Kang SA, Kuehl WM, Gray NS, Sabatini DM. (2009). DEPTOR is an mTOR inhibitor frequently overexpressed in multiple myeloma cells and required for their survival. *Cell*, 137: 873-886.

Petersen-Jones SM, Occelli LM, Winkler PA, Lee W, Sparrow JR, Tsukikawa M, Boye SL, Chiodo V, Capasso JE, Becirovic E, Schon C, Seeliger MW, Levin AV, Michalakis S, Hauswirth WW, Tsang SH. (2018). Patients and animal models of CNGβ1-deficient retinitis pigmentosa support gene augmentation approach. *J Clin Invest*, 128(1):190-206.

Petit L, Ma S, Cipi J, Cheng SY, Zieger M, Hay N, Punzo C. (2018). Aerobic glycolysis is essential for normal rod function and controls secondary cone death in retinitis pigmentosa. *Cell Rep*, 23(9): 2629-2642.

Petrin D, Baker A, Coupland SG, Liston P, Narang M, Damji K, Leonard B, Chiodo VA, Timmers A, Hauswirth W, Korneluk RG, Tsilfidis C. (2003). Structural and functional protection of photoreceptors from MNU-induced retinal degeneration by the X-linked inhibitor of apoptosis. *Invest Ophthalmol Vis Sci*, 44(6): 2757-63.

Petrs-Silva H, Dinculescu A, Li Q, Min SH, Chiodo V, Pang JJ, Zhong L, Zolotukhin S, Srivastava A, Lewin AS, Hauswirth WW. (2009). High-efficiency transduction of the mouse retina by tyrosine-mutant AAV serotype vectors. *Mol Ther,* 17(3): 463-471.

Petrs-Silva H, Dinculescu A, Li Q, Deng WT, Pang J, Min SH, Chiodo V, Neeley AW, Govindasamy L, Bennett A, Agbandje-McKenna M, Zhong L, Li B, Jayandharan GR, Srivastava A, Lewin AS, Hauswirth WW. (2011). Novel properties of tyrosine-mutant AAV vectors in the mouse retina. *Mol Ther,* 19(2): 293-301.

Pettinelli CB, McFarlin DE. (1981). Adoptive transfer of experimental allergic encephalomyelitis in SJL/J mice after in vitro activation of lymph node cells by myelin basic protein: requirement for Lyt 1+2- T lymphocytes. *J Immunol,* 127(4): 1420-3.

Piantadosi CA, Carraway MS, Babiker A, Suliman HB. (2008). Hemo oxygenase-1 regulates cardiac mitochondrial biogenesis via Nrf2-dependent transcriptional control of nuclear respiratory factor-1. *Circ Res*, 103(11): 1232-40.

Pillay S, Meyer NL, Puschnik AS, Davulcu O, Diep J, Ishikawa Y, Jae LT, Wosen JE, Nagamine CM, Chapman MS, Carette JE. (2016). An essential receptor for adeno-associated virus infection. *Nature*, 530(7588):108-12.

Pillay S, Zou W, Cheng F, Puschnik AS, Meyer NL, Ganaie SS, Deng X, Wosen JE, Davulcu O, Yan Z, Engelhardt JF, Brown KE, Chapman MS, Qiu J, Carette JE. (2017). AAV serotypes have distinctive interactions with domains of the cellular receptor AAVR. *J Virol*, 91(18):e00391-17.

Potheraveedu VN, Schopel M, Stoll R, Heumann R. (2017). Rheb in neuronal degeneration, regeneration, and connectivity. *Biol Chem*, 398(5-6): 589-606.

Prusky GT, Alam NM, Beekman S, et al. (2004). Rapid quantification of adult and developing mouse spatial vision using a virtual optomotor system. *Invest Ophthalmol Vis Sci*, 45: 4611–4616.

Punzo C, Kornacker K, Cepko CL. (2009). Stimulation of the insulin/mTOR pathway delays cone death in a mouse model of retinitis pigmentosa. *Nat Neurosci*, 12(1): 44-52.

Punzo C, Xiong W, Cepko CL. (2012). Loss of daylight vision in retinal degeneration: are oxidative stress and metabolic dysregulation to blame? *J Biol Chem*, 287(3): 1642-8.

Qi LS, Larson MH, Gilbert LA, Doudna JA, Weissman JS, Arkin AP, Lim WA. (2013). Repurposing CRISPR as an RNA-guided platform for sequence-specific control of gene expression. *Cell*, 152(5): 1173-1183.

Qi X, Lewin AS, Sun L, Hauswirth WW, Guy J. (2006). Mitochondrial protein nitration primes neurodegeneration in experimental autoimmune encephalomyelitis. *J Biol Chem*, 281(42): 31950-62.

Qi X, Lewin AS, Sun L, Hauswirth WW, Guy J. (2007). Suppression of mitochondrial oxidative stress provides long-term neuroprotection in experimental optic neuritis. *Invest Ophthalmol Vis Sci*, 48(2): 681-91.

Qi X, Sun L, Lewin AS, Hauswirth WW, Guy J. (2007). Long-term suppression of neurodegeneration in chronic experimental optic neuritis: antioxidant gene therapy. *Invest Ophthalmol Vis Sci*, 48(12): 5360-70.

Quinn TA, Dutt M, Shindler KS. (2011). Optic neuritis and retinal ganglion cell loss in a chronic murine model of multiple sclerosis. *Front Neurol,* 2(50).

Rajala A, Wang Y, Rajala RVS. (2018). Constitutive activation mutant mTOR promote cone survival in retinitis pigmentosa mice. *Adv Exp Med Biol*, 1074: 491-497.

Ramachandran PS, Lee V, Wei Z, Song JY, Casal G, Cronin T, Willett K, Huckfeldt R, Morgan JI, Aleman TS, Maguire AM, Bennett J. (2017). Evaluation of dose and safety of AAV7m8 and AAV8BP2 in the non-human primate retina. *Hum Gene Ther*, 28(2): 154-167.

Ravikumar B, Vacher C, Berger Z, Davies JE, Luo S, Oroz LG, Scaravilli F, Easton DF, Duden R, O'Kane CJ, Rubinsztein DC. (2004). Inhibition of mTOR induces autophagy and reduces toxicity of polyglutamine expansions in fly and mouse models of Huntington disease. *Nat Genet*, 36(6): 585-595.

Rayapudi S, Schwartz SG, Wang X, Chavis P. (2013). Vitamin A and fish oils for retinitis pigmentosa. *Cochrane Database Syst Rev*, 12: CD008428.

Reichenbach A, Bringmann A. (2013). New functions of muller cells. *Glia*, 61(5): 651-78.

RetNet: retinal information network. (2018, September 18). Retrieved from https://sph.uth.edu/retnet/.

Ries V, Henchcliffe C, Kareva T, Rzhetskaya M, Bland R, During MJ, Kholodilov N, Burke RE. (2006). Oncoprotein AKT/PKB induces trophic effects in murine models of Parkinson's disease. *Proc Natl Acad Sci U S A,* 103(49): 18757-18762.

Rog DJ, Mottershead JP. (2006). The role of interferon beta in multiple sclerosis management. *Future Prescriber*, 7(3): 15-19.

Rudick RA, Goelz SE. (2011). Beta-interferon for multiple sclerosis. *Exp Cell Res*, 317(9): 1301-11.

Russell S, Bennett J, Wellman JA, Chung DC, Yu ZF, Tillman A, Wittes J, Pappas J, Elci O, McCague S, Cross D, Marshall KA, Walshire J, Kehoe TL, Reichert H, Davis M, Raffini L, George LA, Hudson FP, Dingfield L, Zhu X, Haller JA, Sohn EH, Mahajan VB, Pfeifer W, Weckmann M, Johnson C, Gewaily D, Drack A, Stone E, Wachtel K, Simonelli F, Leroy BP, Wright JF, High KA, Maguire AM. (2017). Efficacy and safety of voretigene neparvovec (AAV2-hRPE65v2) in patients with RPE65-mediated inherited retinal dystrophy: a randomized, controlled, open-label, phase 3 trial. *Lancet*, 390(10097): 849-860.

Saijo K, Glass CK. (2011). Microglial cell origin and phenotypes in health and disease. *Nat Rev Immunol,* 11: 775-787.

Salganik M, Hirsch ML, Samulski RJ. (2015). Adeno-associated virus as a mammalian DNA vector. *Microbiol Spectr,* 3(4): doi:10.1128/microbiolspec.MDNA3-0052-2014.

Sancak Y, Thoreen CC, Peterson TR, Lindquist RA, Kang SA, Spooner E, Carr SA, Sabatini DM. (2007). PRAS40 is an insulin-regulated inhibitor of the mTORC1 protein kinase. *Mol Cell*, 25: 903-915.

Santiago CP, Keuthan CJ, Boye SL, Boye SE, Imam AA, Ash JD. (2018). A drug-tunable gene therapy for broad-spectrum protection against retinal degeneration. *Mol Ther,* S1525-0016(18)30341-1.

Sarbassov DD, Ali SM, Kim DH, Guertin DA, Latek RR, Erdjument-Bromage H, Tempst P, Sabatini DM. (2004). Rictor, a novel binding partner of mTOR, defines a rapamycin-insensitive and raptor-independent pathway that regulates the cytoskeleton. *Curr Biol*, 14: 1296-1302.

Sarchielli P, Orlacchio A, Vicinanza F, Pelliccioli GP, Tognoloni M, Saccardi C, Gallai V. (1997). Cytokine secretion and nitric oxide production by mononuclear cells of patients with multiple sclerosis. *J Nueroimmunol*, 80(1-2): 76-86.

Sato T, Nakashima A, Guo L, Tamanoi F. (2009). Specific activation of mTORC1 by Rheb G-protein in vitro involves enhanced recruitment of its substrate protein. *J Biol Chem*, 284: 12783-12791.

Saxena A, Bauer J, Scheikl T, Zappulla J, Audebert M, Desbois S, Waisman A, Lassmann H, Liblau RS, Mars LT. (2008). Cutting edge: multiple sclerosis-like lesions induced by effector CD8 T cells recognizing a sequestered antigen on oligodendrocytes. *J Immunol*, 181(3): 1617-21.

Saxton RA, Sabatini DM. (2017). mTOR signaling in growth, metabolism, and disease. *Cell*, 169(2): 361-371.

Shalem O, Sanjana NE, Hartenian E, Shi X, Scott DA, Mikkelsen TS, Heckl D, Ebert BE, Root DE, Doench JG, Zhang F. (2014). Genome-scale CRISPR-Cas9 knockout screening in human cells. *Science*, 343(6166): 84-87.

Shen J, Yang X, Dong A, Petters RM, Peng YW, Wong F, Campochiaro PA. (2005). Oxidative damage is a potential cause of cone cell death in retinitis pigmentosa. *J Cell Physiol*, 203(3): 457-64.

Shindler KS, Ventura E, Dutt M, et al. (2010). Oral resveratrol reduces neuronal damage in a model of multiple sclerosis. *J Neuroophthalmol*, 30: 328–339.

Shindler KS, Ventura E, Rex TS, Elliott P, Rostami A. (2007). SIRT1 activation confers neuroprotection in experimental optic neuritis. *Invest Ophthalmol Vis Sci*, 48(8): 3602-3609.

Shu Q, Xu Y, Zhuang H, Fan J, Sun Z, Zhang M, Xu G. (2014). Ras homolog enriched in brain is linked to retinal ganglion cell apoptosis after light injury in rats. *J Mol Neurosci*, 54(2): 243-51.

Simonelli F, Maguire AM, Testa F, Pierce EA, Mingozzi F, Bennicelli JL, Rossi S, Marshall K, Banfi S, Surace EM, Sun J, Redmond TM, Zhu X, Shindler KS, Ying GS, Ziviello C, Acerra C, Wright JF, McDonnell JW, High KA, Bennett J, Auricchio A. (2010). Gene therapy for Leber's congenital amaurosis is safe and effective through 1.5 years after vector administration. *Mol Ther,* 18(3): 643-50.

Sochor MA, Vasireddy V, Drivas TG, Wojno A, Doung T, Shpylchak I, Bennicelli J, Chung D, Bennett J, Lewis M. (2015). An autogenously regulated expression system for gene therapeutic ocular applications. *Sci Rep,* 5: 17105.

Sospedra M, Martin R. (2016). Immunology of multiple sclerosis. *Semin Neurol*, 36(2): 115-27.

Sparrow JR, Hicks D, Hamel CP. (2010). The retinal pigment epithelium in health and disease. *Curr Mol Med*, 10(9): 802-823.

Spilman P, Podlutskaya N, Hart MJ, Debnath J, Gorostiza O, Bredesen D, Richardson A, Strong R, Galvan V. (2010). Inhibition of mTOR by rapamycin abolishes cognitive deficits and

reduces amyloid-β levels in a mouse model of Alzheimer's disease. *PLOS One*, 5(4): e9979.

Srivastava A. (2016). In vivo tissue-tropism of adeno-associated viral vectors. *Curr Opin Virol*, 21:75-80.

Stein-Streilein J, Taylor AW. (2007). An eye's view of T regulatory cells. *J Leukoc Biol*, 81(3): 593-8.

Sugita Y, Miura K, Araki F, et al. (2013). Contributions of retinal direction-selective ganglion cells to optokinetic responses in mice. *Eur J Neurosci,* 38(6):2823-2831.

Sun D, Whitaker JN, Huang Z, Liu D, Coleclough C, Wekerle H, Raine CS. (2001). Myelin antigen-specific $CD8^+$ T cells are encephalitogenic and produce severe disease in C57BL/6 mice. *J Immunol*, 166(12): 7579-87.

Syed YY. (2018). Ocrelizumab: a review in multiple sclerosis. *CNS Drugs,* 1-8.

Takahashi K, Igarashi T, Miyake K, Kobayashi M, Yaguchi C, Lijima O, Yamazaki Y, Katakai Y, Miyake N, Kameya S, Shimada T, Takahashi H, Okada T. (2017). Improved intravitreal AAV-mediated inner retinal gene transduction after surgical internal limiting membrane peeling in cynomolgus monkeys. *Mol Ther,* 25(1): 296-302.

Talla V, Yu H, Chou TH, Porciatti V, Chiodo V, Boye SL, Hauswirth WW, Lewin AS, Guy J. (2013). NADH-dehydrogenase type-2 suppresses irreversible visual loss and neurodegeneration in the EAE model of MS. *Mol Ther*, 21(10):1876-88.

Talla V, Porciatti V, Chiodo V, Boye SL, Hauswirth WW, Guy J. (2014). Gene therapy with mitochondrial heat shock protein 70 suppresses visual loss and optic atrophy in experimental autoimmune encephalomyelitis. *Invest Ophthalmol Vis Sci*, 55(8): 5214-5226.

Talla V, Koilkonda R, Porciatti V, Chiodo V, Boye SL, Hauswirth WW, Guy J. (2015). Complex I subunit gene therapy with NDUFA6 ameliorates neurodegeneration in EAE. *Invest Ophthalmol Vis Sci,* 56(2): 1129-40.

Thomas CE, Ehrhardt A, Kay MA. (2003). Progress and problems with the use viral vectors for gene therapy. *Nat Rev Genet*, 4(5): 346-358.

Trachsel-Moncho L, Benlloch-Navarro S, Fernandez-Carbonell A, Ramirez-Lamelas DT, Olivar T, Silvestre D, Poch E, Miranda M. (2018). Oxidative stress and autophagy-related changes during retinal degeneration and development. *Cell Death Dis*, 9(8): 812.

Tratschin JD, West MH, Sandbank T, Carter BJ. (1984). A human parvovirus, adeno-associated virus, as a eucaryotic vector: transient expression and encapsidation of the procaryotic gene for chloramphenicol acetyltransferase. *Mol Cell Biol*, 4(10): 2072-2081.

Trip SA, Schlottmann PG, Jones SJ, et al. (2005). Retinal nerve fiber layer axonal loss and visual dysfunction in optic neuritis. *Ann. Neurol,* 58: 383-391.

Uren AG, Kool J, Berns A, van Lohuizen M. (2005). Retroviral insertional mutagenesis: past, present and future. *Oncogene*, 24(52): 7656-72.

Usui S, Komeima K, Lee SY, Jo YJ, Ueno S, Rogers BS, Wu Z, Shen J, Lu L, Oveson BC, Rabinovitch PS, Campochiaro PA. (2009). Increased expression of catalase and superoxide dismutase 2 reduces cone cell death in retinitis pigmentosa. *Mol Ther*, 17(5): 778-86.

Vandenberghe LH, Bell P, Maguire AM, Cearley CN, Xiao R, Calcedo R, Wang L, Castle MJ, Maguire AC, Grant R, Wolfe JH, Wilson JM, Bennett J. (2011). Dosage thresholds for AAV2 and AAV8 photoreceptor gene therapy in monkey. *Sci Transl Med*, 3(88): 88ra54.

Vandenberghe LH, Bell P, Maguire AM, Xiao R, Hopkins TB, Grant R, Bennett J, Wilson JM. (2013). AAV9 targets cone photoreceptors in nonhuman primate retina. *PLOS One*, 8(1): e53463.

Vaziri H, Dessain SK, Ng Eaton E, Imai SI, Frye RA, Pandita TK, Guarente L, Weinberg RA. (2001). hSIR2 (SIRT1) functions as a NAD-dependent p53 deacetylase. *Cell*, 107(2): 149-59.

Veleri S, Lazar CH, Chang B, Sieving PA, Banin E, Swaroop A. (2015). Biology and therapy of inherited retinal degenerative disease: insights from mouse models. *Dis Model Mech*, 8(2): 109-129.

Venkatesh A, Ma S, Le YZ, Hall MN, Ruegg MA, Punzo C. (2015). Activated mTORC1 promotes long-term cone survival in retinitis pigmentosa mice. *J Clin Invest,* 125(4): 1446-1458.

Vladimirova O, O'Connor J, Cahill A, Alder H, Butunoi C, Kalman B. (1998). Oxidative damage to DNA in plaques of MS brains. *Mult Scler*, 4(5): 413-8.

Wang J, Yang Z, Liu C, Zhao Y, Chen Y. (2013). Activated microglia provide a neuroprotective role by balancing glial cell-line derived neurotrophic factor and tumor necrosis factor-α secretion after subacute cerebral ischemia. *Int J Mol Med*, 31: 172-178.

Wang L, Harris TE, Roth RA, Lawrence JC. (2007). PRAS40 regulatoes mTORC1 kinase activity by functioning as a direct inhibitor of substrate binding. *J Biol Chem*, 282: 20036-20044.

Wang T, Tsang SH, Chen J. (2017). Two pathways of rod photoreceptor cell death induced by elevated cGMP. *Hum Mol Genet,* 26(12): 2299-2306.

Weber MS, Hemmer B, Cepok S. (2011). The role of antibodies in multiple sclerosis. *Biochimica et biophysica acta,* 1812: 239-245.

Weihbrecht K, Goar WA, Pak T, Garrison JE, DeLuca AP, Stone EM, Scheetz TE, Sheffield VC. (2017). Keeping an eye on Bardet-Biedl syndrome: a comprehensive review of the role of Bardet-Biedl syndrome genes in the eye. *Med Res Arch*, 5(9): 10.18103/mra.v5i9.1526.

Weinreb RN, Aung T, Medeiros FA. (2014). The pathophysiology and treatment of glaucoma. *JAMA*, 311(18): 1901-1911.

Wilhelm H, Schabet M. (2015). The diagnosis and treatment of optic neuritis. *Dtsch Arztebl Int*, 112(37): 616-25.

Willett K, Bennett J. (2013). Immunology of AAV-mediated gene transfer in the eye. *Front Immunol*, 4: 261.

Wolf A, Agnihorti S, Micallef J, Mukherjee J, Sabha N, Cairns R, Hawkins C, Guha A. (2011). Hexokinase 2 is a key mediator of aerobic glycolysis and promotes tumor growth in human glioblastoma multiforme. *J Exp Med*, 208(2): 313-26.

Wright AF, Chakarova CF, Abd El-Aziz MM, Bhattacharya SS. (2010). Photoreceptor degeneration: genetic and mechanistic dissection of a complex trait. *Nat Rev Genet*, 11(4): 273-84.

Wu D, Klaw MC, Kholodilov N, Burke RE, Detloff MR, Cote MP, Tom VJ. (2016). Expressing constitutively active rheb in adult dorsal root ganglion neurons enhances the integration of sensory axons that regenerate across a chondroitinase-treated dorsal root entry zone following dorsal root crush. *Front Mol Neurosci*, 9:49.

Wu D, Klaw MC, Connors T, Kholodilov N, Burke RE, Cote MP, Tom VJ. (2017). Combining constitutively active rheb expression and chondroitinase promotes functional axonal regeneration after cervical spinal cord injury. *Mol Ther,* 25(12):2715-2726.

Xia X, Qu B, Li YM, et al. (2017). NFAT5 protects astrocytes against oxygen-glucose-serum deprivation/restoration damage via the SIRT1/Nrf2 pathway. *J Mol Neurosci,* 61(1): 96-104.

Xiao X, Li J, Samulski RJ. (1998). Production of high-titer recombinant adeno-associated virus vectors in the absence of helper adenovirus. *J Virol*, 72(3): 2224-32.

Xiong W, MacColl Garfinkel AE, Li Y, Benowitz LI, Cepko CL. (2015). NRF2 promotes neuronal survival in neurodegeneration and acute nerve damage. *J Clin Invest*, 125(4): 1433-45.

Yan L, Findlay GM, Jones R, Procter J, Cao Y, Lamb RF. (2006). Hyperactivation of mammalian target of rapamycin (mTOR) signaling by gain-of-function mutant of the rheb GTPase. *J Biol Chem,* 281(29):19793-7.

Yang H, Jiang X, Li B, Yang HJ, Miller M, Yang A, Dhar A, Pavletich NP. (2017). Structural mechanisms of mTORC1 activation by RHEB and inhibition by PRAS40. *Nature*, 552(7685): 368-373.

Yang H, Rudge DG, Koos JD, Vaidialingam B, Yang HJ, Pavletich NP. (2013). mTOR kinase structure, mechanism and regulation. *Nature*, 497: 217-223.

Yang Y, Wang L, Bell P, McMenamin D, He Z, White J, Yu H, Xu C, Morizono H, Musunuru K, Batshaw ML, Wilson JM. (2016). A dual AAV system enables the Cas9-mediated correction of a metabolic liver disease in newborn mice. *Nat Biotechnol*, 34(3): 334-8.

Zagorski T, Dudek I, Berkan L, Mazurek M, Kedziora J, Chmielewski H. (1991). Superoxide dismutase (SOD-1) activity in erythrocytes of patients with multiple sclerosis. *Neurol Neurochir Pol*, 25(6): 725-30.

Zhang L, Cui X, Jauregui R, Park KS, Justus S, Tsai YT, Duong JK, Hsu CW, Wu WH, Xu CL, Lin CS, Tsang SH. (2018). Genetic rescue reverses microglial activation in preclinical models of retinitis pigmentosa. *Mol Ther,* 26(8): 1953-1964.

Zhang L, Du J, Justus S, Hsu CW, Bonet-Ponce L, Wu WH, Tsai YT, Wu WP, Jia Y, Duong JK, Mahajan VB, Lin CS, Wang S, Hurley JB, Tsang SH. (2016). Reprogramming metabolism by targeting sirtuin 6 attenuates retinal degeneration. *J Clin Invest*, 126(12): 4659-4673.

Zhang L, Justus S, Xu Y, Pluchenik T, Hsu CW, Yang J, Duong JK, Lin CS, Jia Y, Bassuk AG, Mahajan VB, Tsang SH. (2016). Reprogramming towards anabolism impedes degeneration in a preclinical model of retinitis pigmentosa. *Hum Mol Genet*, 25(19): 4244-4255.

Zhang P, Li Y, Du Y, et al. (2016). Resveratrol ameliorated vascular calcification by regulating Sirt-1 and Nrf2. *Transplant Proc,* 48(10): 3378-3386.

Zheng Y, Shen W, Zhang J, Yang B, Liu YN, Qi H, Yu X, Lu SY, Chen Y, Xu YZ, Li Y, Gage FH, Mi S, Yao J. (2018). CRISPR interference-based specific and efficient gene inactivation in the brain. *Nat Neurosci*, 21(3): 447-454.

Zhong G, Wang H, Bailey CC, Gao G, Farzan M. (2016). Rational design of aptazyme riboswitches for efficient control of gene expression in mammalian cells. *Elife,* 5: e18858.

Zinn E, Pacouret S, Khaychuk V, et al. (2015). In silico reconstruction of the viral evolutionary lineage yields a potent gene therapy vector. *Cell Rep,* 12(6):1056-1068.

Zuo L, Khan RS, Lee V, et al. (2013). SIRT1 promotes RGC survival and delays loss of function following optic nerve crush. *Invest Ophthalmol Vis Sci*, 54: 5097–5102.